

# Helical flow of non-Newtonian fluids, with reference to drilling fluid flow.

MORTON, J.D.

1978

*The author of this thesis retains the right to be identified as such on any occasion in which content from this thesis is referenced or re-used. The licence under which this thesis is distributed applies to the text and any original images only – re-use of any third-party content must still be cleared with the original copyright holder.*

HELICAL FLOW OF NON-NEWTONIAN FLUIDS,  
WITH REFERENCE TO DRILLING FLUID FLOW.

by

JOHN DOUGLAS MORTON

A thesis presented to the Council for  
National Academic Awards, in conformance  
with the requirements for the degree,  
Master of Philosophy.

School of Mechanical and Offshore Engineering,  
Robert Gordon's Institute of Technology,  
November 1978.

## ACKNOWLEDGEMENTS

I am happy to acknowledge my debts to Mr. J.E. Porter for his support, guidance and insight throughout the course of this research and to Mr. J.G. Black for his constant enthusiasm, advice and encouragement without which this thesis would never have reached fruition.

I am grateful to Mr. B Airey, Mr. F.S. Ashton, Mr. M. Phillip and Mr. D. Shaw for their invaluable discussions and helpful criticism.

I acknowledge my gratitude to the Science Research Council for financing this research.

Finally I would like to thank all members of the School of Mechanical and Offshore Engineering who were of assistance to me in so many ways.

## TABLE OF CONTENTS

CHAPTER 1	INTRODUCTION AND BACKGROUND	
1.1	Introduction	1
1.2	Background	1
1.3	Numerical Values	4
1.3.1	Annular Dimensions	4
1.3.2	Drill String Rotation	5
1.3.3	Flow Rate	5
CHAPTER 2	THEORETICAL DESCRIPTION OF DRILLING FLUID FLOW	
2.1	Governing Equations	8
2.2	Fluid Models	12
2.2.1	Newtonian Fluid Model	13
2.2.2	Shear Rate Dependent Models	14
2.2.3	Viscoelastic Fluid Models	17
2.2.4	Conclusion	20
2.3	Non Dimensional Systems	21
2.3.1	Introduction	21
2.3.2	General Dimensionless System	21
2.3.3	Dimensionless Systems for Particular Fluid Models	22
2.3.4	Derived Parameters	24
CHAPTER 3	WORK ON DRILLING FLUID FLOW	
3.1	Previous Work	25
3.1.1	The Integral Formulation	25
3.1.2	The Differential Formulation	27
3.1.3	Integral Solution Method for One Flow Component Only	28
3.1.4	Integral Solution Method with Two Velocity Components	30
3.1.5	Differential Solution Methods	34
3.1.6	Summary and Discussion	36
3.2	Work of the Present Thesis	37
3.2.1	Basis of the Computer Program	37
3.2.2	Description of the MUDFLO Program	40
3.2.3	Calculations performed using MUDFLO	41
3.2.4	Conclusion	42

CHAPTER 4	RESULTS	
4.1	Comparison with Existing Experimental Data	43
4.2	Predicted Velocity Profiles for Power Law Fluids in Helical Flow	48
4.2.1	Radius Ratio $k = 0.5$	49
4.2.2	Variable Radius Ratio	73
4.2.3	Variable Fluid Index	89
4.3	Physical Representation of Results	100
4.4	Conclusion	100
CHAPTER 5	REVIEW, CONCLUSIONS AND RECOMMENDATIONS	
5.1	Review	103
5.1.1	Chapter 1 : Introduction	103
5.1.2	Chapter 2 : Theoretical Description	103
5.1.3	Chapter 3 : Work on Drilling Fluid Flow	104
5.1.4	Chapter 4 : Results	105
5.2	Results and Conclusions	105
5.3	Recommendations for Further Work	107
APPENDIX A	Components of the Shear Rate Tensor in Helical Flow	A-1
APPENDIX B	COMPUTER PROGRAM	
B.1	Description	B-1
B.2	Program Listing	B-4
B.3	Variable Names Used in the Program	B-17
B.4	Archive Numbers	B-19
NOMENCLATURE		
BIBLIOGRAPHY		

## ABSTRACT

This thesis is motivated by a desire to understand better the complex flow of drilling fluids in oil wells.

After an initial discussion of the flow and its complexities, mathematical models are considered, and a 'helical flow' model adopted as being a reasonable approximation to the flow which may be solved in practice. Rheological models for the fluids are discussed, and it is shown that, with helical flow, a shear rate dependent viscosity model is of considerable generality.

Numerical methods for obtaining velocity profiles from these models are explored and it is suggested that an iterative finite difference procedure is the most suitable to the purpose of understanding better the flow of drilling fluids.

The iterative finite difference procedure is implemented in a computer program 'MUDFLO' which can be operated using either a consistent dimensioned system of units, or using the dimensionless variables defined in the text.

It is shown that three dimensionless parameter groups are sufficient to describe completely the helical flow of a power law fluid. A set of velocity profile graphs is presented, covering typical values of these three parameter groups. From this set of graphs, the velocity profiles for most practically occurring flows of power law fluids may be interpolated.

Some computational difficulties are however reported in calculations using the Bingham plastic fluid model, and using the power law fluid model with very low fluid index.

The results of the computer program with the power law fluid model are supported by comparison with existing experimental data, and by discussion of the general characteristics of the set of dimensionless velocity profile graphs.

## INTRODUCTION AND BACKGROUND

1.1 Introduction

Drilling fluid is used in oil wells to transport rock chips up the annular space between the rotating drill string and the casing during drilling. (See 1.2) Since the drilling fluid or 'mud' must perform several functions under many, often conflicting, constraints it is useful to have accurate information on the interdependence of the various flow parameters involved. Prediction of the characteristics of drilling fluid flow is however made difficult by complex geometry and by the fluid's non-Newtonian properties. Present day drilling technology uses empirical calculations based on past experience to overcome the problems of integrating the conflicting functions of drilling fluid, but there is some concern over the economic efficiency of these methods. (Sifferman et al. 74)

Whilst the present work gives a general discussion of drilling fluid flow and the associated problems in this section, it's main aim is to tackle the specific problem of estimating velocity profiles for the flow.

A mathematical model for the flow consisting of a coupled pair of non-linear ordinary differential equations is constructed (in chapter 2) and solution is performed using an iterative finite difference procedure (in chapter 3). The results of this work are presented (in chapter 4) in the form of velocity profile charts for the ranges of parameters that occur in oil well drilling, with a dimensionless formulation being used to reduce the number of charts involved. Discussion of the results and recommendations for further work are made in chapter 5. The computer programme developed for this thesis has been archived by RGIT Computer Services Section, and full instructions for accessing and running it are included in the text.

1.2 Background

Before discussing the helical flow of drilling fluid, we give a brief description of oil well drilling and the part that drilling fluid plays in this operation.

Oil and gas can be produced in several special geological

formations the important features of which are:

- 1) That the reservoir is bounded on its upper surface by an impermeable rock layer.
- 2) That the oil and gas are held in a permeable rock layer with the lower bound of the reservoir being formed by a water-table, also held in the permeable layer.

Oil well drilling is performed using a 'drill bit' rotated and supported by the 'drill string'. The drill string is made up from several components of different diameters, and may be thought of as cylindrical, but with stepwise changes in diameter. To drill a well or 'hole' a large diameter hole is first drilled, and is then lined with steel 'casing'. Progressively smaller holes are then drilled, each one being cased from the surface before the next is commenced. Oil wells are not drilled straight, but are usually 'deviated', having several changes in direction. As a result of such deviations, the drill string will rarely be concentric with the casing, and its eccentricity will probably vary with time as well as with depth. In order to remove the rock chips produced when drilling a well, drilling fluid is pumped down through the drill string and rises up the 'annular gap' between casing and drill string carrying the chips with it. The drilling fluid consists of a complex mixture of chemicals and also performs many other functions whilst subject to several conflicting constraints. Baroid (76) lists the functions of drilling fluid in a general way as follows:

- " 1) Cool and lubricate the bit and drill pipe,
- 2) Clean the bottom of the hole,
- 3) Remove cuttings from the hole,
- 4) Settle cuttings in the surface pits,
- 5) Wall off permeable formations,
- 6) Overcome formation fluid pressures,
- 7) Prevent caving of the formation,
- 8) Avoid damage to productivity,
- 9) Allow interpretable electric logging,
- 10) Reduce casing costs,
- 11) Prevent drill pipe corrosion fatigue,
- 12) Perform above functions without hazard to the drilling crews".

Regarding conflicting constraints, the reference continues :

" The individual functions in the preceding list are straight-forward and self explanatory, but combinations of functions that affect the efficiency of the drilling operation directly are of special importance. "

The drilling muds are non-Newtonian and exhibit the properties of shear-rate dependent viscosity, thixotropy and viscoelasticity. (Murphy 75, Wilson 76). As a result of the shear-rate dependent viscosity, the fluids will have an 'apparent' viscosity' which varies across the annular gap and its velocity components will be inter-dependent.

A complete analysis of drilling fluid thus seems, at very least, impractical, and we approach the problem using the following philosophy. Firstly, we attempt to gain more insight into drilling fluid flow by studying simplified cases of particular aspects of the subject, and secondly, using such insight, the empirical approaches used in practice may be improved. The ultimate aim of this approach is to increase the profitability of oil well drilling operations.

The particular aspect studied by the present work is that of predicting the velocity profiles in the annulus with a view to gaining insight into the particle transport function of drilling fluids.

We note that there are two main components of flow:

- a) The axial velocity component as the fluid is being pumped up the annulus. This component will be zero at both walls.
- b) The angular velocity component caused by the rotation of the drill string. This will be zero at the casing and will reach a maximum value ( equal to the angular velocity of the drill string ) at the drill string.

It is clear that, neglecting flow into or out of the rock formation, any radial component of velocity will have a zero time-average value.

Several studies have already been carried out on these velocity profiles, and they are summarised in table 1.1.

We observe:

- 1) They have all considered the simplified case of steady-state non-recirculating laminar flow of a non time-dependent fluid through a uniform annulus.
- 2) Most studies have considered only one velocity component,
- 3) Only one study has taken annular eccentricity into account.

These studies are discussed in detail in chapter 3 , and the conclusion is drawn that it would be valuable to attempt solution for the case of a concentric annulus with two non zero components of velocity using finite difference methods. It is solution of this problem that forms the central aim of the present thesis.

### 1.3 Numerical values

For reference we list ranges of ' typical values ' for the parameters of drilling fluid flow. The values are approximate and, as with any list of typical values, there will be some inevitable omissions from this list, but it will serve to orient the reader to the scale of the problem. Input parameter ranges for the results presented in chapter 4 were taken from this section. Values are given in the oil industry's working units.

#### 1.3.1 Annular dimensions

The annulus is bounded by the drill string and either by the outer casing, or by the ' hole wall ' in uncased sections of the well. The drill string diameter is usually  $3\frac{1}{2}$  or 5 inches, though other sizes are occasionally used. (Sivalingham 77). Hole and casing sizes are listed below along with estimates of the depths to which they are used. (STEC 76).

DEPTH (feet)	HOLE SIZE (inches)	CASING SIZE (inches)
2-300	36	30
1500	26	20
3000	17½	13¾
10-20000 (total depth)	12½	9¾

### 1.3.2 Drill string rotation

Drill string rotation speed is varied according to drill bit size and rock hardness. It is usually of the order 100 RPM, but can be as low as 60 RPM or as high as 250 RPM.

### 1.3.3 Flow rate

In the oil industry, axial flow rates through the annulus are usually specified as 'minimum annular velocities' defined as the discharge rate (ft<sup>3</sup>/min) per unit cross sectional area (ft<sup>2</sup>) of the annular gap. Typical values are given below. (Baroid 76).

OUTER DIAMETER OF ANNULUS (inches)	MINIMUM ANNULAR VELOCITY (feet / minute)
15	80
12½	90
10¾	110
8¾	120
7¾	130

### 1.3.4 Fluid parameters

Two fluid models are in common use : the Bingham plastic and the power law fluid. (Baroid 76 , Martin 68).

The Bingham plastic is defined by

$$\underline{\underline{\tau}} = \left\{ \mu_0 + \frac{\tau_0}{\frac{1}{2}\sqrt{(\underline{\underline{\Delta}}:\underline{\underline{\Delta}})}} \right\} \underline{\underline{\Delta}} \quad \text{when} \quad \frac{1}{2}(\underline{\underline{\tau}}:\underline{\underline{\tau}}) \geq \tau_0^2$$

and

$$\underline{\underline{\Delta}} = 0 \quad \text{when} \quad \frac{1}{2}(\underline{\underline{\tau}}:\underline{\underline{\tau}}) < \tau_0^2$$

Where  $\underline{\underline{\tau}}$  is the shear stress tensor,  $\underline{\underline{\Delta}}$  is the shear rate tensor whilst  $\mu_0$  and  $\tau_0$  are constants, referred to as the plastic viscosity and the yield stress for a particular fluid. Typical values for the plastic viscosity and yield stress of drilling muds are (Sivalingham 77)

$$0 \text{ to } 250 \text{ lbs/100 ft}^2 \quad \text{for } \tau_0$$

and

$$10 \text{ to } 135 \text{ centipoise} \quad \text{for } \mu_0$$

The power law fluid model is defined by

$$\underline{\underline{\tau}} = m \left| \frac{1}{2}\sqrt{(\underline{\underline{\Delta}}:\underline{\underline{\Delta}})} \right|^{n-1} \underline{\underline{\Delta}}$$

Typical values for the constant m and the ' index of consistency n for bentonite drilling muds are :

$$.7 \text{ to } .9 \text{ for } n$$

and

$$.1 \text{ to } 2.0 \text{ for } m ,$$

though n can be much lower for different types of mud. (Martin 68). Here n is a dimensionless index whilst m is given in the units of dyne-sec<sup>n</sup> /cm<sup>2</sup>.

TABLE 1.1      PREVIOUS STUDIES OF VELOCITY PROFILES  
IN DRILLING FLUID FLOW.

SIMPLIFICATIONS	AUTHORS					
	1	2	3	4	5	6
Non-recirculating laminar flow	yes	yes	yes	yes	yes	yes
Uniform annulus	yes	yes	yes	yes	yes	yes
Viscosity not time dependent	yes	yes	yes	yes	yes	yes
Concentric annulus	yes	yes	yes	NO	yes	yes
Viscosity dependent on only one component	yes	yes	yes	yes	NO	NO
Computer required for solution	NO	NO	NO	yes	yes	yes

AUTHORS

- 1) Fredrickson & Bird, 1958. (Semi-analytic solution)
- 2) Parslay & Slibar, 1967. (Semi-analytic solution)
- 3) Slawomirski, 1974. (Semi-analytic solution)
- 4) Guickes, 1975. (Finite difference solution)
- 5) Zeinkiewicz, 1974. (Finite element solution)
- 6) Savins & Wallick, 1966. (Trial and error solution)

## THEORETICAL DESCRIPTION OF DRILLING FLUID FLOW

This chapter is concerned with the theoretical description of the problem. In 2.1 mathematical models for the flow are discussed, and the governing equations for the helical flow model introduced. In 2.2 rheological models for drilling fluids are discussed, particularly in the context of helical flow. Finally, in 2.3, systems of dimensionless variables are introduced and discussed.

### 2.1 Governing equations

Whilst the previous studies (Table 1.1) on drilling fluid flow have all made many simplifying assumptions to reduce the governing equations to a soluble form, none have presented the full equations. It is however instructive both in terms of understanding the nature of the simplifications, and of understanding the full complexity of mud flow, to derive the governing equations for helical flow of non-Newtonian fluids from the equations of conservation of mass and linear momentum.

To do this, we must first model the physical flow, as described below. The mud is considered to flow through an annular gap defined by two vertical cylindrical surfaces: the casing, and the drill string which is allowed to undergo step-wise changes in diameter. The drill string need not be concentric with the casing but its eccentricity is considered constant. The flow is taken as laminar, but will have recirculation zones in the wider section of the annulus due to the eccentricity of the drill string, and at the stepwise changes of drill string diameter. The assumption of no fluid slippage at the boundaries is made, and the fluid is considered incompressible.

We define a polar coordinate system  $(r, \theta, z)$  with the positive  $z$ -axis being taken as the axis of the casing in the vertical direction. Such a flow is governed by the equations of conservation of mass and linear momentum given below. (Bird et al. 65).

Continuity

$$\frac{1}{r} \frac{\partial}{\partial r} (r v_r) + \frac{1}{r} \frac{\partial}{\partial \theta} (v_\theta) + \frac{\partial}{\partial z} v_z = 0$$

r-momentum

$$\rho \left\{ \frac{\partial v_r}{\partial t} + \frac{\partial v_r}{\partial r} v_r + \frac{v_\theta}{r} \frac{\partial v_r}{\partial \theta} - \frac{v_\theta^2}{r} + v_z \frac{\partial v_r}{\partial z} \right\}$$

$$= - \frac{\partial P}{\partial r} - \left( \frac{1}{r} \frac{\partial}{\partial r} (r \tau_{rr}) + \frac{1}{r} \frac{\partial \tau_{r\theta}}{\partial \theta} - \frac{\tau_{\theta\theta}}{r} + \frac{\partial \tau_{rz}}{\partial z} \right)$$

\theta-momentum

$$\rho \left\{ \frac{\partial v_\theta}{\partial t} + v_r \frac{\partial v_\theta}{\partial r} + \frac{v_\theta}{r} \frac{\partial v_\theta}{\partial \theta} + \frac{v_r v_\theta}{r} + v_z \frac{\partial v_\theta}{\partial z} \right\}$$

$$= - \frac{1}{r} \frac{\partial P}{\partial \theta} - \left( \frac{1}{r^2} \frac{\partial}{\partial r} (r^2 \tau_{r\theta}) + \frac{1}{r} \frac{\partial \tau_{\theta\theta}}{\partial \theta} + \frac{\partial \tau_{\theta z}}{\partial z} \right)$$

z-momentum

$$\rho \left\{ \frac{\partial v_z}{\partial t} + v_r \frac{\partial v_z}{\partial r} + \frac{v_\theta}{r} \frac{\partial v_z}{\partial \theta} + v_z \frac{\partial v_z}{\partial z} \right\}$$

$$= - \frac{\partial P}{\partial z} - \left( \frac{1}{r} \frac{\partial}{\partial r} (r \tau_{rz}) + \frac{1}{r} \frac{\partial \tau_{\theta z}}{\partial \theta} + \frac{\partial \tau_{zz}}{\partial z} \right) + \rho g$$

with the boundary conditions:

$$v_r = v_z = 0 \text{ at both walls}$$

$$v_\theta = 0 \text{ at casing}$$

$$\text{and } v_\theta = R_1 \omega_1 \text{ at drill string.}$$

Where  $g$  is the gravitational acceleration

$(v_r, v_\theta, v_z)$  is the fluid velocity

$P$  is the fluid pressure

$t$  is time

$\rho$  is the fluid density

$R_1$  is the diameter of the drill string

$\omega_1$  is the angular velocity of the drill string

and  $\underline{\tau} = \begin{bmatrix} \tau_{rr} & \tau_{r\theta} & \tau_{rz} \\ \tau_{\theta r} & \tau_{\theta\theta} & \tau_{\theta z} \\ \tau_{zr} & \tau_{z\theta} & \tau_{zz} \end{bmatrix}$  is the stress tensor.

For Newtonian fluids, solution of the above system effectively involves solution of the full Navier Stokes system ; and thus, clearly, for the more complex non-Newtonian fluids much simplification is required before solution may be attempted.

One such simplification is the assumption of non-recirculating flow which, whilst still retaining the axial and rotational components of velocity, necessitates constraining the drill string to be concentric and of constant diameter. As the fluid is incompressible, the radial component of velocity will then necessarily be zero. Further, with the drill string concentric, all derivatives with respect to  $\theta$  will become zero. The governing equations of continuity of mass and momentum will thus become:

continuity

( a tautology )

r-momentum

$$-\rho \frac{v_\theta^2}{r} = -\frac{\partial p}{\partial r} - \left( \frac{1}{r} \frac{\partial}{\partial r} (r \tau_{rr}) - \frac{\tau_{\theta\theta}}{r} + \frac{\partial \tau_{rz}}{\partial z} \right)$$

$\theta$ -momentum

$$\rho \left\{ \frac{\partial v_\theta}{\partial t} + v_z \frac{\partial v_\theta}{\partial z} \right\} = - \left( \frac{1}{r^2} \frac{\partial}{\partial r} (r^2 \tau_{r\theta}) + \frac{\partial \tau_{\theta z}}{\partial z} \right)$$

z-momentum

$$\rho \left\{ \frac{\partial v_z}{\partial t} + v_z \frac{\partial v_z}{\partial z} \right\} = -\frac{\partial p}{\partial z} - \left( \frac{1}{r} \frac{\partial}{\partial r} (r \tau_{rz}) + \frac{\partial \tau_{zz}}{\partial z} \right) + \rho g$$

The governing equation system has now been reduced to a much simpler form, but velocity profile analysis would still involve solution of three simultaneous partial differential equations with 3 independent variables. We may further simplify the problem by considering that the flow is steady state, with end effects being negligible. Thus all derivatives (except pressure) with respect to  $z$  and  $t$  will become zero, and the resulting system will involve the following three momentum conservation equations.

r-momentum

$$\frac{1}{r} \frac{d}{dr} (r \tau_{rr}) - \frac{\tau_{\theta\theta}}{r} = - \frac{dP}{dr} + \rho \frac{v_\theta^2}{r}$$

$\theta$ -momentum

$$\frac{1}{r^2} \frac{d}{dr} (r^2 \tau_{r\theta}) = 0$$

z-momentum

$$\frac{1}{r} \frac{d}{dr} (r \tau_{rz}) = \rho g - \frac{dP}{dz}$$

E1

We note that some progress may now be made towards integrating the latter two equations of this system.

Integrating with respect to  $r$  we obtain:

$\theta$ -momentum

$$\tau_{r\theta} = \frac{B}{r^2}$$

z-momentum

$$\tau_{rz} = \frac{r}{2} \left( \rho g - \frac{dP}{dz} \right) + \frac{A}{r}$$

where  $A$  and  $B$  are constants of integration. (Rivlin, 56 and others). This approach has formed the basis for much previous work on helical flow, and on axial flow, in annuli. (See section 3.1).

## 2.2 Fluid models

For the solution approach adopted by the present work, it is now necessary to introduce some 'fluid model' relating the components of the shear stress tensor

$$\underline{\underline{\tau}} = \begin{bmatrix} \tau_{rr} & \tau_{re} & \tau_{rz} \\ \tau_{er} & \tau_{ee} & \tau_{ez} \\ \tau_{zr} & \tau_{ze} & \tau_{zz} \end{bmatrix}$$

to the shear rate or 'deformation rate' tensor

$$\underline{\underline{\Delta}} = \begin{bmatrix} \Delta_{rr} & \Delta_{re} & \Delta_{rz} \\ \Delta_{er} & \Delta_{ee} & \Delta_{ez} \\ \Delta_{zr} & \Delta_{ze} & \Delta_{zz} \end{bmatrix}$$

The components of the deformation rate tensor  $\underline{\underline{\Delta}}$  in polar coordinates are (Bird et al. 65)

$$\Delta_{rr} = 2 \left( \frac{\partial v_r}{\partial r} \right) - \frac{2}{3} (\underline{\underline{\nabla}} \cdot \underline{\underline{v}})$$

$$\Delta_{ee} = 2 \left( \frac{1}{r} \frac{\partial v_\theta}{\partial \theta} + \frac{v_r}{r} \right) - \frac{2}{3} (\underline{\underline{\nabla}} \cdot \underline{\underline{v}})$$

$$\Delta_{zz} = 2 \left( \frac{\partial v_z}{\partial z} \right) - \frac{2}{3} (\underline{\underline{\nabla}} \cdot \underline{\underline{v}})$$

$$\Delta_{re} = \Delta_{er} = r \frac{\partial}{\partial r} \left( \frac{v_\theta}{r} \right) + \frac{1}{r} \frac{\partial v_r}{\partial \theta}$$

$$\Delta_{ez} = \Delta_{ze} = \frac{\partial v_\theta}{\partial z} + \frac{\partial v_z}{\partial \theta}$$

$$\Delta_{rz} = \Delta_{zr} = \frac{\partial v_z}{\partial r} + \frac{\partial v_r}{\partial z}$$

$$\text{where } (\underline{\underline{\nabla}} \cdot \underline{\underline{v}}) = \frac{1}{r} \frac{\partial}{\partial r} (r v_r) + \frac{1}{r} \frac{\partial v_\theta}{\partial \theta} + \frac{\partial v_z}{\partial z}$$

It may be shown (see appendix A) that for the steady state laminar helical flow discussed in 2.1 the shear rate tensor takes the form :

$$\underline{\underline{\Delta}} = \begin{bmatrix} 0 & -\frac{V_\theta}{r} + \frac{\partial V_\theta}{\partial r} & \frac{\partial V_z}{\partial r} \\ -\frac{V_\theta}{r} + \frac{\partial V_\theta}{\partial r} & 0 & 0 \\ \frac{\partial V_z}{\partial r} & 0 & 0 \end{bmatrix} \quad (E2)$$

Once a relationship between the stress tensor and the shear rate tensor is known, it may be inserted into the helical flow system (E1) to produce a new system in which the dependent variables are velocity components instead of stress components. As noted in chapter 1, drilling fluids exhibit shear rate dependent viscosity, viscoelasticity and time dependence, and we look in turn at stress/shear rate relationships or 'fluid models' describing these properties. First, however, we consider the case of a Newtonian fluid model and show that use of this model leads to an equation system with a simple analytical solution.

### 2.2.1 Newtonian fluid model

In this model, the elements of the shear stress tensor are linearly proportional to those of the shear rate tensor. That is

$$\underline{\underline{\tau}} = -\mu \underline{\underline{\Delta}}$$

where  $\mu$  is a constant, referred to as the 'viscosity' of the fluid. Insertion of this relationship into the system (E1) gives

r-momentum

$$\frac{V_\theta^2}{r} = \frac{1}{\rho} \frac{dP}{dr}$$

$\theta$ -momentum

$$\frac{d}{dr} \left( r^2 \left( -\frac{V_\theta}{r} + \frac{\partial V_\theta}{\partial r} \right) \right) = 0$$

z-momentum

$$\frac{1}{r} \frac{d}{dr} \left( r \frac{dV_z}{dr} \right) = \frac{1}{\mu} \left( \rho g - \frac{dP}{dz} \right)$$

In this system the r-momentum equation only relates angular velocity to the resulting radial pressure gradient, whilst the  $\theta$  and  $z$  component equations are independent. Thus, in helical flow of Newtonian fluids, there will be no interaction between the axial and angular components of velocity. A simple analytical solution of the momentum conservation equations for velocity profiles is available (Langlois, 64).

### 2.2.2 Shear rate dependent fluid models.

This type of model has a shear stress, shear rate relationship of the form

$$\underline{\underline{\tau}} = f(\underline{\underline{\Delta}}) \underline{\underline{\Delta}}$$

where  $f(\underline{\underline{\Delta}})$  is a scalar function of the shear rate tensor. This type of fluid has been referred to as a "generalised Newtonian fluid" (McEachern, 66, and others). Many non-Newtonian fluids may adequately be described by this type of model, and indeed most engineering calculations for practical applications use such a model. (Bird et al. 65).

Since  $f(\underline{\underline{\Delta}})$  is a scalar function of  $\underline{\underline{\Delta}}$  it must remain unchanged by transformations of the coordinate system. Consequently it must depend only on the three invariants of the tensor  $\underline{\underline{\Delta}}$ .

That is on

$$I_1 := \sum_i \Delta_{ii}$$

$$I_2 := \sum_i \sum_j \Delta_{ij} \Delta_{ji}$$

$$I_3 := \text{DETERMINANT OF } \underline{\underline{\Delta}}$$

The first invariant  $I_1$  can easily be shown to be  $2(\underline{\underline{\nabla}} \cdot \underline{\underline{\nabla}})$  which is zero for incompressible fluids, and for many simple flows including helical flow the third invariant is also zero. The third invariant is often assumed to be unimportant for practical engineering calculations even when it is non-zero. (Bird et al. 65).

Thus, for practical calculations, we may take the constitutive equation for shear rate dependent fluid as

$$\underline{\underline{\tau}} = f(\underline{\underline{\Delta}} : \underline{\underline{\Delta}}) \underline{\underline{\Delta}} \quad (E3)$$

Inserting this relationship into the governing equations (E1), using the values for  $\underline{\underline{\Delta}}$  given by equation (E2), we obtain:

r-momentum

$$\psi \frac{v_e^2}{r} = \frac{dP}{dr}$$

e-momentum

$$\frac{d}{dr} \left\{ r^3 f\left(\frac{\Delta}{z} : \frac{\Delta}{z}\right) \frac{dw}{dr} \right\} = 0$$

z-momentum

$$\frac{1}{r} \frac{d}{dr} \left\{ r f\left(\frac{\Delta}{z} : \frac{\Delta}{z}\right) \frac{dv}{dr} \right\} = \rho$$

where  $w = v_e/r$

$v = v_z$

$$\rho = \rho_g - \frac{dP}{dz}$$

It is sufficient to solve only the e and z momentum equations to obtain the velocity profiles, as the r-momentum equation merely relates the angular velocity to the resulting radial pressure distribution. The two equations must however be solved simultaneously since they are coupled through the term  $f\left(\frac{\Delta}{z} : \frac{\Delta}{z}\right)$ .

For the present research a computer program "MUDFLO" was developed to solve these e and z momentum equations simultaneously. The equations are solved in the above form, with the fluid model being introduced numerically during solution, rather than analytically before solution is attempted. MUDFLO can thus attempt solution for any fluid model of the form (E3), and with only minor modifications could attempt solution using tabular fluid behaviour data instead of a mathematically defined model.

Many empirical models of the type (E3) have been used in practice and we list the more common ones below.

#### BINGHAM PLASTIC

Used by the oil industry to describe the behaviour of drilling muds, this model has the property of a 'yield stress'. The model is defined as follows

$$\tau_z = - \left\{ \mu_0 + \frac{\tau_0}{\sqrt{\frac{1}{2} \left( \frac{\Delta}{z} \right)}} \right\} \frac{\Delta}{z} \quad \text{when } \frac{1}{2} \left( \frac{\Delta}{z} \right) \geq \tau_0^2$$

$$\underline{\underline{\tau}} = 0 \text{ when } \frac{1}{2}(\underline{\underline{\tau}} : \underline{\underline{\tau}}) < \tau_0^2$$

where the constants  $\mu_0$  and  $\tau_0$  are the ' plastic viscosity ' and the ' yield stress ' respectively.  $\tau_0$  has the units of stress and  $\mu_0$  has the units of viscosity.

#### POWER LAW MODEL

This is another model used by the oil industry to describe the behaviour of drilling fluids. It takes the form

$$\underline{\underline{\tau}} = - \left\{ m \sqrt{\frac{1}{2}(\underline{\underline{\Delta}} : \underline{\underline{\Delta}})} \right|^{n-1} \right\} \underline{\underline{\Delta}}$$

where the constant m has the units of viscosity and n is a dimensionless index.

#### ROBERTSON AND STIFF MODEL

Robertson and Stiff (76) proposed a model for drilling fluids incorporating the yield stress property of the Bingham model and the stress shear rate characteristic of the power law model. The proposed model is actually a generalisation of these two models and takes the form

$$\underline{\underline{\tau}} = \left\{ A \left( \sqrt{\frac{1}{2}(\underline{\underline{\Delta}} : \underline{\underline{\Delta}})} + C \right)^B \sqrt{\frac{1}{2}(\underline{\underline{\Delta}} : \underline{\underline{\Delta}})} \right\} \underline{\underline{\Delta}}$$

where A, B and C are constants.

Robertson and Stiff found that, using this model, they were able to predict actual drilling mud behaviour with consistently greater accuracy than with using either the Bingham or power law models.

#### BRIANT MODEL

Another generalisation of both the Bingham plastic and power law models is the "systeme de Briant" described by Martin (68). It is defined as follows

$$\underline{\underline{\tau}} = \left\{ \tau_0 + \frac{\tau_\infty}{m \sqrt{\frac{1}{2}(\underline{\underline{\Delta}} : \underline{\underline{\Delta}})}} \right\}^m \underline{\underline{\Delta}}$$

where  $\gamma_\infty$ ,  $\lambda_\infty$  and  $m$  are constants.

Many other models of the form (E3) have been proposed, but those mentioned above are the most commonly used. (Coulson, 71; Skelland, 67; Slawomirski, 75 ; Bird, 65).

### 2.2.3 Viscoelastic Fluid models

We next consider fluid models which take into account the more complex fluid properties of viscoelasticity as well as shear-rate dependent viscosity. Whilst many papers exist discussing this type of fluid model, few practical applications have been made.

Nevertheless, we show that as might be expected, in steady helical flow of viscoelastic fluids, the elastic characteristics will exert an influence only at the inlet and outlet of the flow. Consequently, an analysis based on the constitutive equations of purely viscous liquids should be adequate for engineering design purposes where the inlet and outlet conditions are of less importance. That is, in many cases we may use the constitutive equation (E3) to describe with reasonable accuracy steady helical flow of viscoelastic fluids.

#### OLDROYD and MAXWELL MODELS

The Oldroyd fluid model is a simple model incorporating viscoelastic characteristics. It is defined by:

$$\underline{\underline{\tau}} + \lambda_1 \frac{d}{dt}(\underline{\underline{\tau}}) = \mu^* \left( \underline{\underline{\Delta}} + \lambda_2 \frac{d}{dt}(\underline{\underline{\Delta}}) \right)$$

where  $\mu^*$  is a constant term with the units of viscosity, and  $\lambda_1$  and  $\lambda_2$  are known as relaxation times for the fluid.

The Maxwell model is a special case with  $\lambda_2 = 0$ . (Skelland 67).

Clearly, with steady state flow, all derivatives with respect to time will be zero and hence the constitutive equation for these fluids will reduce to that of a Newtonian fluid:

$$\underline{\underline{\tau}} = \mu^* \underline{\underline{\Delta}}$$

Thus with this model, in steady state flow, the viscoelastic properties will have no effect, and the viscosity could be taken as shear rate independent.

GENERAL VISCOELASTIC FLUID MODELS

Several papers have been written by theoretical rheologists on the helical flow of more complex viscoelastic fluids. Such fluids include provision for the stresses that arise in viscoelastic fluids normal to the direction of flow, known as the Weissenberg effect. (Fredrickson 64).

Both Fredrickson (59) and Rivlin (56) used the " model for fluids of the differential type " developed by Rivlin (55). In this model, the stress tensor is expressed as a polynomial in the Rivlin/Ericksen tensors  $A_1, A_2, A_3, \dots, A_n$ . The coefficients of this polynomial are scalar invariants of these tensors and are expressible as polynomials in the traces (I.E. sums of diagonal elements) of products formed from them.

The Rivlin/Ericksen tensors are defined recursively as:

$$A_r = [A_{ij}^{(r)}] \quad \text{for } r = 1, \dots, n$$

where

$$A_{ij}^{(1)} = \frac{v_i}{x_j} + \frac{v_j}{x_i}$$

and

$$A_{ij}^{(r+1)} = \frac{\partial A_{ij}^{(r)}}{\partial t} + \sum_{l=1}^3 v_l \frac{\partial A_{ij}^{(r)}}{\partial x_l} + \sum_{m=1}^3 \left\{ A_{mi}^{(r)} \frac{\partial v_m}{\partial x_j} + A_{mj}^{(r)} \frac{\partial v_m}{\partial x_i} \right\}$$

for  $r = 2, \dots, n$ ,

where  $(x_1, x_2, x_3) = (r, \theta, z)$ ;  $(v_1, v_2, v_3) = (v_r, v_\theta, v_z)$  and the indices  $i, j, l, m$  run from 1 to 3.

Rivlin shows that in helical flow of incompressible fluids  $A_r = 0$  for all  $r$  greater than 2, and so the stress tensor may be written :

$$\begin{aligned} &= -pI + \alpha_1 A_1 + \alpha_2 A_2 + \alpha_3 A_1^2 + \alpha_4 A_2^2 + \alpha_5 (A_1 A_2 + A_2 A_1) + \\ &+ \alpha_6 (A_1^2 A_2 + A_2 A_1^2) + \alpha_7 (A_1 A_2^2 + A_2^2 A_1) + \alpha_8 (A_1^2 A_2^2 + A_2^2 A_1^2) \end{aligned}$$

Where  $\alpha_1, \alpha_2, \dots, \alpha_8$  are polynomials in the ten scalar invariant traces of the non zero products of  $\underline{\underline{A}}_1$  and  $\underline{\underline{A}}_2$  ; and  $\underline{\underline{I}}$  is the identity tensor.

Rivlin further shows that for helical flow,

$$\underline{\underline{A}}_1 = \begin{bmatrix} 0 & r \frac{dw}{dr} & \frac{dv}{dr} \\ r \frac{dw}{dr} & 0 & 0 \\ \frac{dv}{dr} & 0 & 0 \end{bmatrix}$$

$$\underline{\underline{A}}_2 = \begin{bmatrix} 2 \left\{ r^2 \left( \frac{dw}{dr} \right)^2 + \left( \frac{dv}{dr} \right)^2 \right\} & 0 & 0 \\ 0 & 0 & 0 \\ 0 & 0 & 0 \end{bmatrix}$$

Hence as indicated by Fredrickson (59), the non zero traces of products of  $\underline{\underline{A}}_1$  and  $\underline{\underline{A}}_2$  are:

$$\begin{aligned} \text{tr}(\underline{\underline{A}}_1^2) &= \alpha & \text{tr}(\underline{\underline{A}}_2) &= \alpha & \text{tr}(\underline{\underline{A}}_2^2) &= \alpha^2 \\ \text{tr}(\underline{\underline{A}}_2^3) &= \alpha^3 & \text{tr}(\underline{\underline{A}}_1^2 \underline{\underline{A}}_2) &= \frac{1}{2} \alpha^2 & \text{tr}(\underline{\underline{A}}_1^2 \underline{\underline{A}}_2^2) &= \frac{1}{2} \alpha^2 \end{aligned}$$

where  $\alpha = 2 \left\{ \left( r \frac{dw}{dr} \right)^2 + \left( \frac{dv}{dr} \right)^2 \right\}$

Thus, all the polynomials above are functions of  $\alpha$ . We notice also that  $\underline{\underline{A}}_1 = \underline{\underline{\Delta}}$  and  $\alpha = (\underline{\underline{\Delta}} : \underline{\underline{\Delta}})$ , and hence substituting the values for  $\underline{\underline{A}}_1$  and  $\underline{\underline{A}}_2$  into the above expression for  $\underline{\underline{\gamma}}$ , we see that the components of  $\underline{\underline{\gamma}}$  may be written as follows.

$$\begin{aligned} \gamma_{rr} &= -p + \lambda_1(\alpha) \\ \gamma_{\theta\theta} &= -p + \lambda_2(\alpha) \{rw'\}^2 \\ \gamma_{zz} &= -p + \lambda_2(\alpha) \{v'\}^2 \\ \gamma_{r\theta} &= \gamma_{\theta r} = \lambda_3(\alpha) rw' \end{aligned}$$

$$\tau_{rz} = \tau_{zr} = \lambda_3(\alpha) v'$$

$$\tau_{\theta z} = \tau_{z\theta} = \lambda_2(\alpha) r w' v'$$

where  $\lambda_1(\alpha)$ ,  $\lambda_2(\alpha)$  and  $\lambda_3(\alpha)$  are polynomials in  $\alpha$  and ' denotes differentiation with respect to  $r$ .

Comparing these expressions for the components of the stress tensor with those obtained earlier for shear rate dependent fluids, we see that since only the  $\tau_{r\theta}$  and  $\tau_{rz}$  stress terms are of importance for velocity profile calculations, we may consider viscoelastic fluids of the differential type as being simply shear rate dependent fluids. That is, for the purpose of velocity profile calculations, we may once again use the model (E3) with  $f(\underline{\underline{\Delta}} : \underline{\underline{\Delta}})$  being a polynomial.

Coleman and Noll (59) perform a similar analysis for the "general fluid model" (fully described by Noll(58)) in which the state of stress at a time  $t$  is determined not only by the state of motion at that time, but by the kinematic history of the fluid up to the time  $t$ . The general fluid model includes the model for fluids of the differential kind as a special case and according to Coleman and Noll is "believed to cover almost all real fluids (whenever thermal and other non mechanical effects can be disregarded) and in particular includes fluids which exhibit long range hereditary effects such as stress relaxation."

The results from this analysis are virtually identical, and the conclusions regarding the present work remain the same. That is that the model (E3)

$$\underline{\underline{\tau}} = f(\underline{\underline{\Delta}} : \underline{\underline{\Delta}}) \underline{\underline{\Delta}}$$

is sufficient for the calculation of velocity profiles for general fluids in steady state helical flow.

#### 2.2.4 Conclusion

The extreme importance of the fluid model (E3) in steady state helical flow is evident from the above discussion. Accordingly the computer model developed in this work was designed to handle any model of this type, though calculations were only performed for the models currently in use by the oil industry : that is the Bingham plastic and the power law fluid.

## 2.3 Non dimensional systems

### 2.3.1 Introduction

At this stage it is appropriate to consider the introduction of dimensionless variables to the governing equations for helical flow. Using these dimensionless variables, we may collect the various normalising constants into a small number of dimensionless groups with each representing one degree of freedom of the flow system. In this way, the number of parameters required to specify a particular flow situation is reduced from the number of physical variables to the number of independent degrees of freedom for the flow. For power law fluids and Bingham plastics this number turns out to be three.

### 2.3.2 General dimensionless system

We note that since the viscosity function  $f(\underline{\underline{A}} : \underline{\underline{A}})$  depends on the shear rate  $(\underline{\underline{A}} : \underline{\underline{A}}) = 2( (rw')^2 + (v')^2 )$  which clearly depends on both velocity components, and since the two governing ODE's are coupled by the viscosity term, we cannot use an axial velocity reference value as well as a rotational velocity reference value, but must normalise both flow components with respect to the same reference value. Since  $W_1$  is the (known) drill rotation speed, we take this as the reference and define dimensionless variables as follows

$$r^* = r/R_2$$

$$w^* = w/W_1$$

$$v^* = v/W_1 R_2$$

where  $R_2$  is the outer radius of the annulus.

It is usual to normalise body force terms against the value  $\rho g$ , but since the only body force term is the constant term  $\rho$ , this seems a pointless exercise.

The dimensionless groups involved will clearly depend on the particular fluid model being considered, but we may define a general non dimensional viscosity as

$$f^*(\alpha^*) = \frac{1}{F} f(\alpha)$$

where  $F$  has the units of  $(\text{mass})(\text{length})^{-1}(\text{time})^{-1}$

Inserting these dimensionless parameters into the governing equation system for helical flow, we obtain the dimensionless system:

$$\frac{d}{dr^*} \left\{ r^{*3} f^*(\alpha^*) w^{*'} \right\} = 0 \quad (E4)$$

$$\frac{1}{r^*} \frac{d}{dr^*} \left\{ r^* f^*(\alpha^*) v^{*'} \right\} = \frac{\rho R_2}{W_1 F}$$

Where  $\alpha^*$  is defined in the following way

$$\begin{aligned} \alpha &= 2 \left\{ (rw')^2 + (v')^2 \right\} \\ &= 2 W_1^2 \left\{ (rw^{*'})^2 + (v^{*'})^2 \right\} \\ &= W_1^2 \alpha^* \end{aligned}$$

The above system is dimensionless and applies to any fluid model. In 2.3.3 and 2.3.4, we develop a more detailed system for the particular models of power law fluids and Bingham plastics.

### 2.3.3 Dimensionless systems for particular fluid models

For power law fluids, we have

$$\begin{aligned} f(\alpha) &= m \left| \frac{1}{2} \sqrt{\alpha} \right|^{n-1} \\ &= m W_1^{n-1} \left| \frac{1}{2} \sqrt{\alpha^*} \right|^{n-1} \end{aligned}$$

and so we take

$$f^*(\alpha^*) = \left| \frac{1}{2} \sqrt{\alpha^*} \right|^{n-1}$$

$$\text{and } F = m W_1^{n-1}$$

Thus the RHS of the second equation of (E4) becomes  $\frac{\rho R_2}{m W_1^n}$ .

It is now clear that for power law fluids, there are only three degrees of freedom for the velocity profile solution. These are:

- 1) The radius ratio of the annulus  $k = R_1/R_2$

2) The fluid parameter  $n$

3) A global 'system parameter'  $\frac{\rho R_2}{m W_1^n}$  which may be

considered as a nondimensional number relating the axial driving force to the speed of rotation of the inner cylinder.

For Bingham plastics, we have

$$f(\alpha) = \mu_0 + \frac{\tau_0}{\sqrt{\frac{1}{2}\alpha}}$$

which covers all cases, provided the convention

$$f(\alpha) = \infty \Rightarrow \underline{\Delta} = 0$$

is accepted.

Now, 
$$f(\alpha) = \mu_0 \left\{ 1 + \frac{\tau_0}{W_1 \mu_0 \sqrt{\frac{1}{2}\alpha}} \right\}$$

and thus, we take

$$F = \mu_0$$

and 
$$f^*(\alpha^*) = 1 + \left\{ \frac{\tau_0}{\mu_0 W_1} \right\} \frac{1}{\sqrt{\frac{1}{2}\alpha^*}}$$

In this case the RHS of the second equation in (E4) becomes  $\frac{\rho R_2}{\mu_0 W_1}$

and again we have the three degrees of freedom :

1) The radius ratio  $k$

2) The fluid parameter  $\frac{\tau_0}{\mu_0 W_1}$

3) The global 'system parameter'  $\frac{\rho R_2}{\mu_0 W_1}$  .

In both Bingham plastics and power law fluids, then the interdependence of parameters is such that only three degrees of freedom are possible. For power law fluids these are split conveniently into geometric, fluid and system parameters. It can be seen from the definition of these parameters that for power law fluids, increasing the scale of the annulus (I.E. increasing  $R_2$ ) is equivalent to increasing the axial pressure gradient, increasing the consistency index of the fluid, or decreasing the rotation speed by a suitable amount.

Clearly there is a similar inter dependence between parameters for Bingham plastics, though the second dimensionless parameter is not purely a fluid parameter, but also depends on rotation speed.

#### 2.3.4 Derived parameters

Any dimensionless parameter (e.g. volumetric flow rate) which may be defined in terms of the above dimensionless variables will also be dependent only on these three degrees of freedom, and thus if solutions are calculated for ranges of the degrees of freedom, then they will be applicable to any particular real system simply by scaling up.

Because of this, the computer program MUDFLO was used to produce velocity profile graphs for the ranges of the degree of freedom parameters that occur in oil well drilling.

CHAPTER 3  
WORK ON DRILLING FLUID FLOW

In this chapter we discuss work relevant to the helical flow of drilling fluid that has been carried out. 3.1 is concerned with previous work whilst 3.2 covers the work of the present thesis and its relation to the previous work.

### 3.1 Previous work

Much work on subjects related to the helical flow of non-Newtonian fluids has been carried out, with most of the papers being directly concerned with obtaining a better understanding of drilling fluid flow.

Previous studies may be classified according to the solution method used and also according to the number of velocity components considered. The earlier work on the subject, and more recent work on developing velocity profiles have concentrated on one flow component only; usually the axial one. This may be thought of as an approximation to helical flow or as a particular case of helical flow when the rotational component is zero.

Solution methods may be divided into those which use the integral form of the momentum equations and those which use the differential statement of the equations. Most literature uses the integral equation formulation, but the papers which tackle the more complex flow fields generally resort to the differential formulation as does the present work.

We start in 3.1.1 and 3.1.2 by giving a description of the integral and differential formulations and the solution methods employed in each case. This is followed by the discussion of previous work.

#### 3.1.1 The integral formulation

Recall from chapter 2 that the equations of conservation of momentum may be written in terms of the shear stress tensor  $\tau$  as follows:

$$\frac{d\gamma_{re}}{dr} + \frac{2}{r} \gamma_{re} = 0 \quad (E5)$$

$$\frac{d\gamma_{rz}}{dr} + \frac{1}{r} \gamma_{rz} = \rho$$

with  $\rho$  a constant.

Rivlin(56) and others showed that integration of this system leads to the 'integral formulation' of

$$\begin{aligned} \gamma_{re} &= B/r^2 \\ \gamma_{rz} &= \frac{1}{2} \rho r + A/r \end{aligned} \quad (E6)$$

where A and B are constants of integration.

Fredrickson (60 & 64) and Coleman & Noll (59) showed that knowledge of A and B and the viscosity profile leads to knowledge of the velocity profiles through the integral equation system

$$\begin{aligned} w &= W_1 - B \int_r^{R_2} \frac{1}{r^3 f(\alpha)} dr \\ v &= - \int_r^{R_2} \frac{\frac{1}{2} \rho r^2 + A}{r f(\alpha)} dr \end{aligned}$$

which can be obtained by substituting the fluid model  $\underline{\underline{\gamma}} = f(\underline{\underline{\alpha}})$  into (E6) and integrating with respect to r.

Fredrickson(60) and Savins & Wallick(66) showed also that knowledge of A and B leads to knowledge of the viscosity profile. Fredrickson's relation between A&B and the viscosity profile was based on a trial and error calculation method ; whilst Savins and Wallick developed a more practical method based on the equation

$$\begin{aligned} f(\alpha)^2 \alpha &= 2 \left\{ \gamma_{re}^2 + \gamma_{rz}^2 \right\} \\ &= \left( \frac{1}{2} \rho / r + A/r \right)^2 + \left( B^2 / r^4 \right) \end{aligned}$$

Finally, the integral formulation solution method hinges on the calculation of A and B by trial and error method.

For one velocity component only, the procedure is much the same, though simpler since A will be zero for rotational flows and B will be zero for axial flows.

### 3.1.2 The differential formulation method

This method is based on the direct substitution of the fluid model  $\tilde{\tau} = f(\alpha)\Delta$  into the equation system (E5) resulting (after rearrangement) in the system

$$w'' + \left\{ \frac{3}{r} \frac{f'(\alpha)}{f(\alpha)} \right\} w' = 0 \quad (E7)$$

$$v'' + \left\{ \frac{1}{r} \frac{f'(\alpha)}{f(\alpha)} \right\} v' = \frac{\rho}{f(\alpha)}$$

Solution of this system is usually (see Zienkiewicz(74) and Guickes(75)) performed numerically by the following algorithm.

Firstly a discretized form of system (E7) is set up, and separately, a fluid model relating velocity estimates to an estimated viscosity distribution is constructed.

Solution proceeds as follows:

- i) An initial guess is made for the viscosity distribution.
- ii) The discretised system is solved using the viscosity distribution to give estimated velocity profiles.
- iii) The fluid model is used to construct a new estimated viscosity distribution.
- iv) Convergence of the calculation is tested.

If convergence has been achieved, then stop ; if not, return to (ii) and continue.

This algorithm is further discussed later and forms the basis of MUDFLO.

### 3.1.3 Integral solution method for one flow component only.

In this section we discuss papers which have used the integral formulation for one component only flows. Of these only one (Slawomirski (74)) considered rotational flow, and its discussion is left till last. The rest concern the axial flow of non-Newtonian fluids in an annulus which may be considered as an approximation to helical flow.

The integral solution method is essentially the same whichever fluid model is used, and first appeared in a paper by Laird(57) referring to Bingham plastic flow. Fredrickson and Bird (58) extended the method to power law fluids of index  $n=1/s$  for  $s$  integral, and presented tabular results of global flow parameters such as flow rate, radius of zero shear stress and ratio of maximum to average velocity for both Bingham plastics and power law fluids.

These tabular results have been referred to by many of the later authors, and were substantiated by experimental work discussed below. (M<sup>C</sup>Eachern (66), Tiu & Bhattach (74)).

It was considered that these results might also form a basis for testing any computer model for helical flow developed for the present thesis.

Parslay & Slibar (57) also produced a paper concerning the flow of Bingham plastics. The paper was described as dealing with helical flow, but the assumption that the angular velocity had little influence on viscosity was made, and the very complex expressions obtained for velocities and volumetric flow rates really concern axial flow only. No numerical results were presented by Parslay & Slibar.

In a paper by M<sup>C</sup>Eachern(66) the integral formulation method was used to calculate pressure drops, flow rates and radii of zero axial shear stress for Ellis<sup>†</sup> fluid models which are a generalisation of the power law fluids. Some experimental measurement of flow rates and pressure drops was carried out and the results compared with theoretical predictions made using three fluid model approximations to measured viscometric data.

The models used were:

- i) Generalised non-Newtonian fluid represented by direct interpolation of tabular viscometric data.
- ii) Ellis fluid model.
- iii) Power law fluid model.

<sup>†</sup> Note: The Ellis fluid model is not widely used, and accordingly was not defined in 2.2. We are however interested in M<sup>C</sup>Eachern's work, since it applies to power law fluids also.

The conclusions were that the generalised Newtonian and Ellis fluid models produced good results in all cases investigated, whilst the power law model produced good results only if great care was exercised in applying the model to the viscometric data. That is, with the power law model, " particular attention must be paid to the range of shear stress over which the power law parameters are evaluated."

Tiu & Bhattach (73) extend Fredrickson & Bird's work on fully developed velocity profiles for power law fluids to developing flows by introducing a boundary layer calculation.<sup>†</sup> Photographic measurement of the velocity profiles by the same authors (74) was found to support this work and " not only establish the measurement technique for velocity profiles in an annulus, but also substantiated the theoretical work of Fredrickson & Bird (58) which had never been compared with velocity profile data before."

Mishra & Mishra (76) used the integral formulation method as a basis for developing a simple approximation to Fredrickson and Bird's solution for use in boundary layer calculations. Mishra & Mishra provide a useful summary of some of the previous work, but otherwise, the paper is of little relevance to the present study.

Slawomirski (74) discusses the helical flow of drilling fluid flow quite generally, and gives a clear statement of the assumptions that must be made to approximate drilling fluid flow by a helical flow model. In order to obtain a simple analytical solution however, the author makes the further approximation that the axial velocity gradients have little effect on viscosity (C.F. opposite assumption by Parslay & Slibar above). Because of the simpler nature of the rotational governing ODE, this leads to an analytical solution of the integral formulation.

The paper serves as a useful link between the solution oriented papers discussed above and the theoretical rheology-based papers of the next section.

<sup>†</sup> Note: This work concerned axial flow only.

### 3.1.4 Integral solution method with two velocity components

As mentioned previously, work falling into the scope of this section may be neatly divided into papers that theoretically discuss rheological concepts using helical flow as an example, and those concerned with obtaining solutions. We separate our discussion accordingly and treat the theoretical papers in subsection A and the solution oriented papers in subsection B.

#### 3.1.4A Theoretical work

Much of the following discussion was presented in 2.2 and 3.1.1 but is repeated here for completeness.

The integral formulation of the governing equations was first introduced by Rivlin(56) who discussed helical flow of fluids of the differential type as a superposition of axial and rotational flows. Solution of the integral formulation was not discussed and Rivlin proceeded to derive explicit expressions for the components of the shear stress tensor in terms of the fluid parameters and the velocity profiles.

Using the same fluid model, Fredrickson(60) developed expressions for velocity profiles, volumetric flow rate and torque in terms of pressure gradient, relative rotational speed and rheological parameters. Fredrickson proposed a feasible though impractical method for the solution of these expressions by trial and error.

The work of Coleman and Noll (59), though using a slightly different approach, produced expressions similar to those of Fredrickson for the velocity profiles, flow rate and applied torque with a fluid of the general type.

A short review of these three papers is given by Fredrickson(64).

#### 3.1.4B Solution oriented papers.

The work discussed in this section was all directly concerned with the problems of drilling fluid flow, and much of it was directly supported by oil companies.

Savins and Wallick(66) developed a practical solution method for the equations of Fredrickson(60) based on the numerical evaluation of the constants of integration A and B, as defined in 3.1.1. The utility of this work was considerably reduced by its restriction to fluid models having a finite positive apparent viscosity  $f(\omega)$  for all values of  $\omega$  in the range zero to infinity.

This requirement is not met by the commonly used power law and Bingham plastic models.

Computations were carried out by Savins and Wallick for the Oldroyd 2 model which may be defined as follows

$$f(\alpha) = \lambda_0 \left[ \frac{1 + \tau_2(\alpha^2)}{1 + \tau_1(\alpha^2)} \right]$$

where  $\lambda_0$ ,  $\tau_1$ , and  $\tau_2$  are constants with  $\lambda_0$  having the units of viscosity and  $\tau_1$  &  $\tau_2$  having the units of time.

It is clear that this model satisfies the restrictions imposed by the computation method.

Numerical investigations were carried out with fluid parameter values fixed as

$$\begin{aligned}\tau_1 &= .06 \text{ seconds} \\ \tau_2 &= .02 \text{ seconds} \\ \lambda_0 &= 10.0 \text{ g(cm)}^{-1} \text{ (sec)}^{-1}\end{aligned}$$

for radius ratios of .95, .8 and .5.

Results were presented graphically, demonstrating the variation of viscosity profiles, flow rate and torque with axial pressure gradient and relative rotation speed. Velocity profile results were not presented.

Between 1970 and 1974, Walker, in conjunction with personnel directly employed by the oil industry, developed a computer program suitable for the 'in field' evaluation of drilling mud flow parameters. The computer calculation was based on a mathematical model similar to that of Savins and Wallick, and was first described in Walker(70). Walker (71,73 & 74) describe the development of this basic calculation into a sophisticated tool designed to assist those responsible for the control of drilling mud flow parameters. The outputs from this computer calculation (as described by Walker (74)) were in the form of empirical indices giving information on predicted annular velocity, annular pressure loss due to circulation and laminar/turbulent flow transition.

Walker(70) describes experimental verification of the basic model for helical flow which relies on the work of Fredrickson(60) and Coleman & Noll(58). The author states that "the method of calculation has been shown experimentally to be correct for a polymer liquid in helical flow (Ref. Rea & Showalter 67) and was used by Savins and Wallick to predict velocity profiles and pressure drops in the annulus of a drilling well assuming that the liquid followed a 3-constant Oldroyd model." Whilst the theory outlined in the paper does seem in line

with the work of Fredrickson, Coleman & Noll, and Savins & Wallick, this statement is contradictory since the calculation method used by Rea & Showalter was that described in the thesis of Dierckes(65) and was very different (see 3.1.5).

It therefore seems reasonable to suppose that, despite the applicability of Rea & Schowalter's computer program to power law fluids, the work of Walker in this paper suffers the same restrictions on fluid models as the work of Savins & Wallick and can not be applied to power law fluids.

Walker(70) appears to have used direct interpolation of viscometric data in his computer program rather than introducing a specific fluid model.

Experimental measurements of the variation of pressure drop with volumetric flow rate and rotation speed for four different bentonite solutions in a helical flow test rig were carried out by Walker and the results, when compared with predictions, were found to be within 25% in most cases. In two cases, however, differences of up to 45% were found. A comprehensive discussion of the errors and possible causes is presented, and the conclusion is drawn that:

" The method of laminar helical flow calculation proposed by Coleman & Noll and also by Fredrickson is valid for bentonite systems and is recommended for calculating annular pressure drops with rotating drill pipe."

Sufficient data is presented in this paper to allow comparisons with the MUDFLO predictions either by:

- i) Using a power law model approximation to the viscometric data given by Walker.
- or ii) Modifying MUDFLO so that it can run using interpolation of viscometric data instead of a specific fluid model.

It is recommended that this be carried out in conjunction with an experimental test program in order to obtain a more meaningful analysis of any comparisons made.

Walker(71) describes the extension of the basic mathematical model with the calculation of empirical indices to describe predicted drilling rate, hole cleaning efficiency, and possible erosion of the

hole for any given flow conditions with a given fluid. The rheological model used for the computer calculations described in this paper was "mathematically simulated by a series of power and 3-constant models",

Examples of considerable cost savings made through the use of this computer program are given in the paper.

Walker(73 & 74) describe the same work, but with Walker(73) being presented at the Society of Petroleum Engineers conference in London, April 1973, and walker(74) being published subsequently in the Journal of Petroleum Technology.

These papers describe the further development of the computer calculation, and the solution of difficulties associated with its field operation. A turbulent/laminar transition prediction index is introduced in the form of a "z-stability parameter" based on the work of Ryan & Johnstone(59) on the laminar/turbulent flow transition of non-Newtonian liquid flow in straight tubes. This z-value is a function of radius and may be defined as

$$z(r) = 0.2078 (R_2 - R_1) \frac{\gamma}{g} \frac{v(r)}{\tau_w} \frac{dv}{dr}$$

and may be approximated by

$$z(r) = \frac{\gamma}{m} (\bar{v})^{2-n} \quad \text{for power law fluids}$$

where

$\tau_w$  is the shear stress at the tube wall ( $lb_f \text{ sec} / 100ft^2$ )

and  $\bar{v}$  is the average annular velocity (ft/min).

The criterion is accepted by Walker(73) in that laminar flow is assumed if the maximum value of z(r) is less than 808. Charts of z(r) values for various flow conditions and fluid parameters are presented in both papers.

The fluid model used in this version of Walker's computer program consisted of two power law models: one to be used at low shear rates and the other at high shear rates. It thus appears that the problem of rheological restrictions on Savins & Wallick's calculation method were overcome by Walker, but no indication of how this was done is given in either of the papers.

### 3.1.5 Differential solution methods.

A basic outline of the differential formulation was given in 3.1.1, and we now discuss papers that have used the method.

Zienkiewicz(74) discusses the steady flow of non-Newtonian fluids in parallel sided conduits such as flow through parallel plates or an annular gap. The flow is considered to be in one direction (z say) with all derivatives except pressure being zero in that direction. The governing flow equation is thus the 'Poisson equation':

$$\frac{\partial}{\partial x} \left\{ \frac{\mu}{g} \frac{\partial v}{\partial x} \right\} + \frac{\partial}{\partial y} \left\{ \frac{\mu}{g} \frac{\partial v}{\partial y} \right\} + \rho g - \frac{\partial P}{\partial z} = 0$$

Transformation into polar coordinates, and constraining derivatives with respect to  $\theta$  leads to the equation for axial flow through an annulus (as a particular case).

Zienkiewicz discretizes this equation directly using the Galerkin finite element method. Application of the boundary conditions allows the resulting nonlinear algebraic system to be solved using the iterative algorithm outlined in 3.1.2.

Examples of solutions are given for flow of Bingham plastics through circular pipes, through an annulus, and between parallel plates, and for power law fluids in conduits of square cross-section.

Guickes(75) considered the case of axial flow of non-Newtonian fluids in an eccentric annulus. Solution was performed using a bipolar coordinate system to describe the annular space.

Once again, the governing equation was a nonlinear partial differential equation. The flow equation was discretised using finite difference methods, and the resulting system solved using the algorithm of 3.1.2. Results are presented for Bingham plastics and for power law fluids and show the interdependence of volumetric flow rate, pressure gradient, relative displacement of the cylinders and fluid properties. Comparison of results for the particular case of concentric annulus with the results of Fredrickson & Bird showed good agreement (within 1%) for power law fluids with index  $n \geq \frac{1}{2}$ . Computational difficulties were encountered, however, for  $n < \frac{1}{2}$ , and for Bingham plastics. Guickes attributed this to the existence of very small velocity gradients over a large section of the annular space, and suggested that the use of an unevenly spaced grid might be of some assistance in overcoming this problem.

Two papers co-authored by Schowalter (66 & 67) concerned the experimental verification of some experimental concepts using helical flow of a polymer solution. The work program involved the experimental verification of computed flow rate and, later, velocity profiles, but only covered one set of flow conditions. Schowalter & Dierckes (66) describe the experimental flow rig and the flow rate measurements whilst Schowalter & Rea (67) describe the optical technique used for measuring velocity profiles. Schowalter & Dierckes discuss integral formulations for the solution of the governing equations for helical flow but conclude that "it was found more convenient to form differential equations for the two components of velocity." This was done by substituting the power law fluid model directly into the governing equations (E7) and resulted in the following pair of equations which apply specifically to the flow of power law fluids.

$$\begin{aligned}
 w'' + \frac{w'}{nr} \left\{ \frac{(2n-1)(v')^2 + (n-2)(rw')^2}{(v')^2 + (rw')^2} \right\} \\
 - \frac{w'}{nr} \left\{ (n-1)rv' \frac{\rho}{m} \left[ (v')^2 + (rw')^2 \right]^{\frac{1}{2}(1-n)} \right\} &= 0 \\
 v'' + \frac{1}{n} \left\{ \frac{(v')^2 + (2-n)(rw')^2}{(v')^2 + (rw')^2} \right\} \frac{v'}{r} \\
 + \frac{\rho}{nm} \left\{ \frac{n(rw')^2 + (v')^2}{\left[ (v')^2 + (rw')^2 \right]^{\frac{1}{2}(n+1)}} \right\} &= 0
 \end{aligned}$$

The complexity of this analysis arises from the inclusion of the specific fluid model at this stage. In the algorithm of 3.1.2, the inclusion of the fluid model is left till the computation, with the analysis being left simpler and of more general applicability. Dierckes(65) developed a novel solution method based on the transformation of the above two 2nd order ODEs to a system of four first order ODEs. Solution of the transformed system was performed by a trial and error application of the Runge-Kutta-Gill procedure. Schowalter & Rea (67) present the computed and measured velocity profiles for the flow and conclude good agreement. The results are compared with MUDFLO calculations in chapter 4.

### 3.1.6 Summary and discussion.

In the above two methods of solving the governing equations of helical flow have been presented:

- i) The integral formulation in which the governing equations are analytically integrated and solution is effected by evaluation of the constants of integration.
- ii) The differential formulation in which a numerical procedure is directly applied to the governing equations to obtain a solution.

It is significant that the more complex cases of flow in an eccentric annulus (Guickes 75) and flow with two non zero velocity components (Zienkiewicz 74) which involve partial differential equations have been tackled using the differential formulation.

Indeed it is difficult to imagine the successful extension of the integral formulation to these and other more complex cases such as those discussed in chapter 2. On the other hand, the differential formulation with a finite element or finite difference procedure is of more general applicability and could prove readily adaptable to such cases.

Savins & Wallick (69) compare the integral and differential formulations as they apply to axial flow of power law fluids. Their integral formulation is an extension of Fredrickson & Bird's (58) to real power law index  $n$ , whilst their differential formulation was based on the equation

$$nv'' + \frac{v'}{r} + \frac{\rho}{n} (v')^2 \frac{1}{2}(1-n) = 0$$

which is obtained by substituting the power law fluid model directly into the governing equation. Solution of this equation was performed using conventional (non-iterative) finite difference methods.

Whilst Savins & Wallick conclude that the integral formulation is more accurate for this problem, the flow rates predicted by the differential formulation were within 1% of those obtained from the integral formulation. It is therefore reasonable to expect good results from the differential formulation.

It was thus decided that the present work should utilise the differential formulation to investigate the helical flow of non-Newtonian

fluids, and should consider the extension of this method to more complex cases. A further advantage gained by using this formulation is that the computer program developed in this work is applicable to any simple fluid model and the restrictions of Savins & Wallick (66) for the integral formulation are avoided.

### 3.2 Work of the present thesis.

The work undertaken for this thesis included the production of a set of dimensionless charts from which the velocity profiles of drilling fluids in helical flow may be determined.

To do this a computer program 'MUDFLO' was developed using finite difference techniques and the differential formulation described in 3.1. The program is described in 3.2.1 and 3.2.2, and is listed in the appendices. 3.2.3 gives details of the calculations performed using MUDFLO, whilst the results are presented in chapter 4.

#### 3.2.1 Basis of the computer program.

We recall from chapter 3 (E7) that the governing equations for helical flow may be written :

$$w'' + \left\{ \frac{3}{r} + \frac{f'(\alpha)}{f(\alpha)} \right\} w' = 0$$

$$v'' + \left\{ \frac{1}{r} + \frac{f'(\alpha)}{f(\alpha)} \right\} v' = \frac{\rho}{f(\alpha)}$$

where  $\underline{\tau} = f(\alpha)\underline{\Delta}$  describes a fluid of the simple type. The quantity  $f(\alpha)$  is often referred to (Zeinkiewicz 74 , Guickes 75) as the 'apparent viscosity', and its dependence on both  $v$  and  $w$  makes the above system difficult to solve. As discussed in 3.1, it was decided to attempt solution of the system using the differential formulation in which the viscosity profile is first estimated by a constant distribution. Velocity distributions are calculated for this viscosity estimate using finite difference methods, and a new viscosity profile calculated using the fluid model. The process is continued in this way until the changes in velocity between iterations is very small.

The basic structure of the calculation, and of the program, is then as shown in figure 3.1.

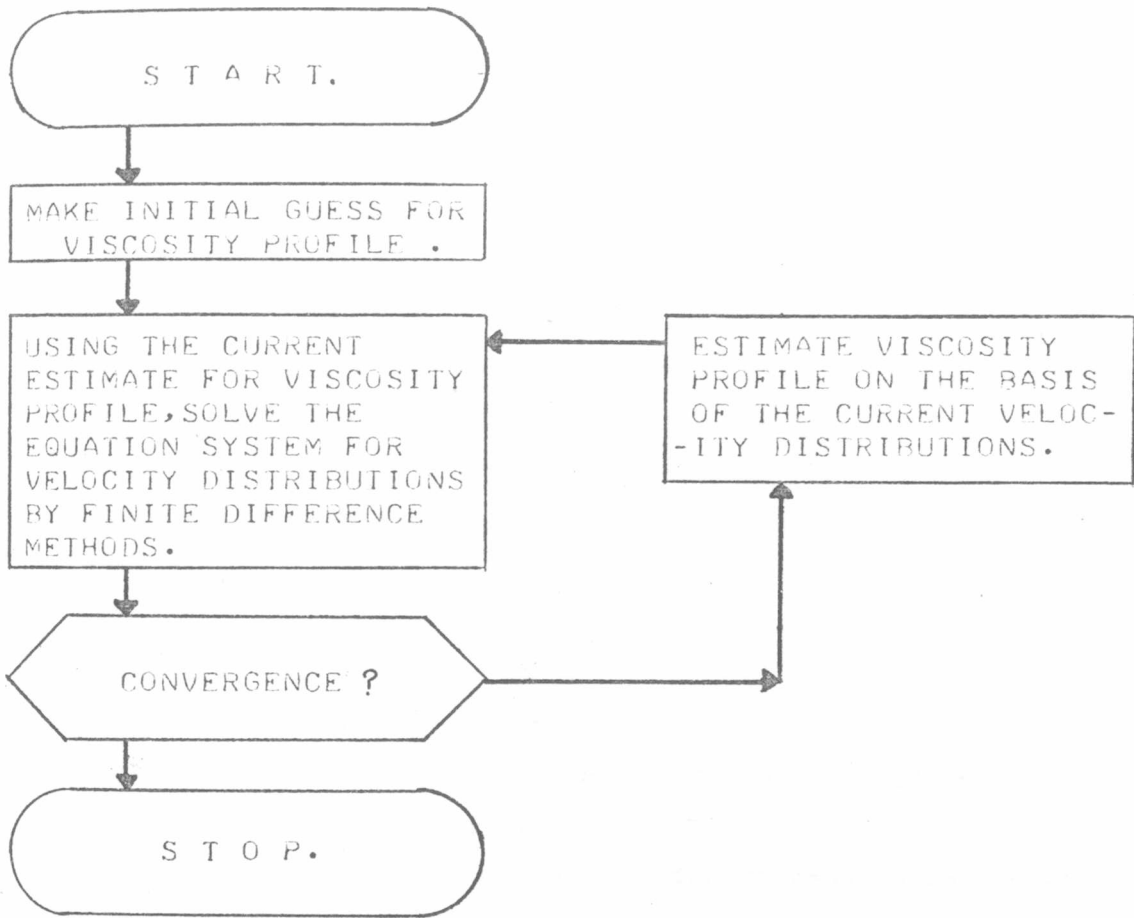


Fig. 3.1 BASIC STRUCTURE OF THE COMPUTER PROGRAM

To aid interpretation and further development of the program, the finite difference application in the algorithm was written to solve any general ordinary differential equation of the form

$$y''(r) + P(r) y'(r) + Q(r) y(r) = R(r)$$

where  $P(r)$ ,  $Q(r)$  and  $R(r)$  are continuous functions, and the boundary conditions are known. The notation used in the program was mnemonically based on that of Greenspan(71) who adequately describes the finite difference method. Greenspan(71) and Spalding(70) give central difference scheme (CDS) and upwind difference scheme (UDS) formulae for the solution of the above equation and discuss the relative merits of each scheme; the CDS being generally more accurate, but the UDS guaranteeing a solution. MUDFLO was initially written incorporating both schemes with the UDS being used when the CDS failed to provide a solution. Whilst the increased inaccuracy of the UDS was found to be negligible with Newtonian fluids where only one iteration is required, the inaccuracy was found to be cumulative with errors of up to 30% occurring in iterative solutions for non-Newtonian fluids. The UDS option was consequently disallowed in MUDFLO. Solution of the finite difference matrices was performed using the direct algorithm described by Greenspan(71).

Since experimental verification of results was outwith the scope of this research project, a criterion for assessing the computer predictions was developed. This criterion was based on the integral formulation results that

$$f(\infty) r \frac{dw}{dr} = \tau_{re} = B/r^2 \quad (E8)$$

$$f(\infty) \frac{dv}{dr} = \tau_{rz} = \frac{1}{2} \rho r + A/r$$

where A and B are constants and:

- i) the radius of zero shear stress in the rz plane is given by  $r = \sqrt{(-2/\rho)}$
- ii) the torque applied per unit length to maintain the relative rotation of the cylinders is  $2\pi B$ .

Since the MUDFLO calculation gives the velocity and viscosity distributions and their derivatives at a number of nodes across the annulus,

an estimate for the constants A and B may be calculated at each node from (E8). If the variation in estimates for either constant was greater than  $\frac{1}{2}\%$ , the results were assumed poor and were not included in the thesis. In this way some measure of the program's performance was obtained, and values of the physically important parameters A and B were included in the computer printout.

### 3.2.2 Description of the MUDFLO program

The MUDFLO computer program is fully self documenting and was written using FORTRAN in a 'structured' style, with the various functions of the program being performed by independent program 'modules'. In this way, generality and flexibility of the program were maximised and testing and development made more simple. Three numerical procedures : 'MOVSET' (to set up finite difference matrices), 'SOLVSR' (to solve matrices) and 'DIFF' (differentiator) were used in the program. They were developed independently as subroutines and can be replaced without program editing. References to the theory used for the numerical procedures are included in the program listing given in the appendices. The block structures of the whole program and of its modules were kept identical to those of the respective algorithms used, and all the variable names were mnemonically based either on physical meaning or on the notation of a reference text. Full details of the program may be obtained by referring to the listing in the appendix. Copies of the program and operating instructions have been archived on magnetic tape by the RGIT Computer Services Unit and can be accessed using the archive numbers quoted in the appendix. A list of variable names is also included in the appendix.

The inner and outer radius, speed of rotation of the inner cylinder, axial applied body force ( $\rho$ ) and fluid model and parameters form the data input to the calculation; whilst the output includes flow rate average annular velocity, torque and drag lift per unit length on the cylinders and the radius of zero  $r_z$  shear stress, as well as values of the radius, shear rate, viscosity, velocities and velocity derivatives at various points across the annulus.

Graphical presentation of velocity and viscosity distributions was possible using a semi-automatic sequence of data handling programs, including a CALCOMP digital plotter control package written by W M<sup>c</sup>Ombie of RGIT.

### 3.2.3 Calculations performed using MUDFLO

As an initial check on the performance of the program, some finite difference calculations were performed for Newtonian fluids and the results compared with the exact solution described by Langlois (64). Results were found to be in excellent agreement, with CDS predictions being within .05% of the exact solution.

The only experimentally measured velocity profiles for helical flow of non-Newtonian fluids available are those presented by Rea and Schowalter (67) for power law fluids. A detailed comparison of MUDFLO predictions with this experimental data is presented in chapter 4, and excellent agreement is again concluded.

It was desired to produce dimensionless velocity profile charts for both Bingham plastic and power law fluid models, but difficulty was encountered in computations for Bingham plastics. Similar difficulty was encountered with axial flow of all but very nearly Newtonian fluids (e.g. power law with  $n \gg .8$ ). It is thought that these difficulties arose from the very low velocity derivatives occurring over most of the annular gap in these flows and are related to those reported by Guickes(75).

Calculations were performed for power law fluids in helical flow with parameters varying over the ranges encountered in oil well drilling. The variables and velocity profile charts involved were reduced to a reasonable number by using the non dimensional formulation of chapter 2 with the three parameters  $n$ ,  $k$ , and  $\frac{\rho R_2}{m W_1^n}$  covering all possible independent variations of the physical values. The required ranges of  $n$  and  $k$  are available from chapter 1, but it is more difficult to estimate the range of the third parameter. For any value of  $k$ , however, a recommended average velocity is available (chapter 1), and thus knowing the range of drill string rotation speeds, a range of non dimensional average annular velocity may be calculated.

Calculations using MUDFLO were therefore performed in the following way:

- i) Choose  $n$  and  $k$ .
- ii) Calculate the appropriate range of non dimensional average annular velocity.
- iii) Run MUDFLO with various values of  $\frac{\rho R_2}{m W_1^n}$  till the range of non dimensional average annular velocity has been covered by the values obtained as output from the calculation.

In this way, a full picture of the velocity profiles and their dependence on the various parameters was built up. The results are presented and discussed in chapter 4.

Calculations for all the practically occurring cases converged, however a few results were rejected on the basis of the result assessment criterion described earlier in this chapter. Those rejected were once again cases where very low velocity gradients occurred over large sections of the annulus.

#### 3.2.4 Conclusion

The conclusion is drawn that application of the present algorithm is limited to cases with significant velocity gradients over most of the annular gap. Investigation of the exact nature of this limitation and possible methods of overcoming it are left as a matter for further research to be carried out after experimental verification of existing results and of the suitability of the result assessment criterion.

## CHAPTER 4

### RESULTS

#### 4.1 Comparison with existing experimental data.

Rea(67) studied the flow behaviour of a power law fluid in an annulus with a rotating outer cylinder. A flow visualisation technique was used to measure velocity profiles in the helical flow. Only one set of flow conditions was studied and these are listed in table 4.1. Rea presented results in the form of two graphs: one of the modulus of velocity and one of the flow angle, at various radial positions across the annulus. Data was extracted from enlarged copies (about 2½ times) of these graphs and compared with results obtained using MUDFLO. The data extracted from Rea's paper is listed in table 4.2 along with a linear interpolation of the MUDFLO calculation, and the results are presented graphically in figs 4.1 and 4.2. Inspection of the table and graphs shows that good agreement exists between the MUDFLO prediction and the experimental results.

Taking the interpolated MUDFLO results to be a statistical expectation and estimating the variance of the experimental results from this expectation, we obtain values of 1.4 (cm/sec)<sup>2</sup> and 1.1 (degrees)<sup>2</sup> for the variances of the velocity magnitude and flow angle respectively. This compares well with the values of 1.4 and 1.5 respectively quoted by Rea for his computational procedure.

The conclusion may therefore be drawn that the MUDFLO finite difference approach produces a good theoretical prediction for Rea's experimental measurements.

Volumetric flow rates obtained by integrating velocity profiles also show good agreement between MUDFLO predictions and experimental measurement as may be seen from the table below.

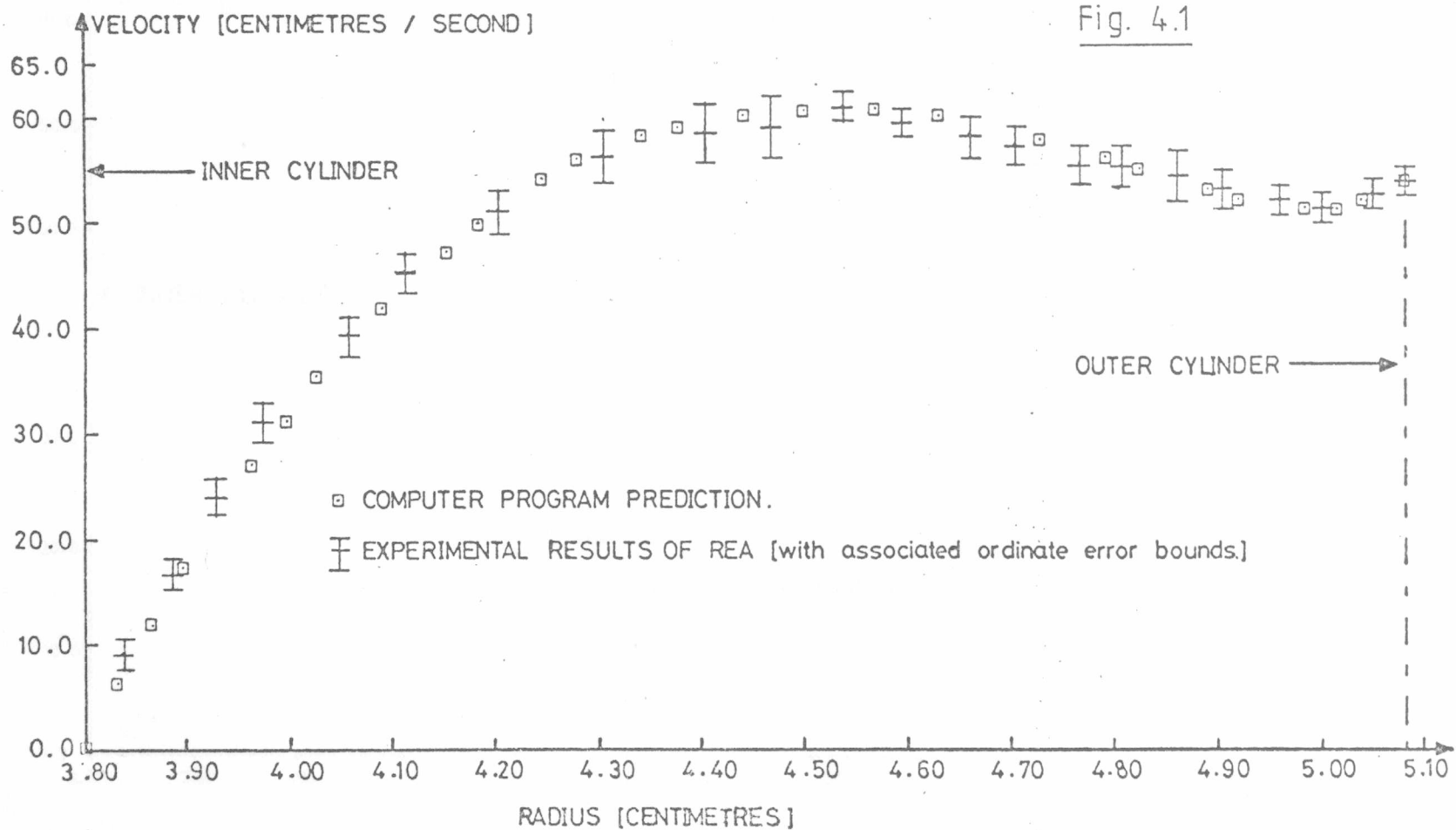
VELOCITY PROFILE	FLOW RATE (GALS/MIN)	INTEGRATION METHOD.
MUDFLO prediction.	20.261	Trapezoid rule.
Rea's experimental data.	20.38 21.18	Graphical method. Least squares rule.

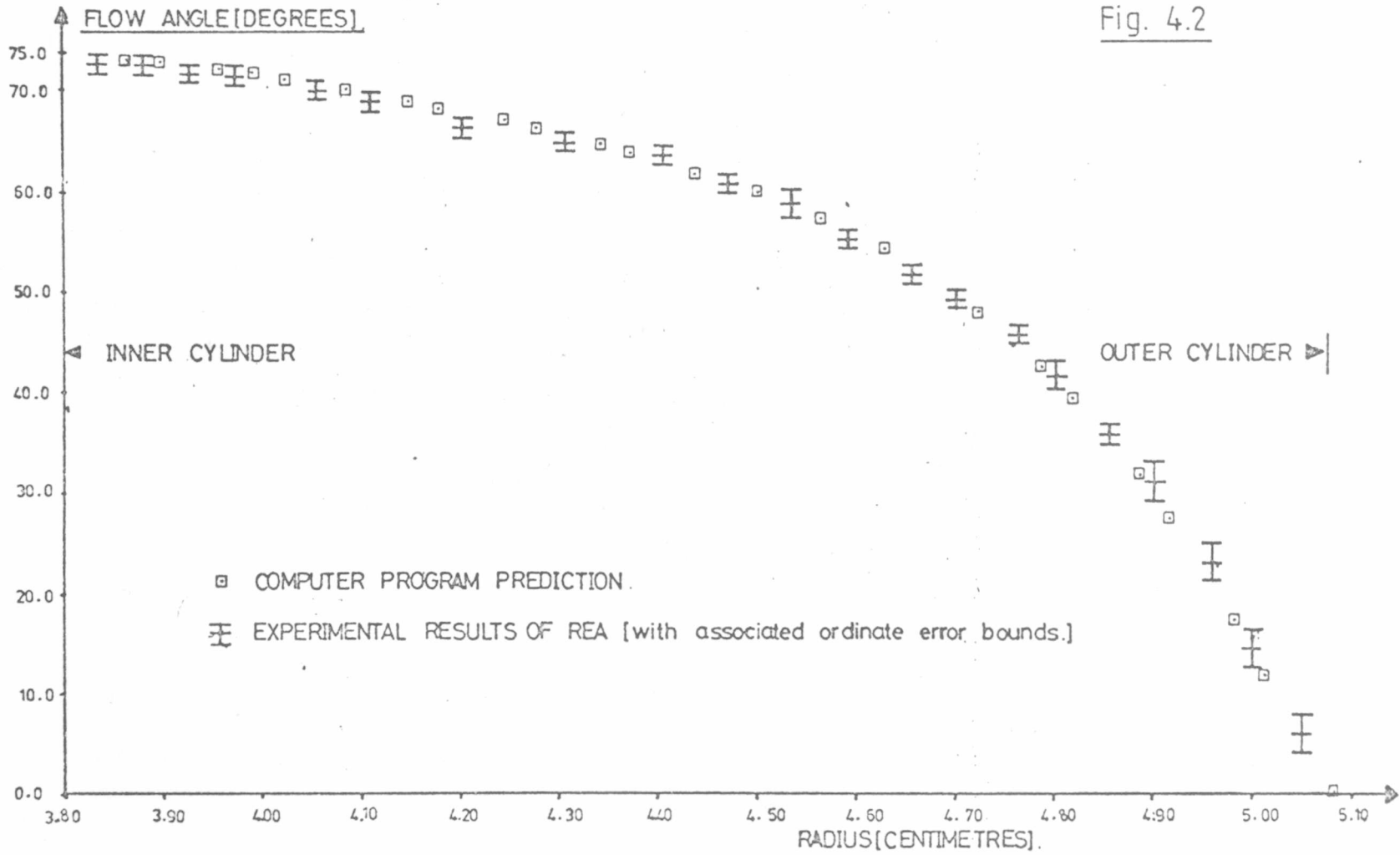
APPARATUS	<p>Inner radius = <math>2.992 \pm .001</math> (inches)</p> <p>Outer radius = <math>4.000 \pm .001</math> (inches)</p>
BOUNDARY VALUES	<p>Outer cylinder rotation speed = <math>100 \pm 1</math> (rpm)</p> <p>Axial pressure drop = <math>787 \pm 6</math> (dyne/cm<sup>2</sup>/cm)</p>
FLUID	<p>Power law fluid with:</p> <p><math>m = 6.93 \pm .08</math> (dyne-sec<sup>0.825</sup> /cm<sup>2</sup>)</p> <p><math>n = 0.825 \pm 0.023</math></p>

TABLE 4.1 Flow conditions used by Rea(67)

NODE NUMBER	RADIAL POSITION (cm)	EXPERIMENTALLY MEASURED		MUDFLO PREDICTION	
		FLOW ANGLE (degrees)	VELOCITY (cm/sec)	FLOW ANGLE (degrees)	VELOCITY (cm/sec)
1	3.800	73.70	3.00	73.70	0
2	3.838	72.81	9.16	73.20	7.31
3	3.881	72.71	16.81	73.03	14.93
4	3.927	71.71	24.11	72.41	22.51
5	3.973	71.21	31.32	71.78	28.98
6	4.055	70.24	39.58	70.50	39.13
7	4.112	68.97	45.44	69.53	44.69
8	4.202	66.04	51.34	67.79	51.67
9	4.306	64.84	56.37	65.46	57.04
10	4.404	62.87	58.78	62.88	60.41
11	4.469	60.74	59.24	60.87	60.71
12	4.538	57.97	60.11	58.30	61.01
13	4.594	54.88	59.63	55.78	60.61
14	4.658	52.59	58.34	52.31	59.12
15	4.708	48.81	57.33	49.02	58.54
16	4.765	45.24	55.42	44.54	57.23
17	4.806	41.69	55.42	40.71	55.69
18	4.859	36.85	54.46	34.98	54.02
19	4.907	30.63	53.23	28.83	52.81
20	4.959	23.49	52.21	21.18	51.84
21	5.009	14.54	51.50	16.02	51.65
22	5.050	6.57	52.70	5.89	52.20
23	5.080	0	53.61	0	52.83

TABLE 4.2 Comparison of Rea's experimental results with MUDFLO prediction.





## 4.2 Predicted velocity profiles for power law fluids in helical flow.

In 4.2 we give graphical presentations of the results obtained by MUDFLO for the ranges of parameters normally encountered in oil well drilling with power law fluids. In order to reduce the number of graphs involved, we use the dimensionless formulation of 2.3.3 with the calculation procedure described in 3.2.3. In 3.2.3, it was shown that the three independent parameters

- n (fluid index)
- k (radius ratio of annulus)

and  $\frac{\rho R_2}{mW_1^n}$  (dimensionless axial pressure gradient, denoted  $\rho$  in this section)

are sufficient to specify any particular flow conditions.

In oil well drilling, n varies from .3 to 1.0 and is usually close to 0.7, whilst k varies from .2 to .7 and is usually close to .5 (Chapter 1). Velocity profiles for flow conditions covering these parameter ranges are presented in this section as follows:

4.2.1 concerns the most common radius ratio of  $k = .5$ , for various values of n and  $\rho$ .

4.2.2 concerns the commonly occurring fluid index values of  $n = .5$  and  $.7$  with k and  $\rho$  varying.

4.2.3 covers the remaining cases of  $k = .3$  and  $.7$  with n and  $\rho$  variable.

An index to the graphs presented in these sections is provided in tables 4.3, 4.4 and 4.5.

#### 4.2.1 Radius ratio $k = .5$ .

This section deals with the results for the commonly occurring radius ratio of  $k = .5$ . Values of  $n = 1.0, .9, .8, .7, .6, .5$ , and  $.4$  are considered with values of  $\beta$  being chosen to cover the required range of dimensionless average annular velocity. Three discussions are included in this section covering angular velocity profiles, axial velocity profiles and average annular velocities in turn.

##### (i) Discussion of the angular velocity curves.

To aid interpretation of these graphs, the curve for  $\beta = 0$  has been included on each graph. This curve represents the angular velocity when axial flow has no effect on viscosity and is the curve obtained when the approximation of Slawomirski(76) (that viscosity is dependent only on angular velocity gradient) is made.

As the fluid index  $n$  decreases the angular velocity graphs (see table 4.3 and figs. 4.3 R to 4.7 R) show increasing gradient near the inner wall, and increasing influence of  $\beta$  on the shape of the curves. The curves on each graph are all quite close, and indeed are all close to the  $\beta = 0$  approximation curve particularly when  $n$  is high.

The angular velocity graphs show a curious grouping with an upper and lower family of curves being formed near the drill string, a mixed region in the middle, and then different upper and lower families near the casing. Since these effects are particularly evident on fig. 4.8 R ( $n = .5, k = .5$ ), this case was studied further.

On examining 4.8 R it can be seen that the  $\beta = -6, -9$  and  $-12$  curves are grouped together near the casing whilst the  $\beta = 0, -3$  and  $-6$  curves are grouped together near the drill string. It is also interesting to note that the  $\beta = -6, -9$  and  $-12$  curves are convex near the casing and thus have a point of inflection.

For ease of discussion, we divide the radial domain into three sections which we refer to as:

- i) The 'LHS', where the upper and lower families are formed near the drill string.
- ii) The 'RHS', where upper and lower families are formed near the casing.
- iii) The 'MIDDLE', where the curves cross.

Now viscosity is dependent on the non dimensional shear rate

$$\left\{ r^* \frac{dw^*}{dr^*} \right\}^2 + \left\{ \frac{dv^*}{dr^*} \right\}^2$$

and increases as shear rate decreases for power law fluids with index less than one. Conversely it is clear that velocity gradients will be low in regions of high viscosity.

We consider the effect on velocity gradients and on viscosity of introducing axial flow to a rotational-only flow. (i.e. of increasing  $\dot{\mathcal{P}}$  from 0 ). In rotational flow, velocity gradients are high at the LHS and low at the RHS, whilst axial flow has high velocity gradients at both the LHS and RHS, but very low velocity gradients in the MIDDLE. Thus, on introducing an axial flow component to a rotating flow, we would expect to see viscosity decreases first on the RHS, and then on the LHS. Consequently, we expect increased angular velocity gradients on the RHS, and then on the LHS. Finally, since the velocity profile must remain continuous across the annular gap, we expect a corresponding decrease in the angular velocity gradients near the MIDDLE.

Examination of fig. 4.8 R reflects the above discussion in that increased angular velocity gradients are apparent at the RHS of the  $\dot{\mathcal{P}} = -6, -9$  and  $-12$  curves, and at the LHS of only the  $\dot{\mathcal{P}} = -9$  and  $-12$  curves. Further information may be obtained from the 'characteristic function' :

$$\left\{ r^* \frac{dw^*}{dr^*} \right\}^2 - \left\{ \frac{dv^*}{dr^*} \right\}^2$$

The characteristic function reflects the relative dependence of viscosity on each of the flow components throughout the annular gap, being positive when the axial velocity gradients are dominant and negative when the angular velocity gradients are dominant. From the characteristic curves in fig. 4.8 (iii) it may be seen that the 'dominant' flow components are as follows:

$\rho$	LHS	MIDDLE	RHS
-3	angular	---	angular
-6	angular	---	axial
-9	axial	---	axial

Dominant velocity components on fig 4.8 (iii).

The viscosity curves on fig. 4.8 (ii) show a similar pattern, but illustrate clearly that increasing axial flow has most influence on the LHS where the contribution to shear rate from the angular component is lowest. The viscosity profiles in fig. 4.8 (ii) may be summarised as follows

$\rho$	LHS	MIDDLE	RHS
-3	low	medium	high
-6	low	medium	low
-9	low	high	low

Summary of viscosity profiles in fig. 4.8 (ii).

(ii) Discussion of the axial velocity curves.

As  $n$  decreases, the axial velocity profiles (figs. 4.3 A to 4.9 A) all become flatter in the MIDDLE and more skewed towards the LHS.

Since the governing differential equation system was made non dimensional by reference to the angular velocity of the drill string (see 2.3.3) it is difficult to see quantitatively the effect of varying

$\rho$  on the shape of the velocity profiles. Accordingly, for the particular case of ( $n = .5$  ;  $k = .5$ ) a graph of 'reduced velocity' versus radius  $r^*$  was produced (fig 4.8(i)) by dividing each velocity profile by the appropriate average annular velocity. Denoting the non dimensional average annular velocity as  $\bar{v}^*$ , the reduced velocity is thus

$$v^* / \bar{v}^* .$$

From this graph it may be seen that as  $\dot{\rho}$  decreases, the reduced velocity curves become less skewed towards the LHS and their peaks become flatter and lower. To explain this, we consider a helical flow in which the axial flow rate is gradually decreased. This is equivalent to reducing  $|\dot{\rho}|$ , and will result in reduced shear rate at both the LHS and RHS. The reduction in shear rate will, however, be more noticeable at the RHS since there is little contribution to shear rate from the angular component in this region. Consequently, the viscosity at the RHS will become increased, and the the point of maximum axial velocity will move towards the LHS. The resulting viscosity profile will be asymmetric, and thus the sharpness of the velocity profile may be expected to increase. These effects may be clearly seen on fig 4.8(i), with the  $\dot{\rho} = -9$  and  $-12$  curves having broad flat peaks near the centre, and the  $\dot{\rho} = -3$  curve being skewed towards the LHS and having a sharper peak. Further support for this discussion may again be obtained by studying the viscosity profiles and characteristic functions on figs. 4.8(ii) and (iii). As  $|\dot{\rho}|$  decreases, the viscosity profiles do indeed increase considerably near the RHS and a slight increase is also apparent at the LHS. The decrease in viscosity in the MIDDLE as  $\dot{\rho}$  decreases is not explained by the simple discussion above, but is due to the interaction of both velocity components.

(iii) Discussion of the average annular velocities.

A graph of the average annular velocities obtained for all the cases considered in this section is given in fig 4.10. It is immediately clear from this graph, that as expected, the average velocity ( $\bar{v}$ ) increases as  $\dot{\rho}$  increases. It is also clear that the rate of increase becomes greater as  $n$  decreases from 1.0.

The Newtonian fluid ( $n = 1.0$ ) curve is a straight line (through the origin) of slope  $-.021$ . Hence  $\bar{v}$  varies linearly with  $\dot{\rho}$  for Newtonian fluids.

It can be shown from the results on this graph that the axial flow rate is unaffected by the speed of rotation of the inner cylinder. This is in accordance with the independence of the governing equations for helical flow of Newtonian fluids.

Comparing the other curves with the  $n = 1.0$  line, it can be seen that the average annular velocity increases non uniformly with  $\dot{\rho}$  for  $n$  less than 1.0 .

It is also clear that the average annular velocity is affected by  $W_1$  though it is not immediately obvious whether increasing  $W_1$  causes an increase or a decrease in  $\bar{v}$ . The situation may be clarified by the following example.

Consider the results for  $n = .7$ . From fig. 4.10,

$$\text{for } \rho = -10 \quad \bar{v}^* = .291$$

$$\text{and for } \rho = -5 \quad \bar{v}^* = .123.$$

Suppose that  $\rho$ ,  $m$  and  $R_2$  are fixed and that for  $\rho = -10$ , the inner cylinder rotates at a speed  $W$ .

Changing  $\rho$  from  $-10$  to  $-5$  is equivalent to increasing the speed of rotation from  $W$  to  $2^{1/n}W$ . I.E. to  $2.692 W$ .

Hence

$$\bar{v} \text{ (for } \rho = -10, W_1 = W) = .291 R_1 W$$

and

$$\begin{aligned} \bar{v} \text{ (for } \rho = -5, W_1 = 2.692 W) &= .123 \times 2.692 R_1 W. \\ &= .331 R_1 W. \end{aligned}$$

Thus the average annular velocity has been increased by increasing the speed of rotation of the drill string, as expected.

This result applies in general when  $n$  is less than 1.0.

Note.

In the above discussions, variations in  $\rho$  have been considered, for the most part, to arise through changes in  $\rho$ . Similar discussions could be built up by considering changes in  $\rho$  to be produced by changes in  $W_1$  or in both  $W_1$  and  $\rho$ . The results of such discussions would be virtually identical, but would be made more complex by the dependence of many non dimensional quantities ( e.g. viscosity and characteristic function) on the angular velocity  $W_1$  of the drill string.

FIGURE	VERTICAL AXIS QUANTITY	n	k	$\beta$
4.3 A 4.3 R	axial velocity angular velocity	1.0	.5	-25,-20,-15, -10,-5.
4.4 A 4.4 R	axial velocity angular velocity	.9	.5	-25,-20,-15, -10,-5.
4.5 A 4.5 R	axial velocity angular velocity	.8	.5	-20,-15,-9, -6,-3.
4.6 A 4.6 R	axial velocity angular velocity	.7	.5	-20,-15,-10, -5,-2.5
4.7 A 4.7 R	axial velocity angular velocity	.6	.5	-15,-10,-5,-2.5
4.8 A 4.8 R 4.8(i)	axial velocity angular velocity axial velocity ratio	.5	.5	-12,-9,-6,-3.
4.8(ii) 4.8(iii)	viscosity characteristic curve	.5	.5	-9,-6,-3.
4.9 A 4.9 R	axial velocity angular velocity	.4	.5	-7,-6,-3.
4.10	Average annular velocity versus $\beta$ for the values of (n,k, $\beta$ ) above.			

TABLE 4.3 List of figures for 4.2.1.

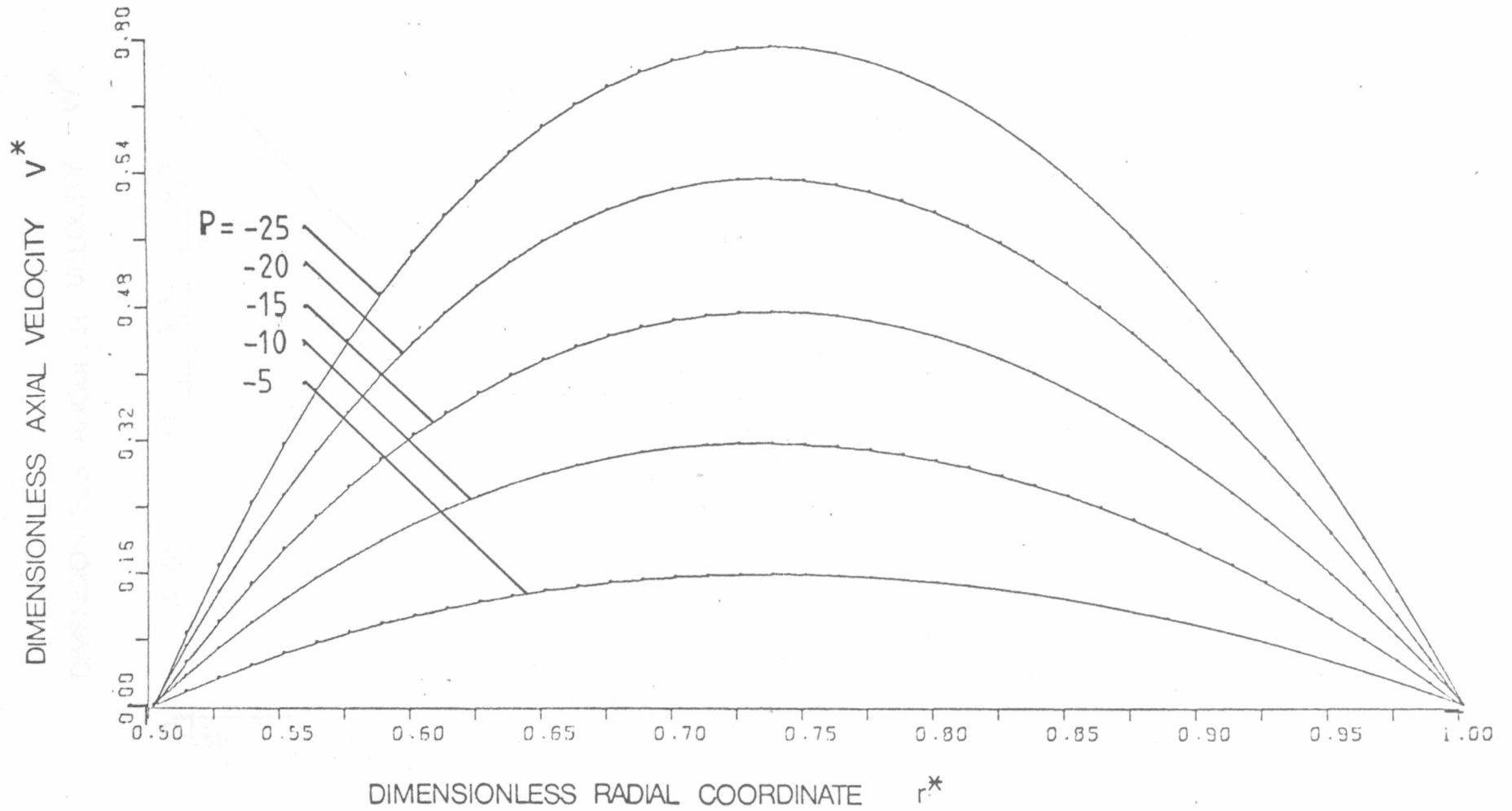
# HELICAL FLOW OF A POWER LAW FLUID

Fig. 4.3 A

$n = 1.0$

$k = 0.5$

55

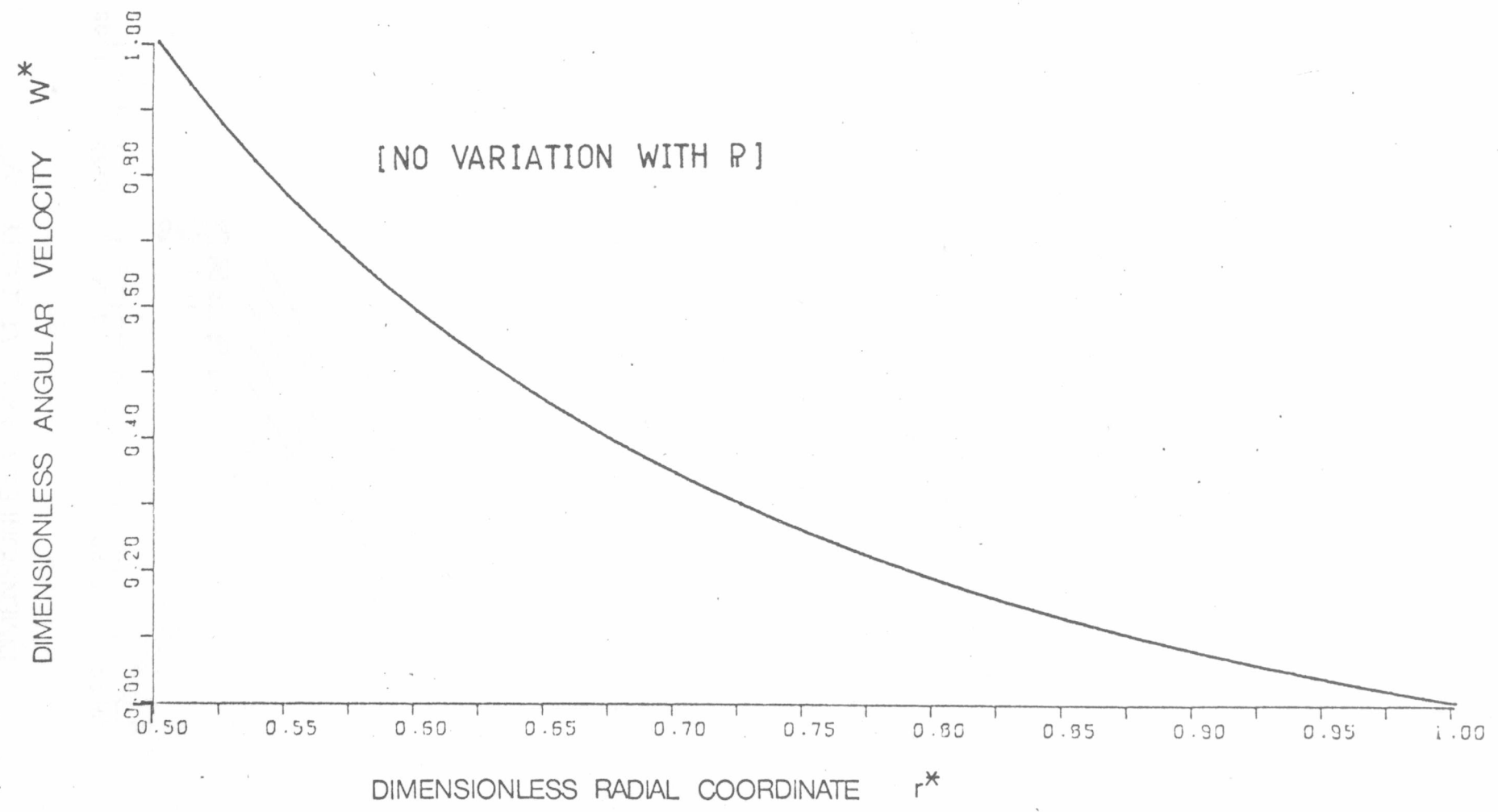


HELICAL FLOW OF A POWER LAW FLUID

Fig. 4.3 R

$n = 1.0$

$k = 0.5$

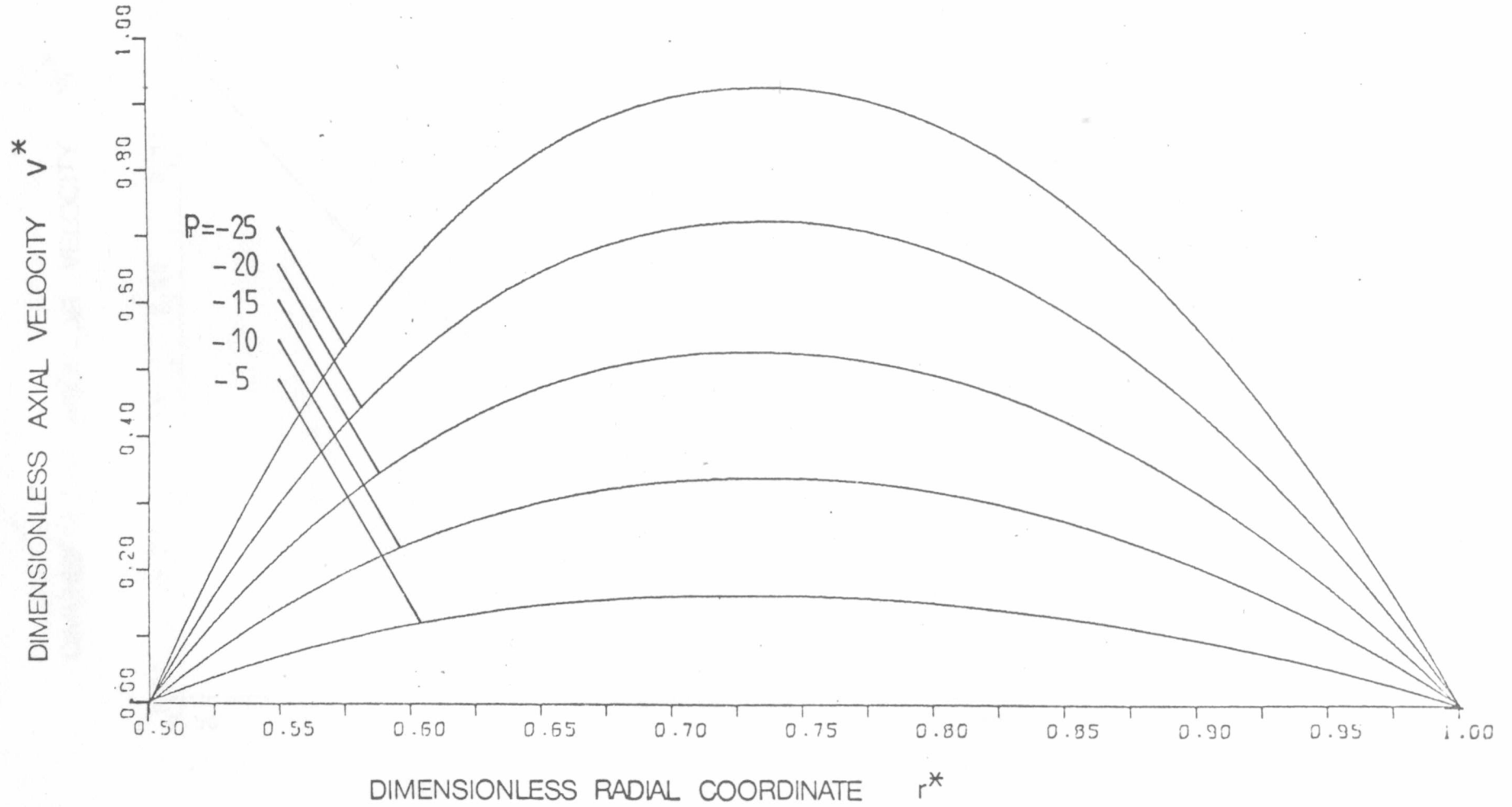


HELICAL FLOW OF A POWER LAW FLUID

Fig. 4.4 A

$n = 0.9$

$k = 0.5$



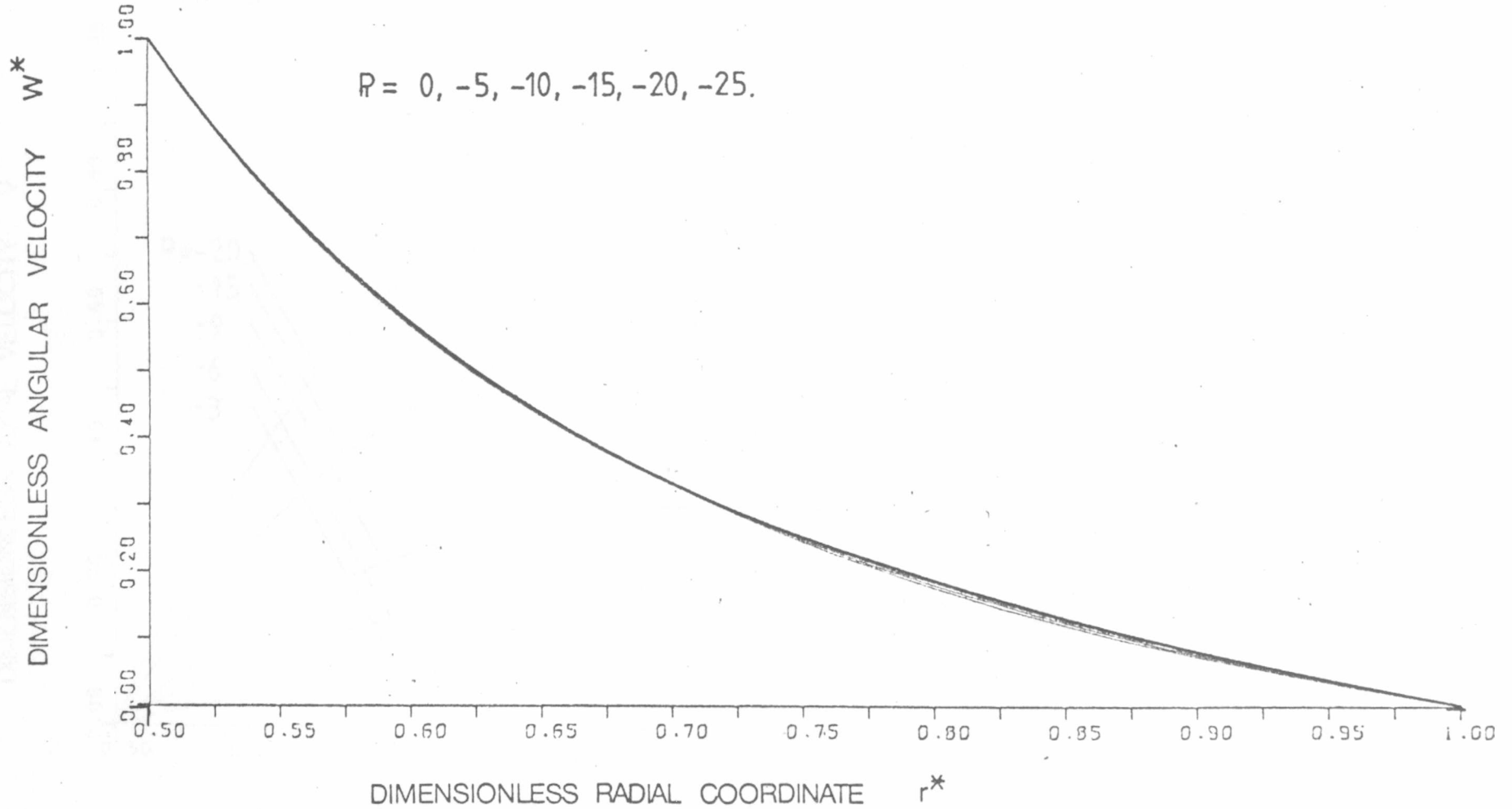
HELICAL FLOW OF A POWER LAW FLUID

Fig. 4.4 R

$n = 0.9$

$k = 0.5$

$R = 0, -5, -10, -15, -20, -25.$

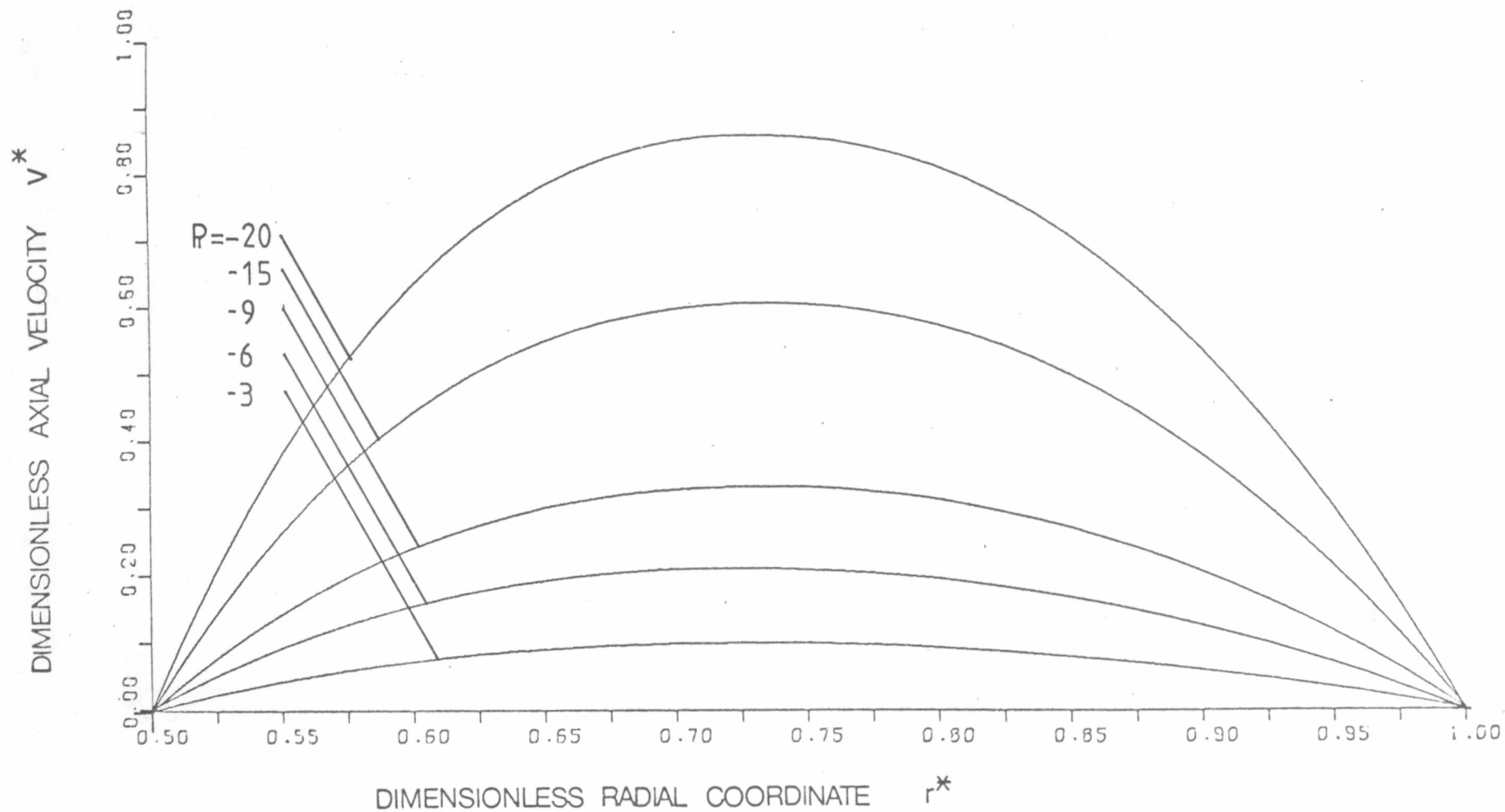


HELICAL FLOW OF A POWER LAW FLUID

Fig. 4.5 A

$n = 0.8$

$k = 0.5$

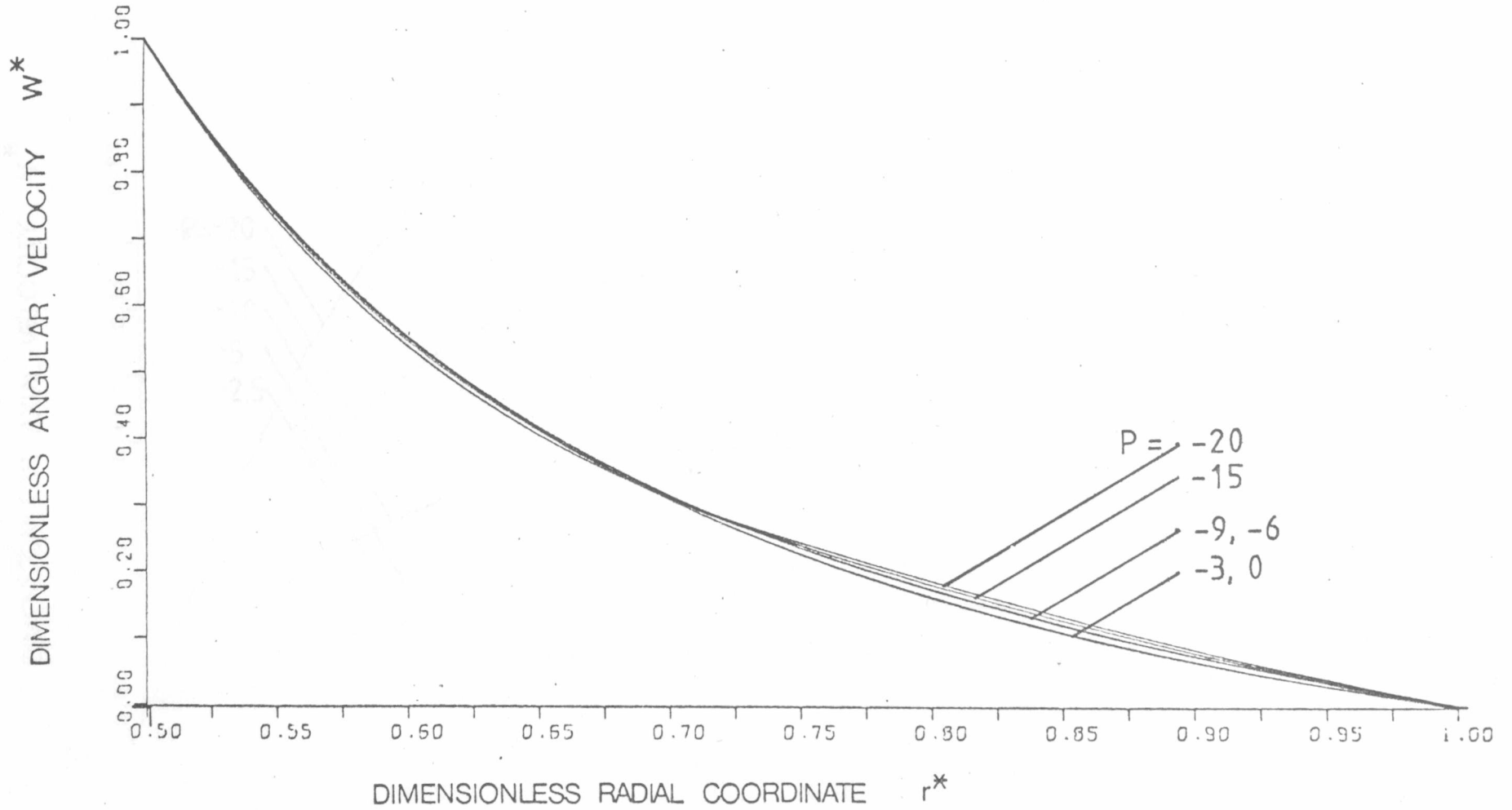


HELICAL FLOW OF A POWER LAW FLUID

Fig. 4.5 R

$n = 0.8$

$k = 0.5$

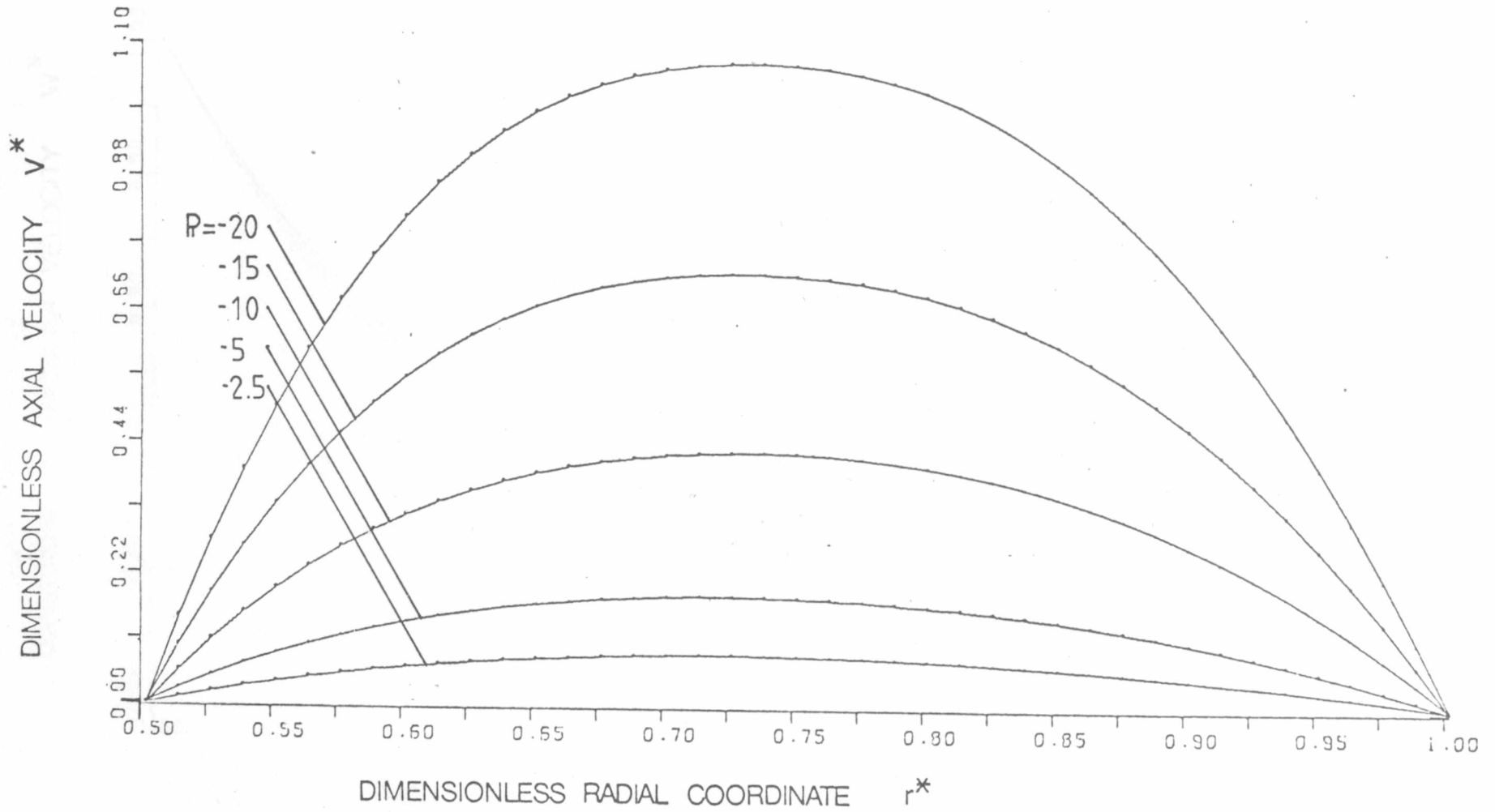


HELICAL FLOW OF A POWER LAW FLUID

Fig. 4.6 A

$n = 0.7$

$k = 0.5$

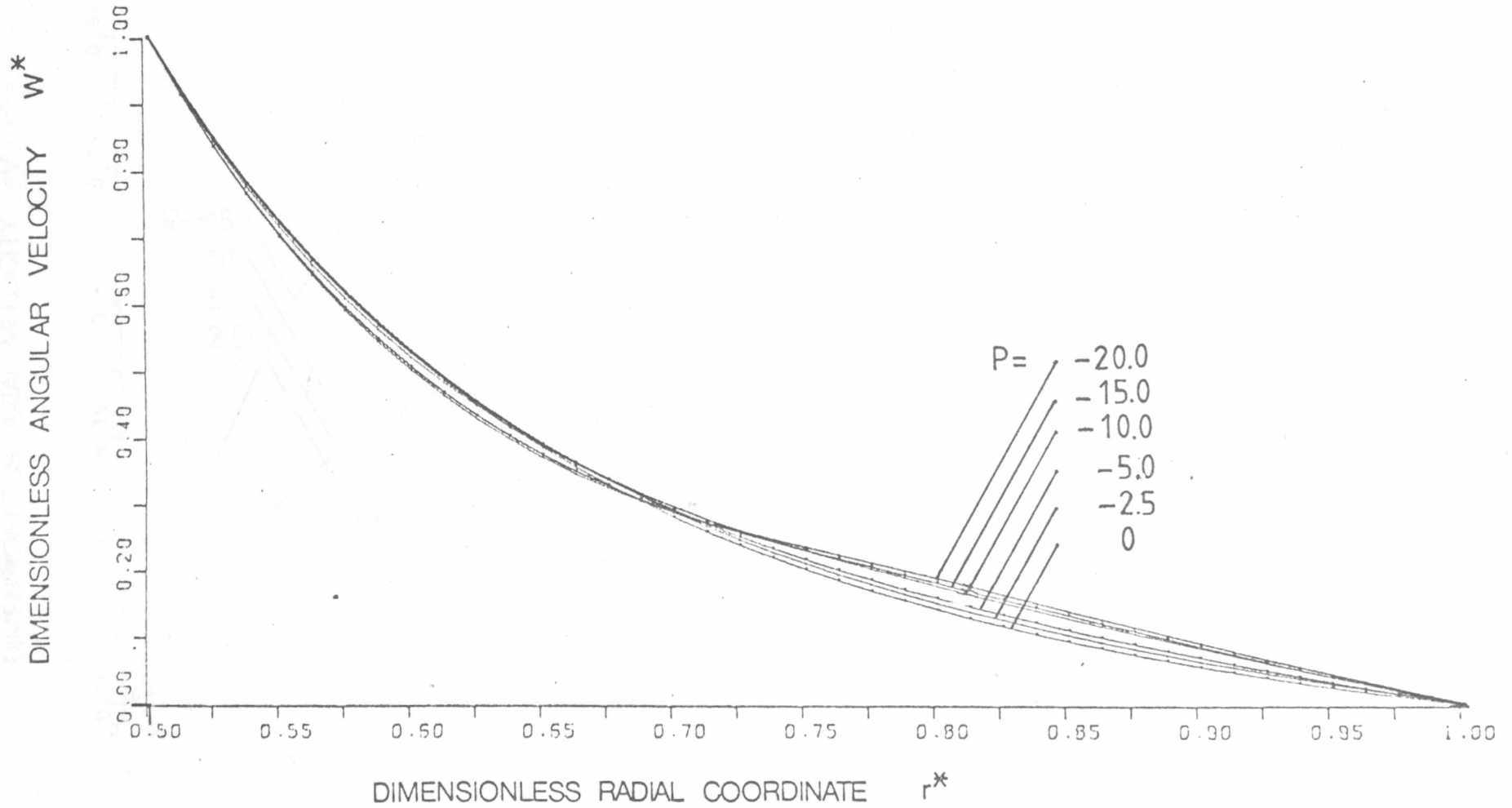


HELICAL FLOW OF A POWER LAW FLUID

Fig. 4.6 R

$n = 0.7$

$k = 0.5$

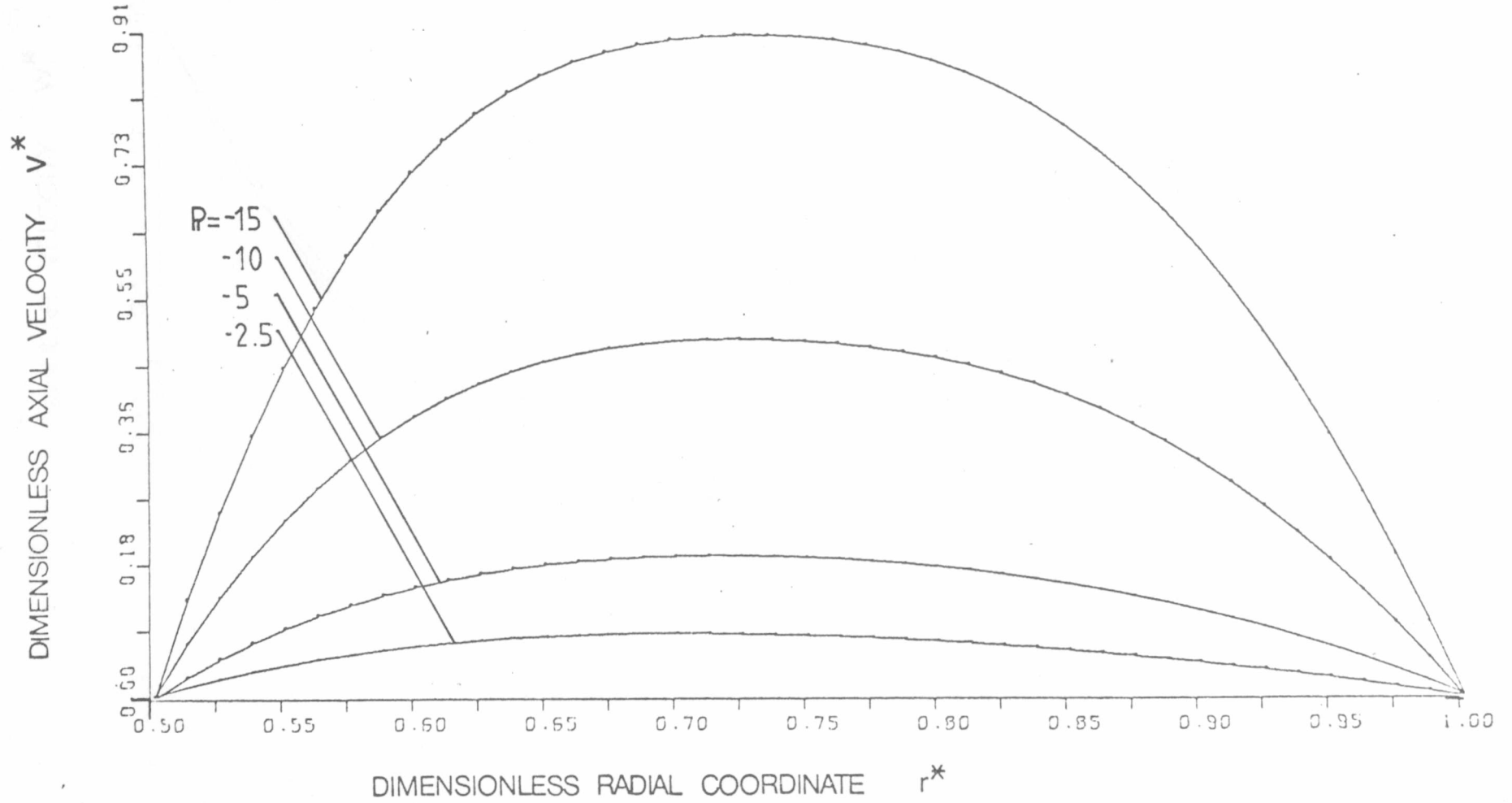


HELICAL FLOW OF A POWER LAW FLUID

Fig. 47 A

$n = 0.6$

$k = 0.5$



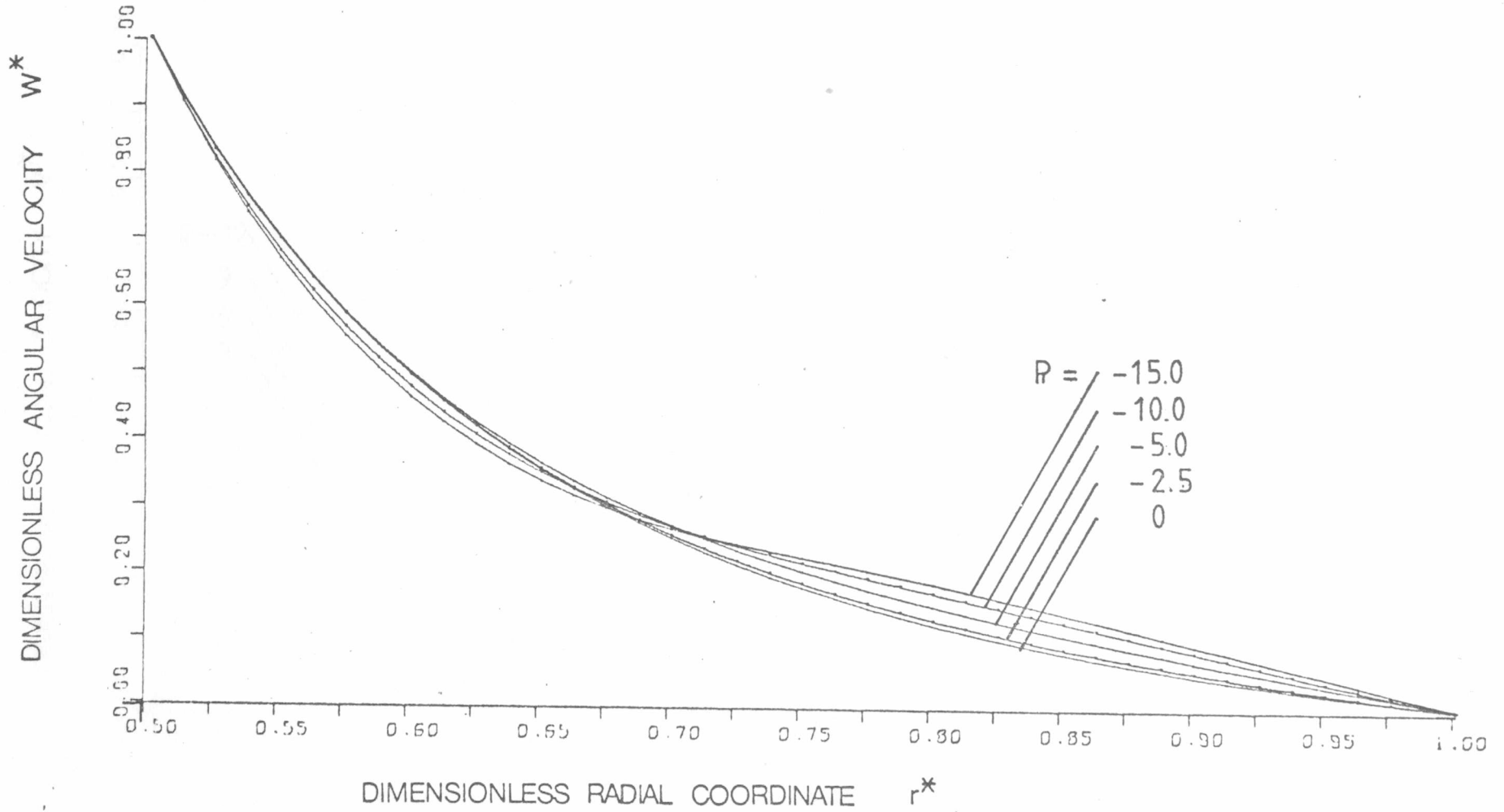
HELICAL FLOW OF A POWER LAW FLUID

Fig. 4.7 R

$n = 0.6$

$k = 0.5$

49

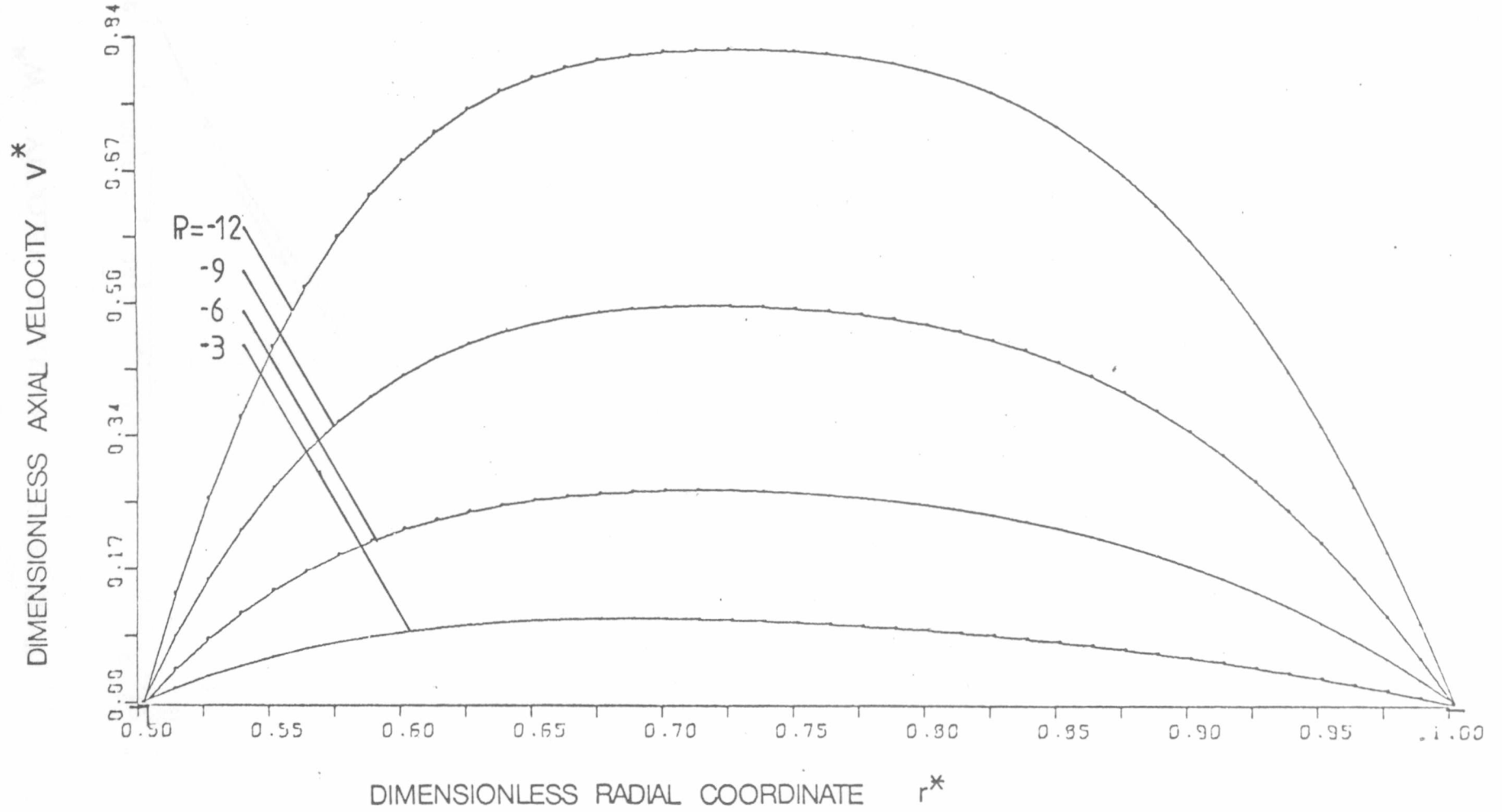


HELICAL FLOW OF A POWER LAW FLUID

Fig. 4.8 A

$n = 0.5$

$k = 0.5$

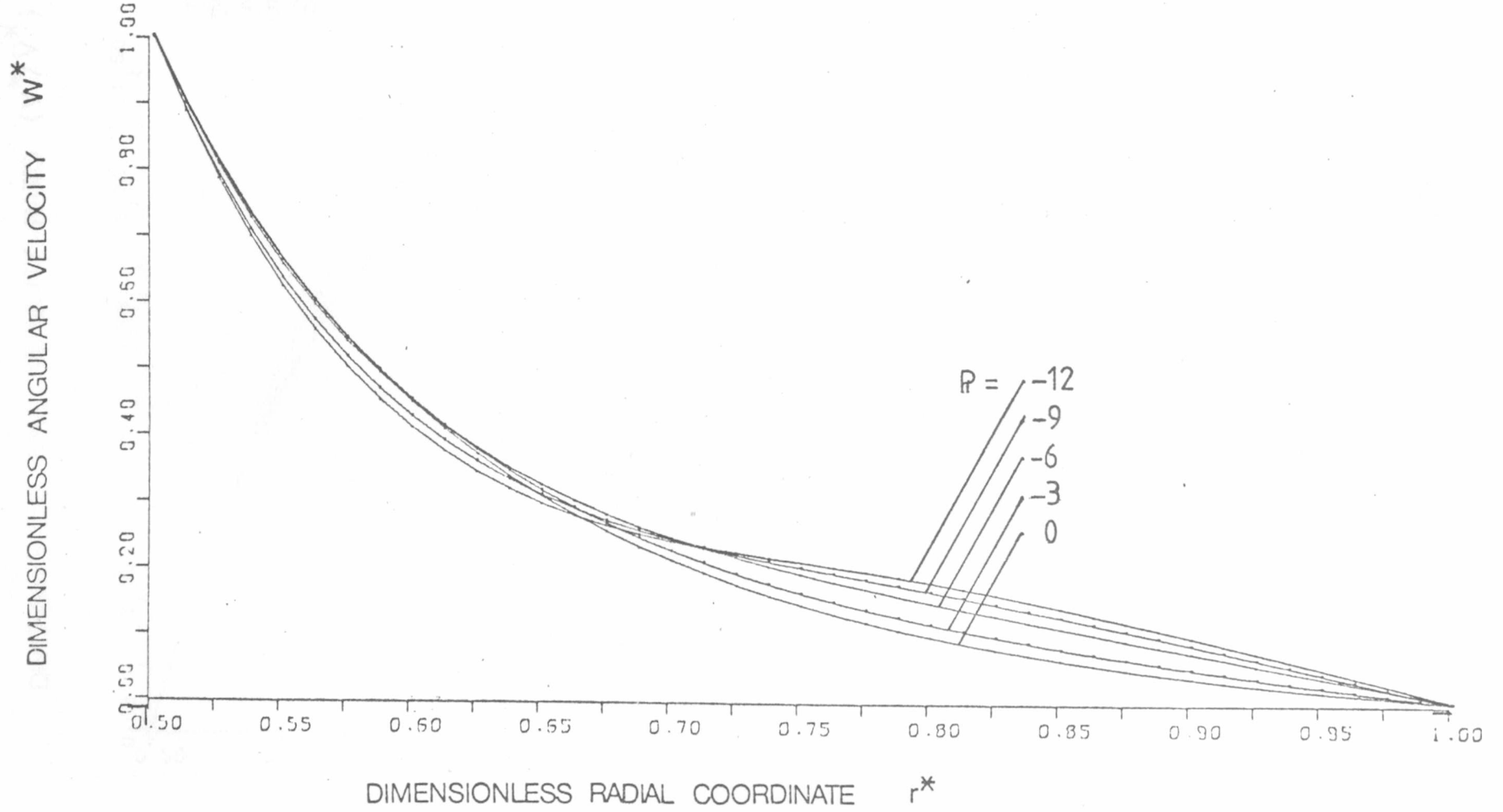


HELICAL FLOW OF A POWER LAW FLUID

Fig. 4.8 R

$n = 0.5$

$k = 0.5$



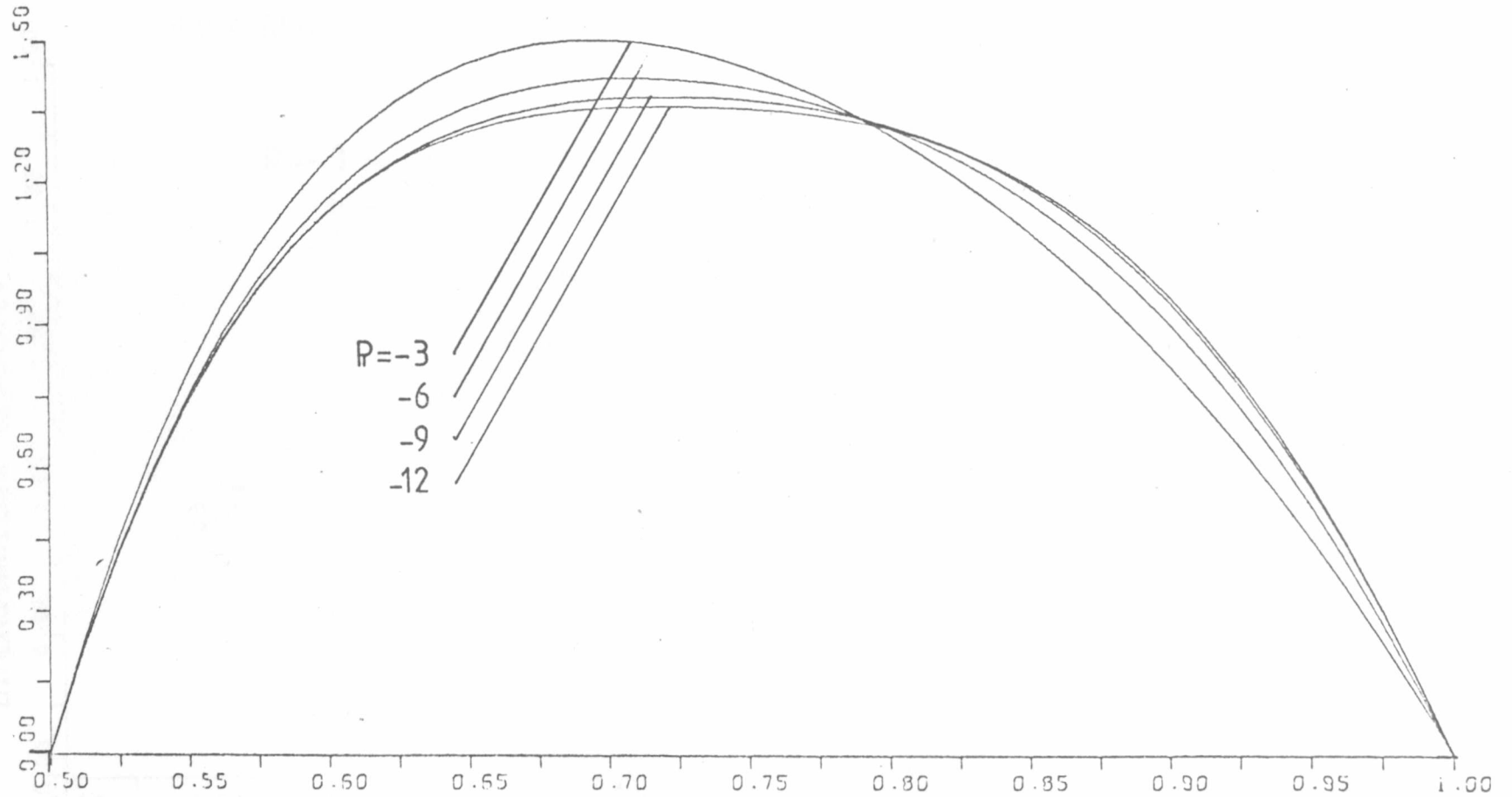
HELICAL FLOW OF A POWER LAW FLUID

Fig. 4.8 (i)

$n = 0.5$

$k = 0.5$

DIMENSIONLESS AXIAL VELOCITY RATIO ( $V^*/V^*$ )



DIMENSIONLESS RADIAL COORDINATE  $r^*$

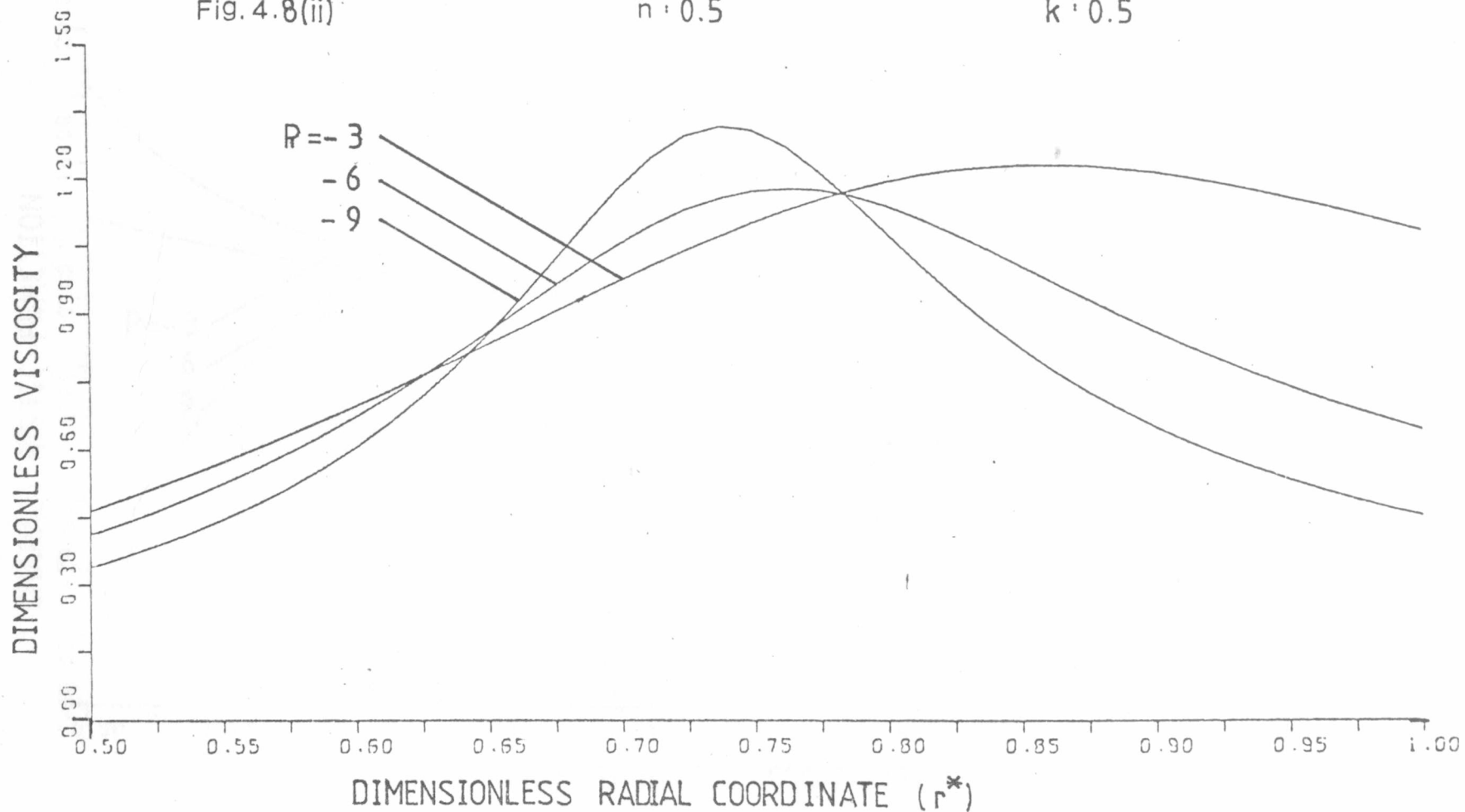
$R = -3$   
 $-6$   
 $-9$   
 $-12$

HELICAL FLOW OF A POWER LAW FLUID

Fig. 4.8(ii)

$n = 0.5$

$k = 0.5$

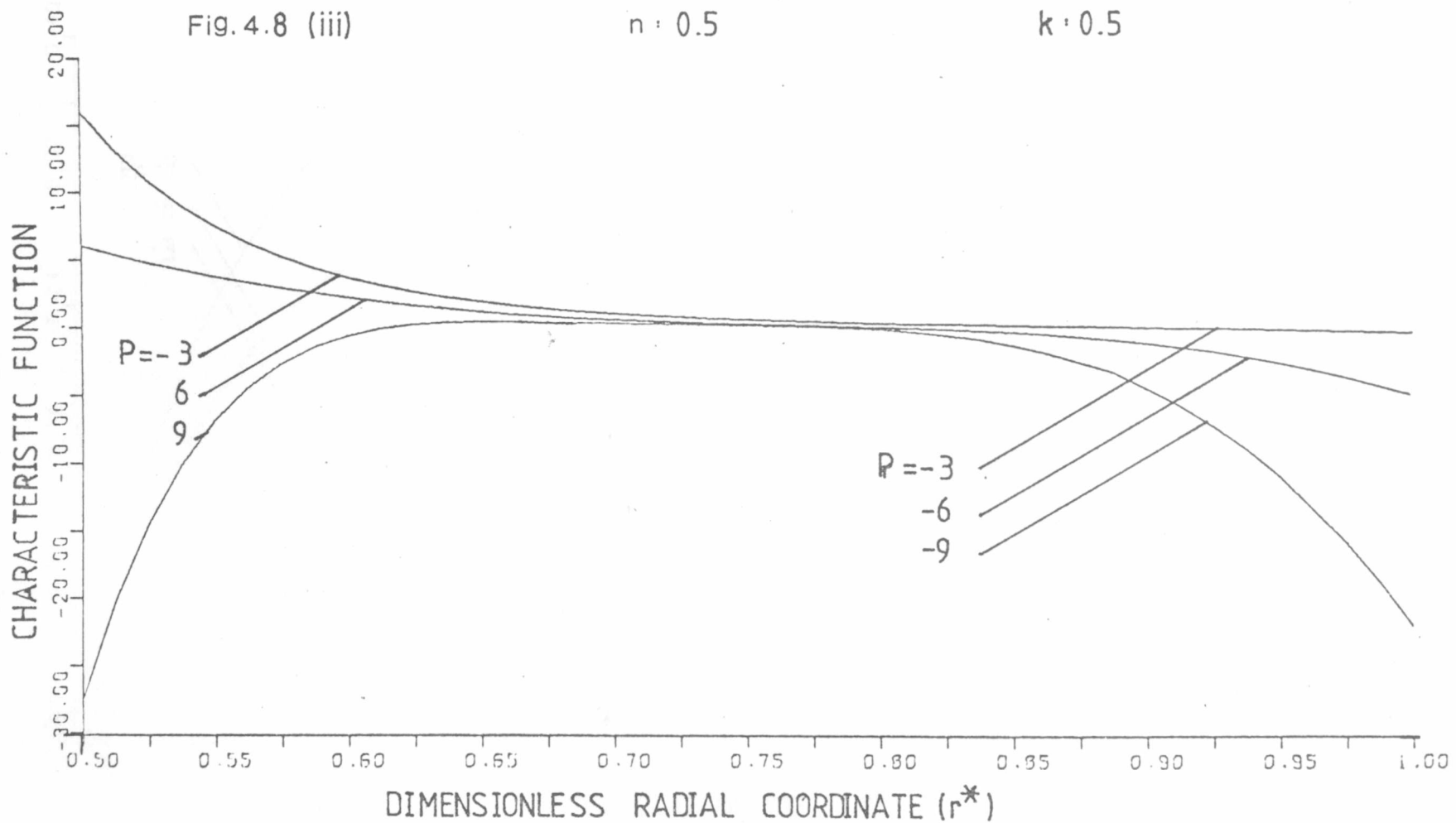


HELICAL FLOW OF A POWER LAW FLUID

Fig. 4.8 (iii)

$n = 0.5$

$k = 0.5$

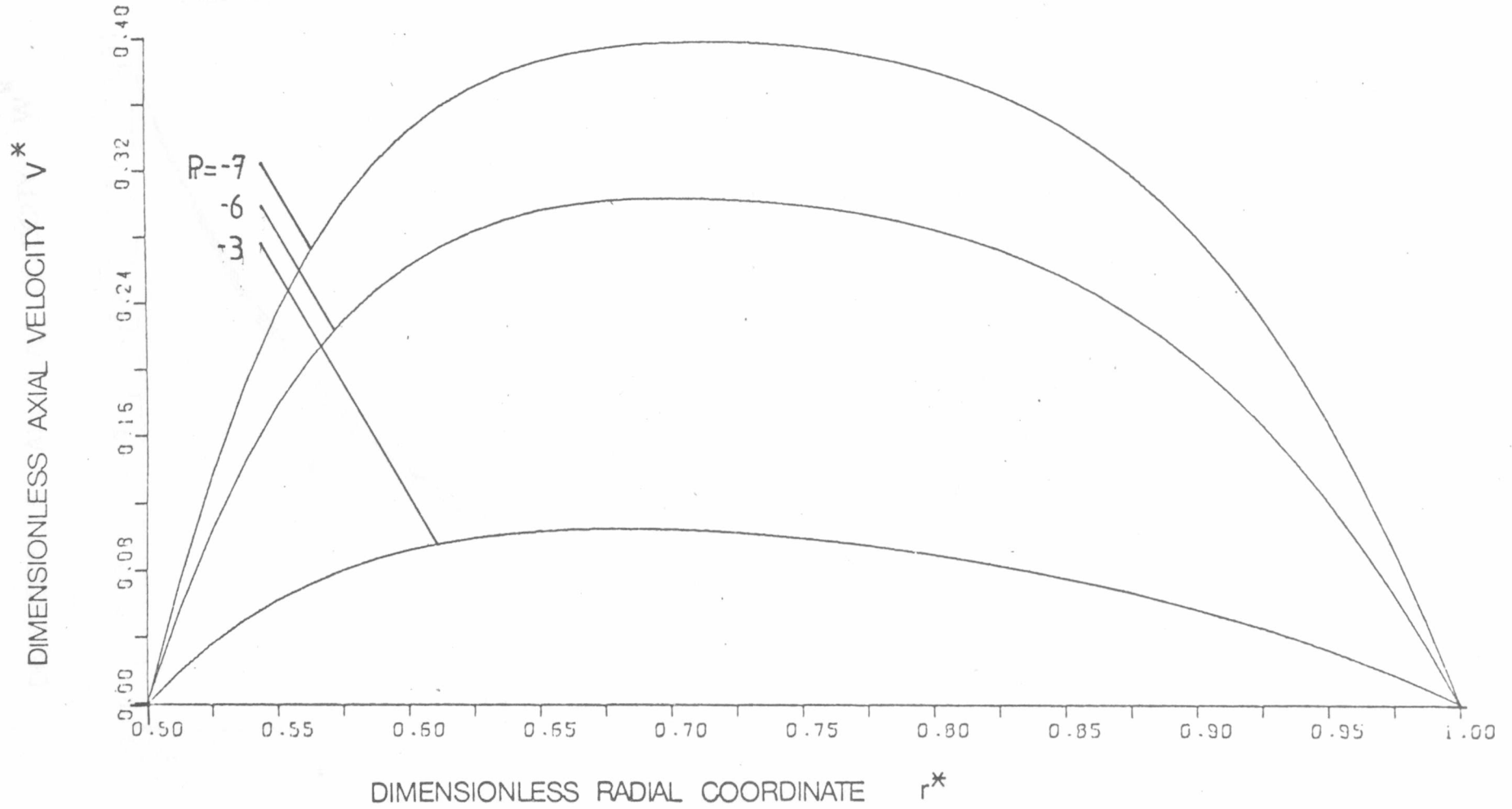


HELICAL FLOW OF A POWER LAW FLUID

Fig. 4.9 A

$n : 0.4$

$k : 0.5$

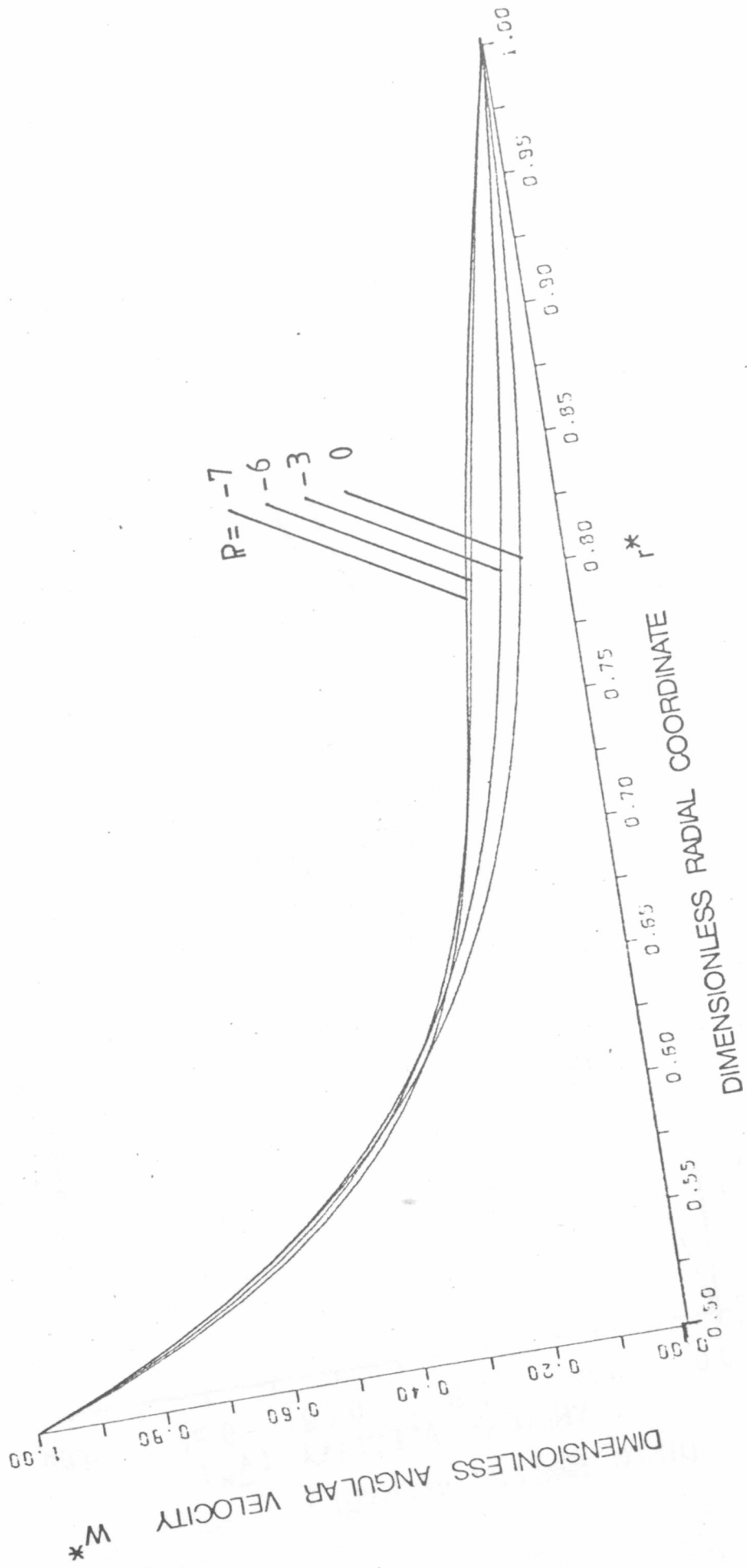


HELICAL FLOW OF A POWER LAW FLUID

$k = 0.5$

$n = 0.4$

Fig. 4.9 R

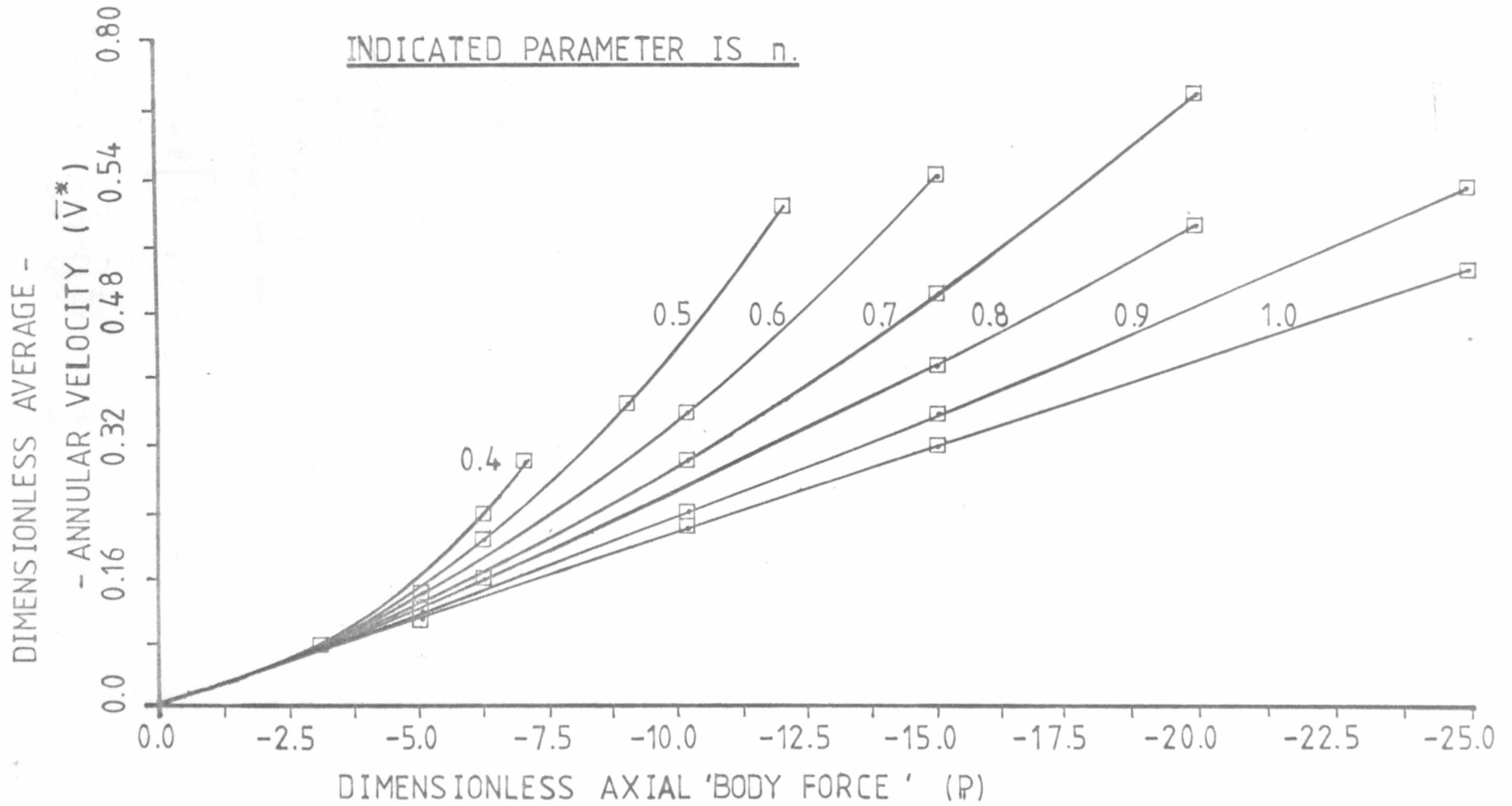


HELICAL FLOW OF A POWER LAW FLUID

Fig. 4.10

$k : 0.5$

INDICATED PARAMETER IS  $n$ .



#### 4.2.2 Variable radius ratio.

In this section we study the effects of varying the radius ratio  $k$  on the velocity profiles. To aid comparison of the results, we plot the velocities versus radial node number instead of the dimensionless radial coordinate  $r^*$ , and we present the axial velocity profiles as plots of axial velocity ratio  $v^*/\bar{v}^*$ . For completeness, a graph of  $\bar{v}^*$  versus  $k$  is included.

The values of  $k$  that occur in oil well drilling range from .2 to .7 (though are normally close to .5) (ref. chapter 1), and so we take values of  $k$  as .2, .3, .4, .5, .6, & .7. The computations for the small values of  $k$ , however, become difficult especially when  $n$  is also small. (c.f. 3.2.3). Some such calculations failed to satisfy the result assessment criterion established in 3.2.1 and accordingly are not presented here.

We note that in the present calculations, 41 equally spaced nodes were used with node 1 being at the inner cylinder and node 41 being at the outer cylinder.

We consider the cases of (i)  $n = .5$  with  $\mathcal{P} = -9$  (axial component dominant) and  $\mathcal{P} = -3$  (angular component dominant) and (ii)  $n = .7$  with  $\mathcal{P} = -10$  (axial component dominant) and  $\mathcal{P} = -5$  (angular component dominant).

For reference we also consider the case of a Newtonian fluid with the arbitrary value of  $\mathcal{P} = -10$ , noting that viscosity is not affected by either velocity component in this case.

Details of the graphs are presented in table 4.4.

Before discussing the results we examine the Newtonian fluid case theoretically. First we recall that an exact analytical expression for the velocity profiles exists in this case. (Langlois 61).

This expression takes the form

$$v^*(r^*) = \mathcal{P} \left[ k^2 - r^{*2} + (1 - k^2) \left\{ \frac{I_n(r^*/k)}{I_n(1/k)} \right\} \right]$$

$$w^*(r^*) = \frac{1}{1-k^2} \left[ \left\{ \frac{k}{r^*} \right\}^2 - k^2 \right]$$

Plotting the curves against nodal number is equivalent to introducing the change of variable

$$\phi^* = (r^* - k) \frac{40}{1 - k} + 1$$

which is effectively the same as the change of variable

$$\phi = (r^* - k) \frac{1}{1 - k}$$

With this change of variable, the exact solution becomes

$$v^*(\phi) = P \left[ -(1 - k)^2 \phi^2 - 2k(1 - k)\phi + (1 - k^2) \frac{\ln(1/k - 1)\phi + 1}{\ln(1/k)} \right]$$

$$w^*(\phi) = \frac{1}{1 - k^2} \left[ \frac{k^2}{((1 - k)\phi + k)^2} - k^2 \right]$$

Both these equations are heavily dependent on  $k$  and so we expect variation of velocity profiles with  $k$  even for the constant velocity Newtonian fluids.

With non-Newtonian fluids we therefore expect the profiles to be affected both 'directly' by altering the radius ratio (in a similar way to the above) and 'indirectly' by the resulting changes in viscosity profile, and thus we must refer to the Newtonian fluid case when analysing results.

For Newtonian fluids the dependence of the angular velocity profiles on  $k$  is shown in fig. 4.11 R. As  $k$  decreases, the curves fall much more steeply near the LHS and become flatter near the RHS, with the angular velocity at the mid point of the annular gap dropping from 3.69 for  $k = .7$  to 0.74 for  $k = .2$ .

The dimensionless axial velocity ratio ( $v^*(\phi) / \bar{v}^*$ ) is not so strongly dependent on  $k$  and fig 4.11 A shows that the shape of the profile is altered most on the LHS. As  $k$  decreases from .7, the curves become skewed towards the LHS, and the peak value of the axial velocity ratio rises from 1.5 at node 20 for  $k = .7$  to 1.54 at node 18 for  $k = .2$ .

As  $k$  decreases, the angular velocity gradients (with respect to  $\phi$ ) increase on the LHS rapidly, whilst those on the RHS decrease. The axial velocity ratio gradients change little with  $k$  but since  $\bar{v}^*$

increases as  $k$  decreases (see fig. 4.16), the gradients of the axial velocity  $v^*$  will increase as  $k$  decreases.

Hence, as  $k$  decreases, the shear rate profile will become more dependent on the axial component both near the MIDDLE and on the RHS.

With non-Newtonian fluids then, we expect the axial component to become more dominant on the RHS and near the MIDDLE as  $k$  decreases. The viscosity profiles for  $n = .7$  and  $\beta = -10$  (fig. 4.12(i)) illustrate this effect with the curves becoming peaked in the centre as  $k$  decreases. The effect can also be seen in the angular velocity profiles for  $n = .5$  and  $\beta = -9$  (fig. 4.14 R) as the  $k = .6$  and  $k = .5$  curves become more convex on the RHS indicating the dominance of the axial component in this region.

In general the effect of decreasing  $k$  on the velocity profiles becomes more pronounced as  $n$  decreases in that the curves fall even more rapidly near the LHS.

With the axial velocity profiles, the direct effect of changing  $k$  and the indirect effect (arising through the resulting changes in viscosity profiles) are in opposition, and this gives rise to a fairly complex set of graphs.

As mentioned above, with Newtonian fluids the axial velocity curves become skewed to the LHS and the maximum value increases as  $k$  is decreased. With non Newtonian fluids however, the viscosity profile develops a peak when  $k$  is decreased, and this will tend to give the axial velocity profile a flatter, more central peak.

On the axial velocity profile graphs for  $n = .7$  with  $\beta = -5$  and  $\beta = -10$  (figs. 4.12 A & 4.13 A) we see that the indirect influence of decreasing  $k$  has the stronger effect on peak height (which decreases) whilst the opposition of the direct and indirect influences is demonstrated near the RHS where the curves are almost identical for all values of  $k$ .

The indirect influence of changing  $k$  on axial velocity profiles is even stronger for the case  $n = .5$  and  $\beta = -9$ , and examination of fig. 4.14 A shows that the curves on the RHS appear in opposite order to those on the LHS of the Newtonian axial velocity profile graph.

Finally the  $n = .5$ ,  $\beta = -3$  graph (fig. 4.15 A) has a confused structure, reflecting the interaction of the various influences on the axial velocity profiles.

FIGURE	VERTICAL AXIS QUANTITY	n	$\rho$	k
4.11 A 4.11 R	axial velocity ratio angular velocity	1.0	-10	.2, .3, .4, .5, .6, .7 .
4.12 A 4.12 R 4.12 (i)	axial velocity ratio angular velocity viscosity	.7	-10	.4, .5, .6, .7
4.13 A 4.13 R	axial velocity ratio angular velocity	.7	-5	.3, .4, .5, .6, .7 .
4.14 A 4.14 R	axial velocity ratio angular velocity	.5	-9	.5, .6, .7 .
4.15 A 4.15 R	axial velocity ratio angular velocity	.5	-3	.4, .5, .6, .7 .
4.16	Average annular velocity versus k for the values of (n,k, $\rho$ ) above			

TABLE 4.4 List of figures for 4.2.2 .

HELICAL FLOW OF A POWER LAW FLUID

Fig. 4.11 A

$n = 1.0$

$R = -10$

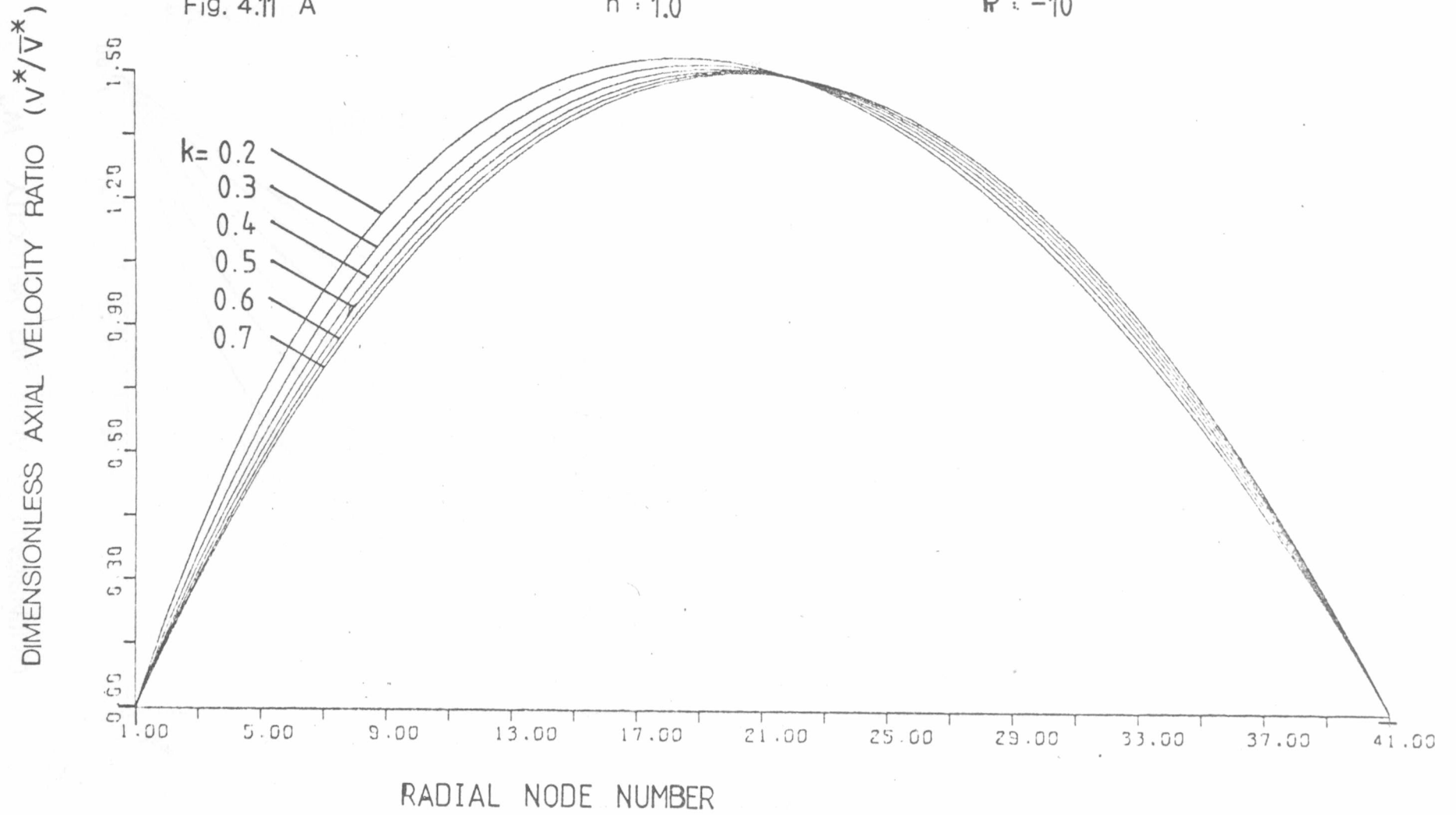
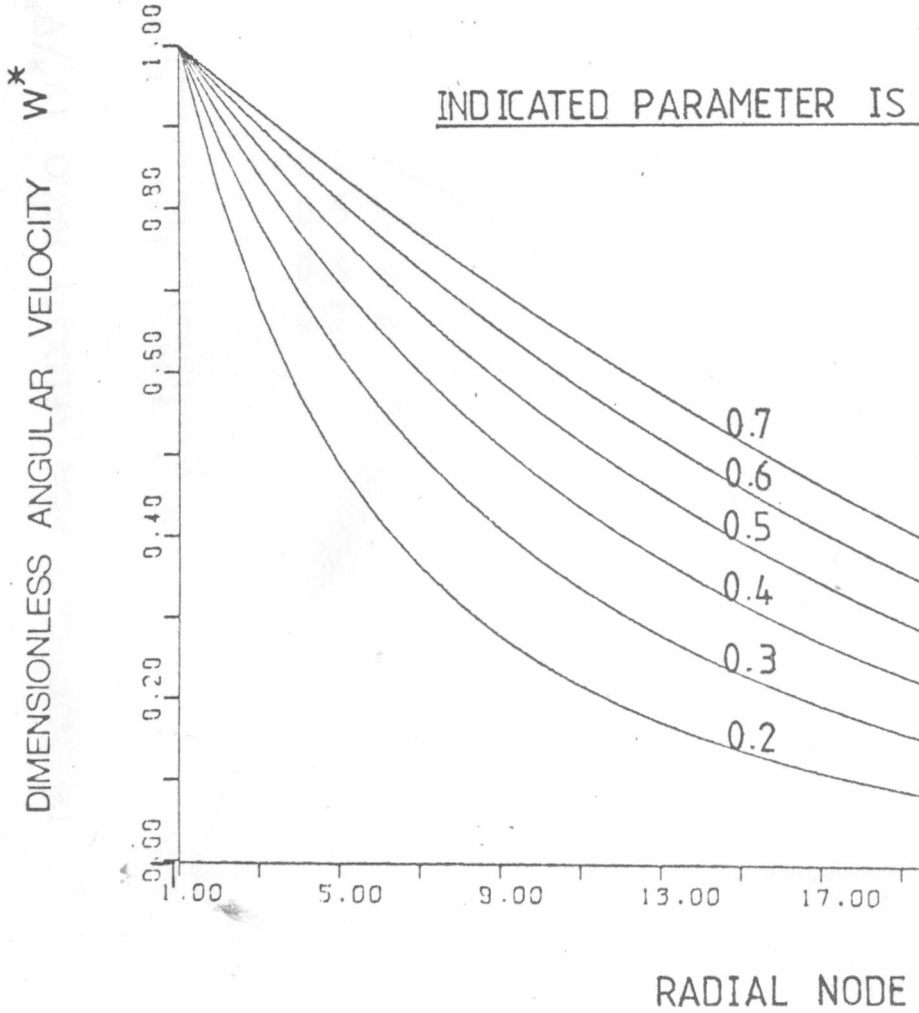


Fig. 4.11 R

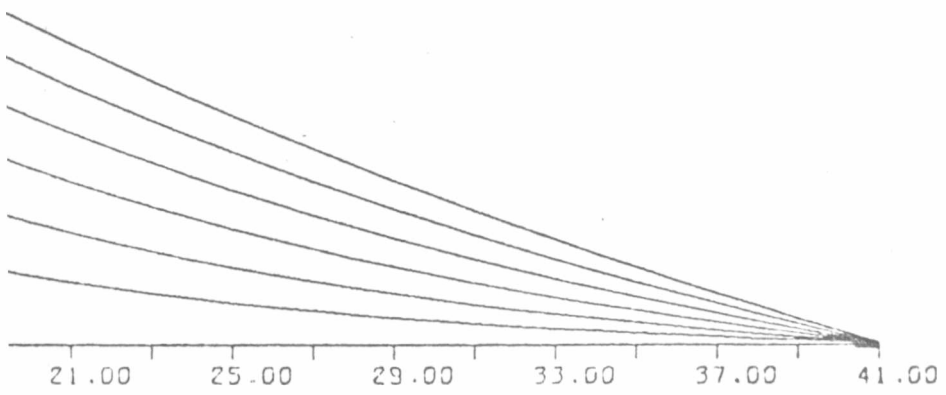
$n = 1.0$



LAW FLUID

P : -10

k



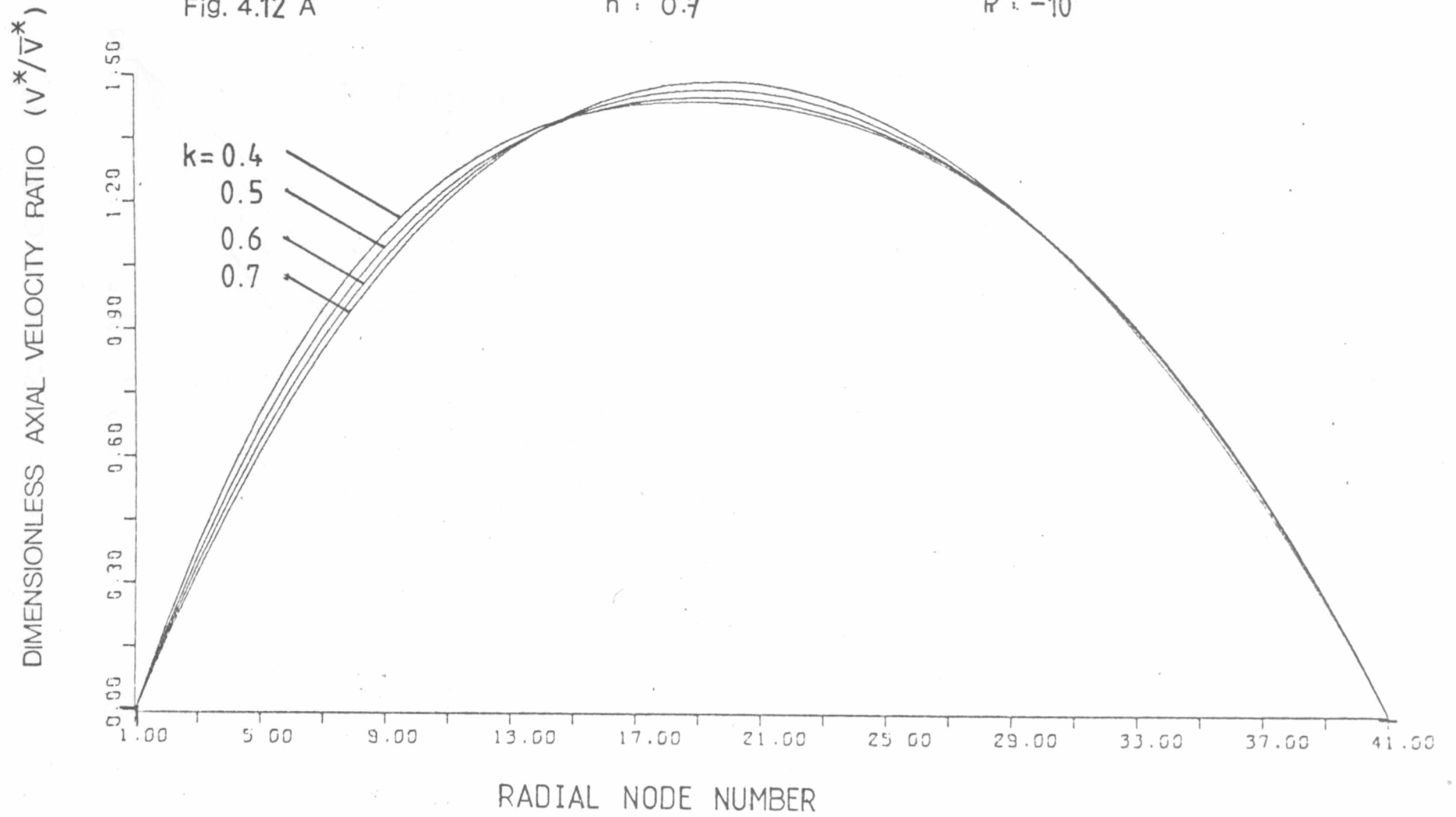
NUMBER

HELICAL FLOW OF A POWER LAW FLUID

Fig. 4.12 A

$n = 0.7$

$R = -10$

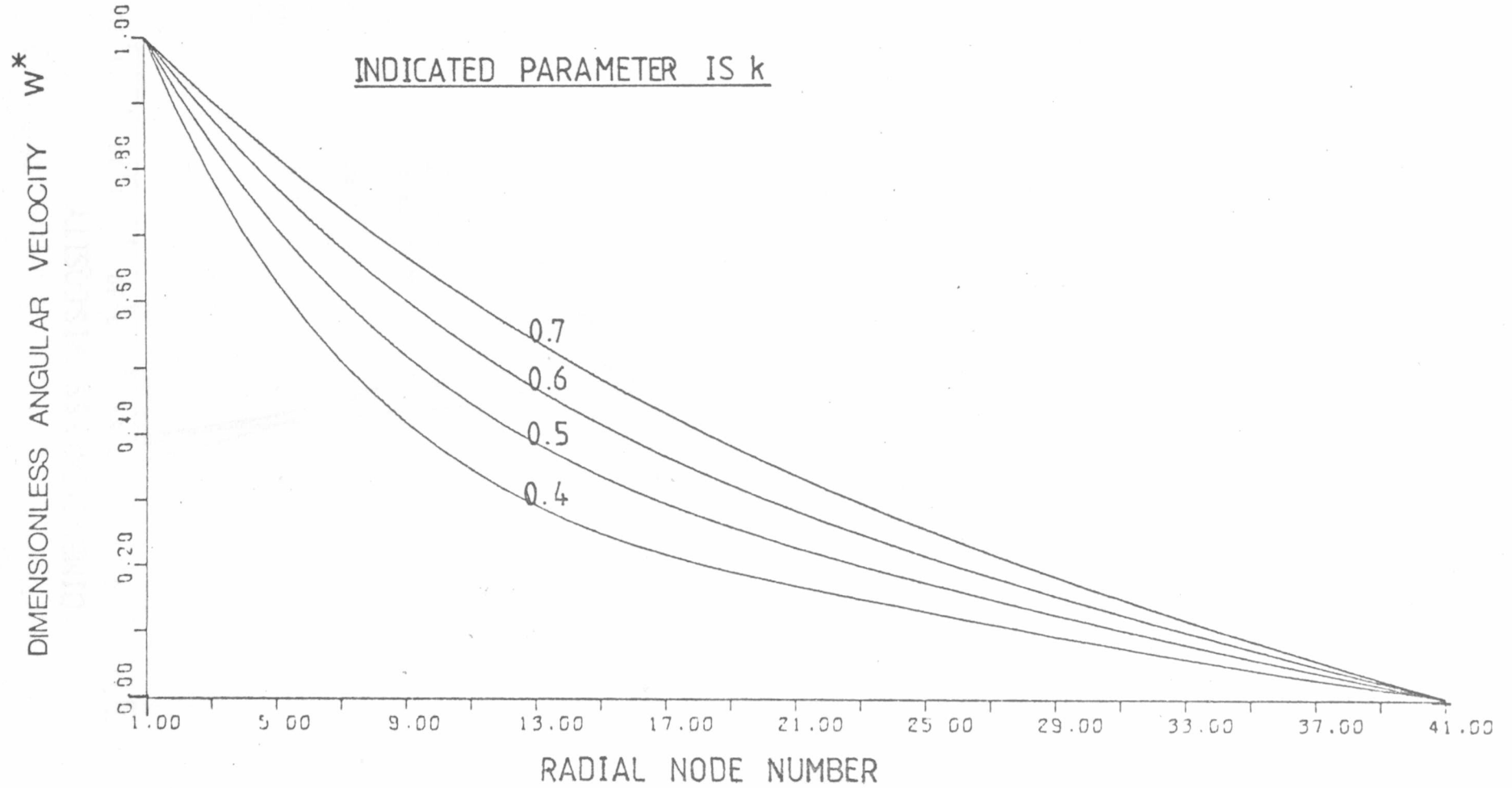


HELICAL FLOW OF A POWER LAW FLUID

Fig. 4.12 R

$n = 0.7$

$R = -10$

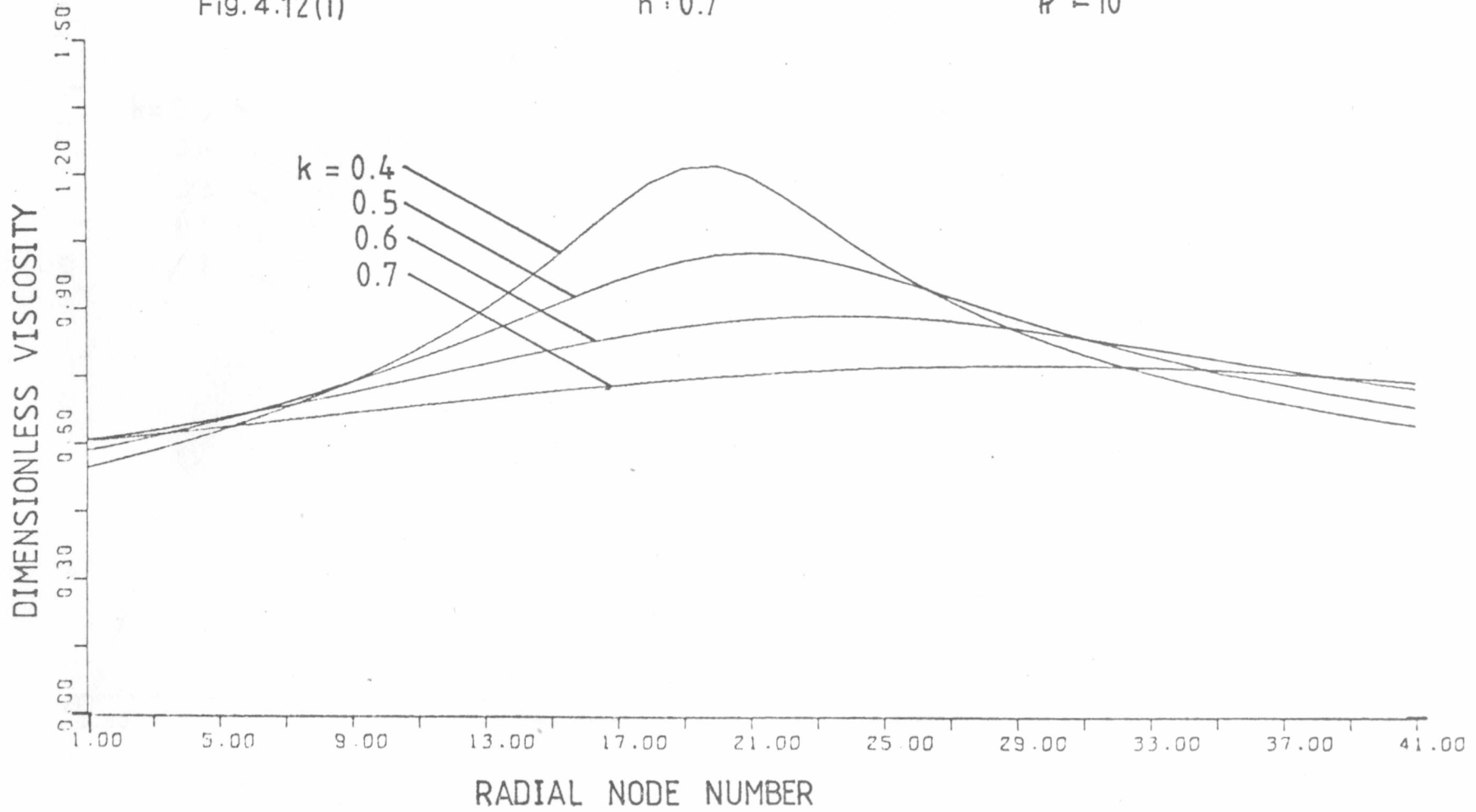


HELICAL FLOW OF A POWER LAW FLUID

Fig. 4.12(i)

$n = 0.7$

$R = 10$

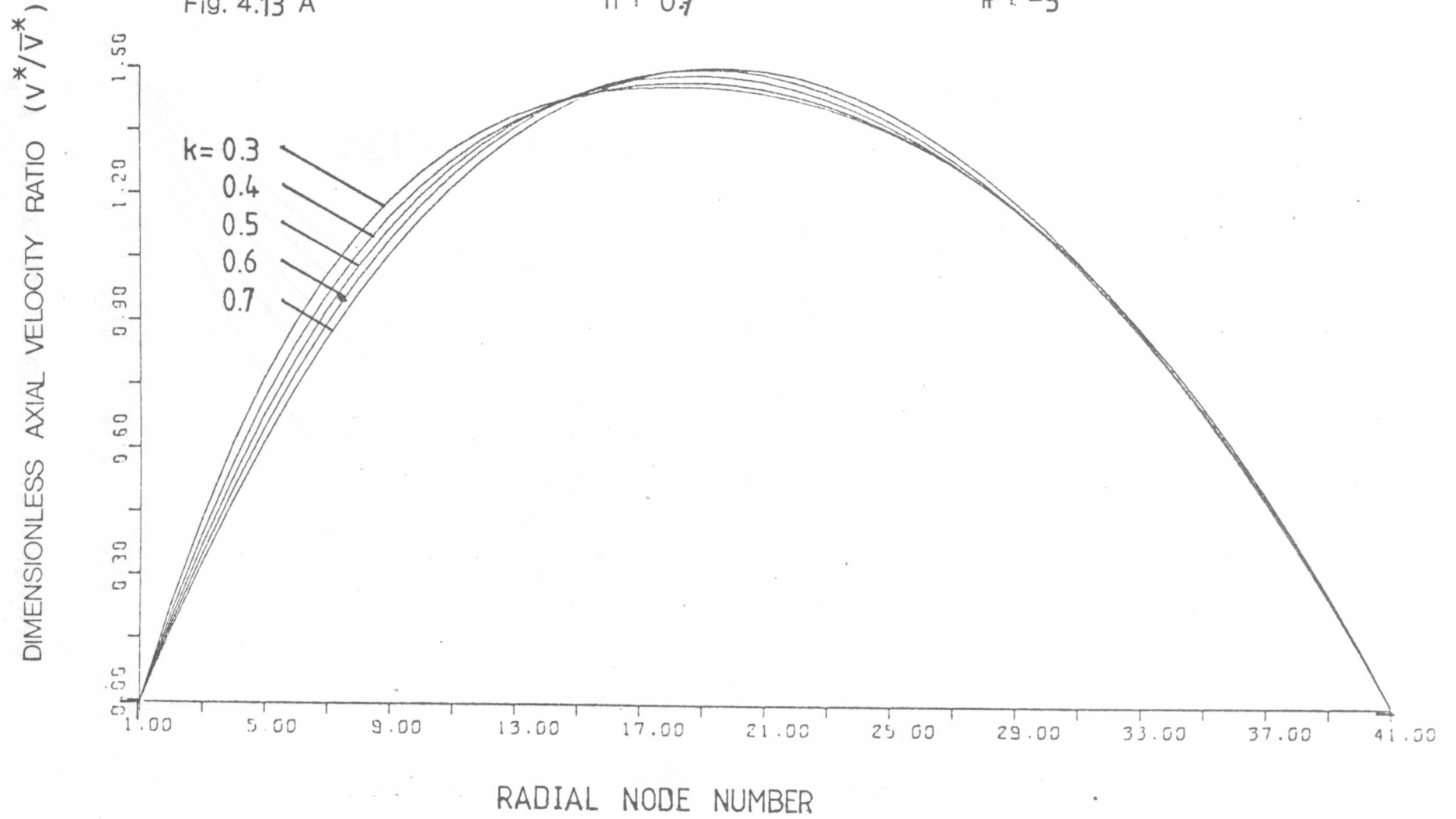


HELICAL FLOW OF A POWER LAW FLUID

Fig. 4.13 A

$n = 0.7$

$R = -5$

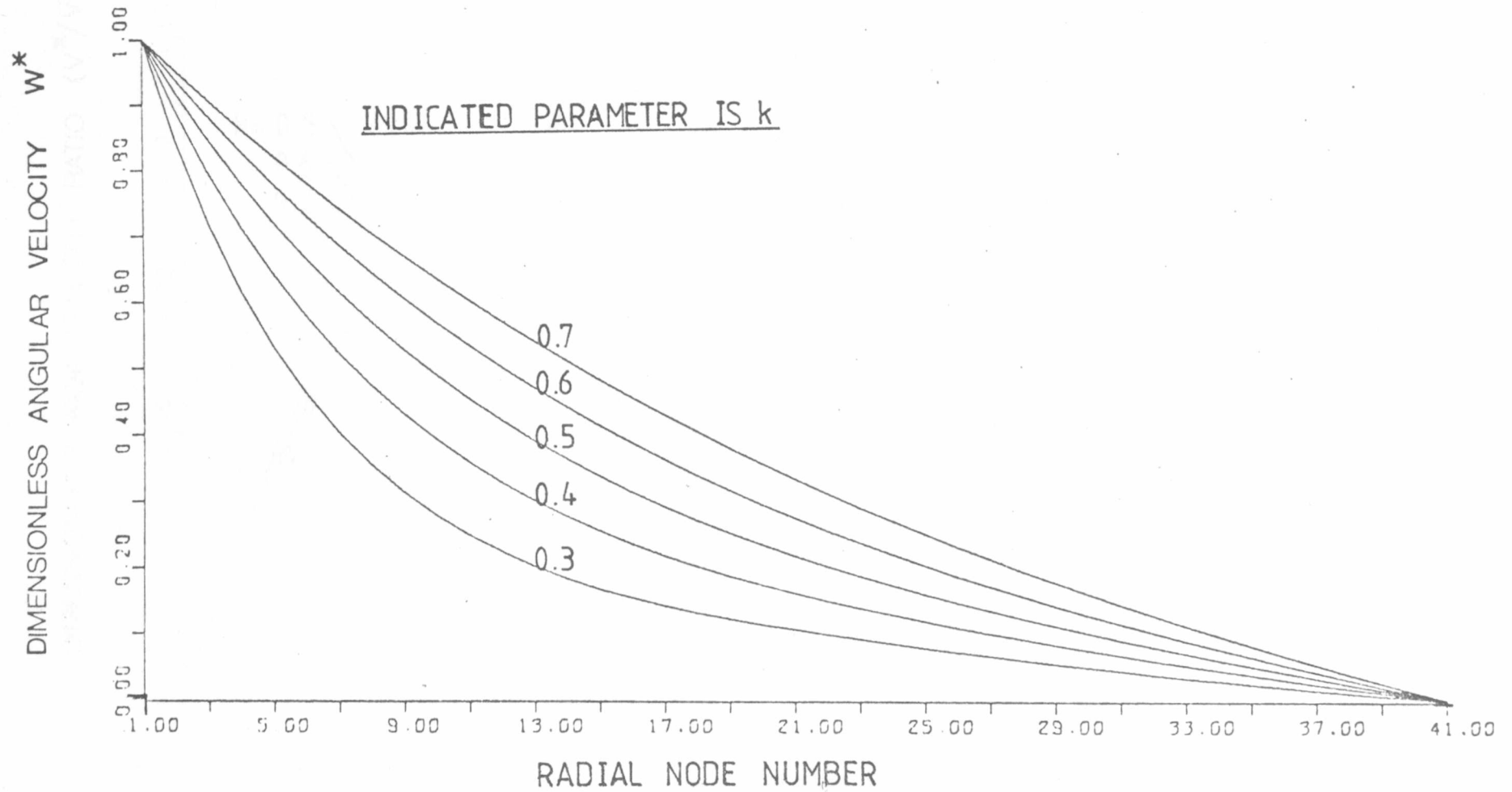


HELICAL FLOW OF A POWER LAW FLUID

Fig. 4.13 R

$n = 0.7$

$P = -5$



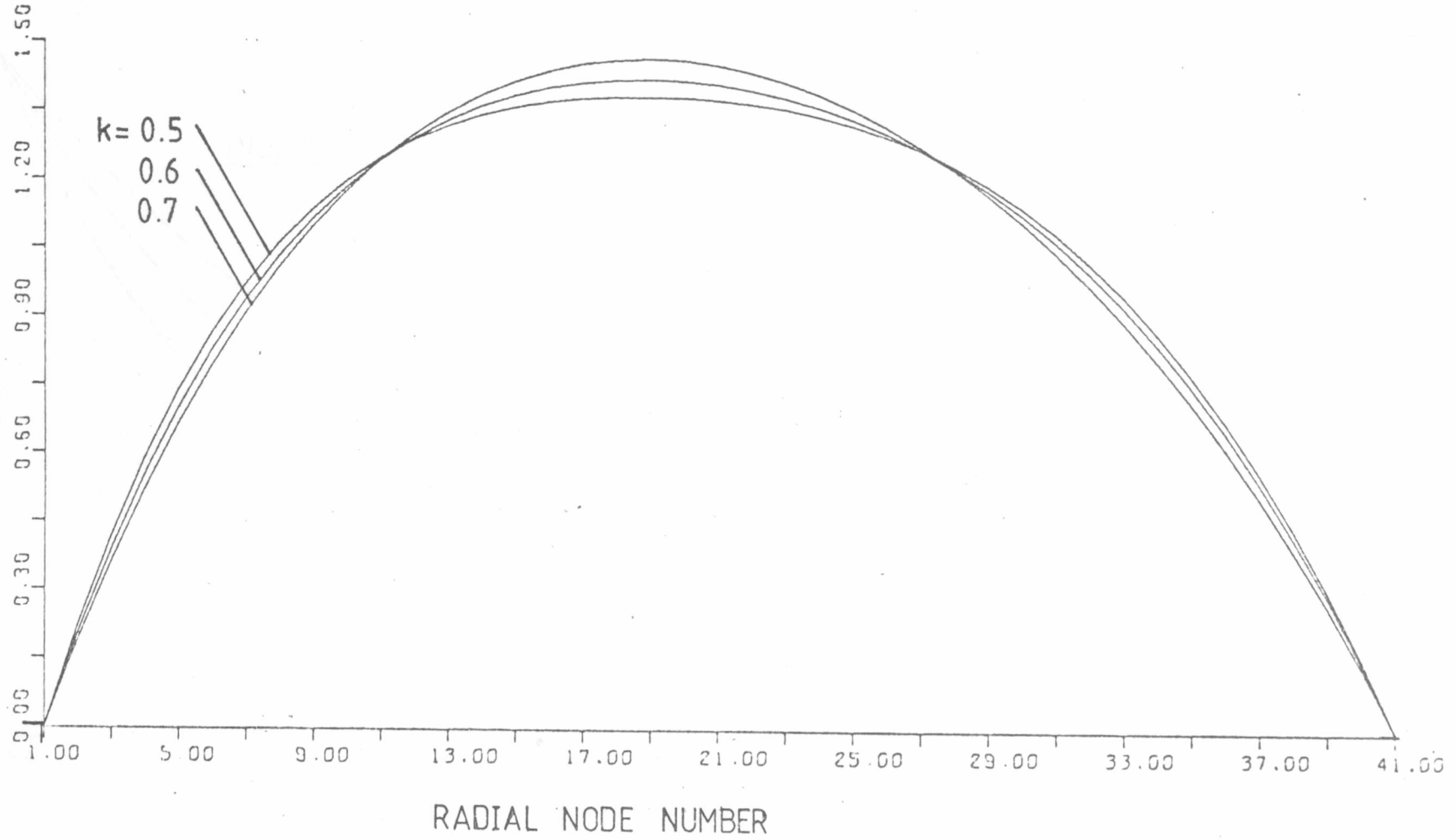
HELICAL FLOW OF A POWER LAW FLUID

Fig. 4.14 A

$n : 0.5$

$R : -9$

DIMENSIONLESS AXIAL VELOCITY RATIO ( $V^*/\bar{V}^*$ )

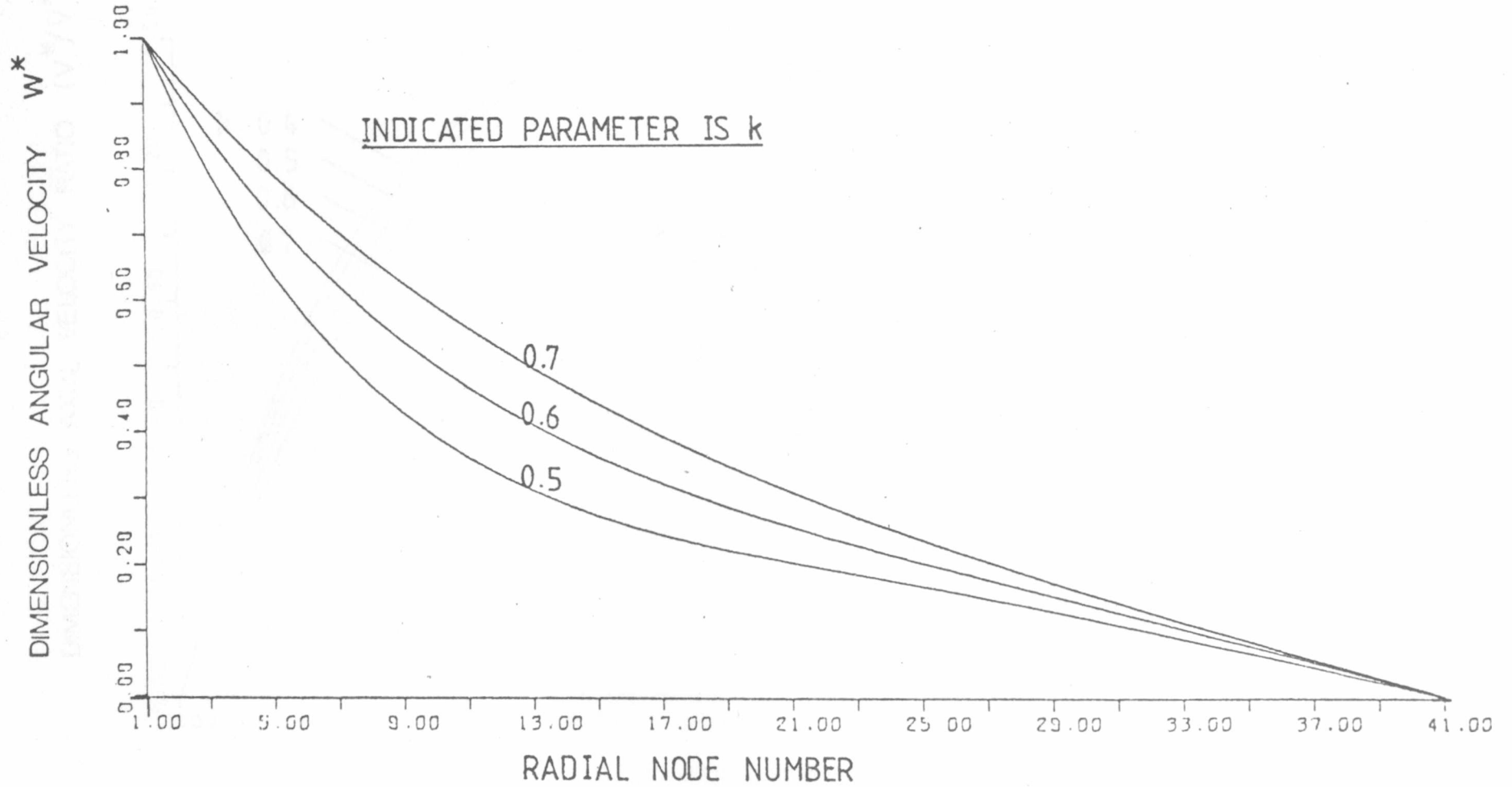


HELICAL FLOW OF A POWER LAW FLUID

Fig. 4.14 R

$n = 0.5$

R = 9



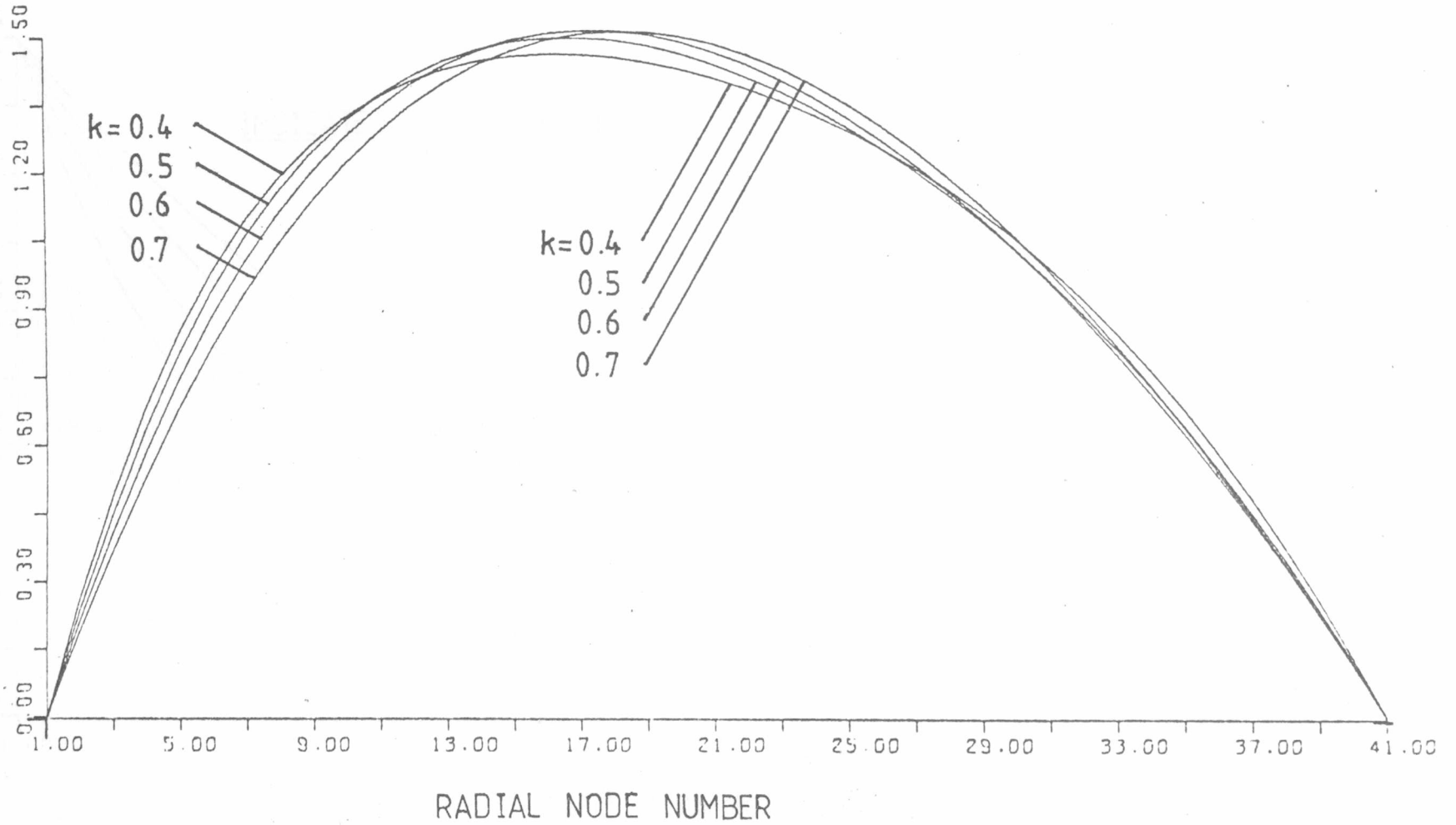
HELICAL FLOW OF A POWER LAW FLUID

Fig. 4.15 A

$n = 0.5$

$R = -3$

DIMENSIONLESS AXIAL VELOCITY RATIO ( $V^*/\bar{V}^*$ )

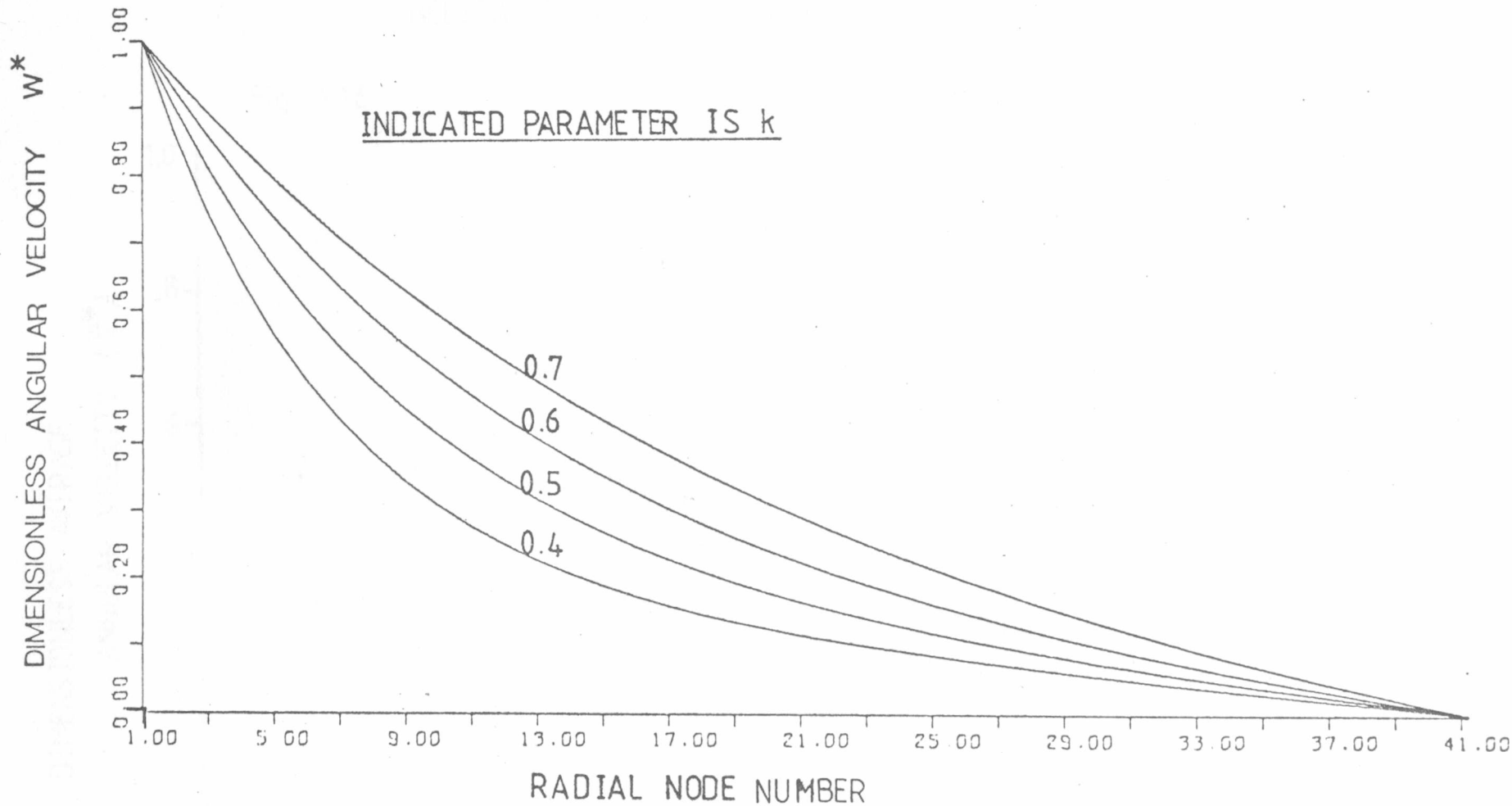


HELICAL FLOW OF A POWER LAW FLUID

Fig. 4.15 R

$n = 0.5$

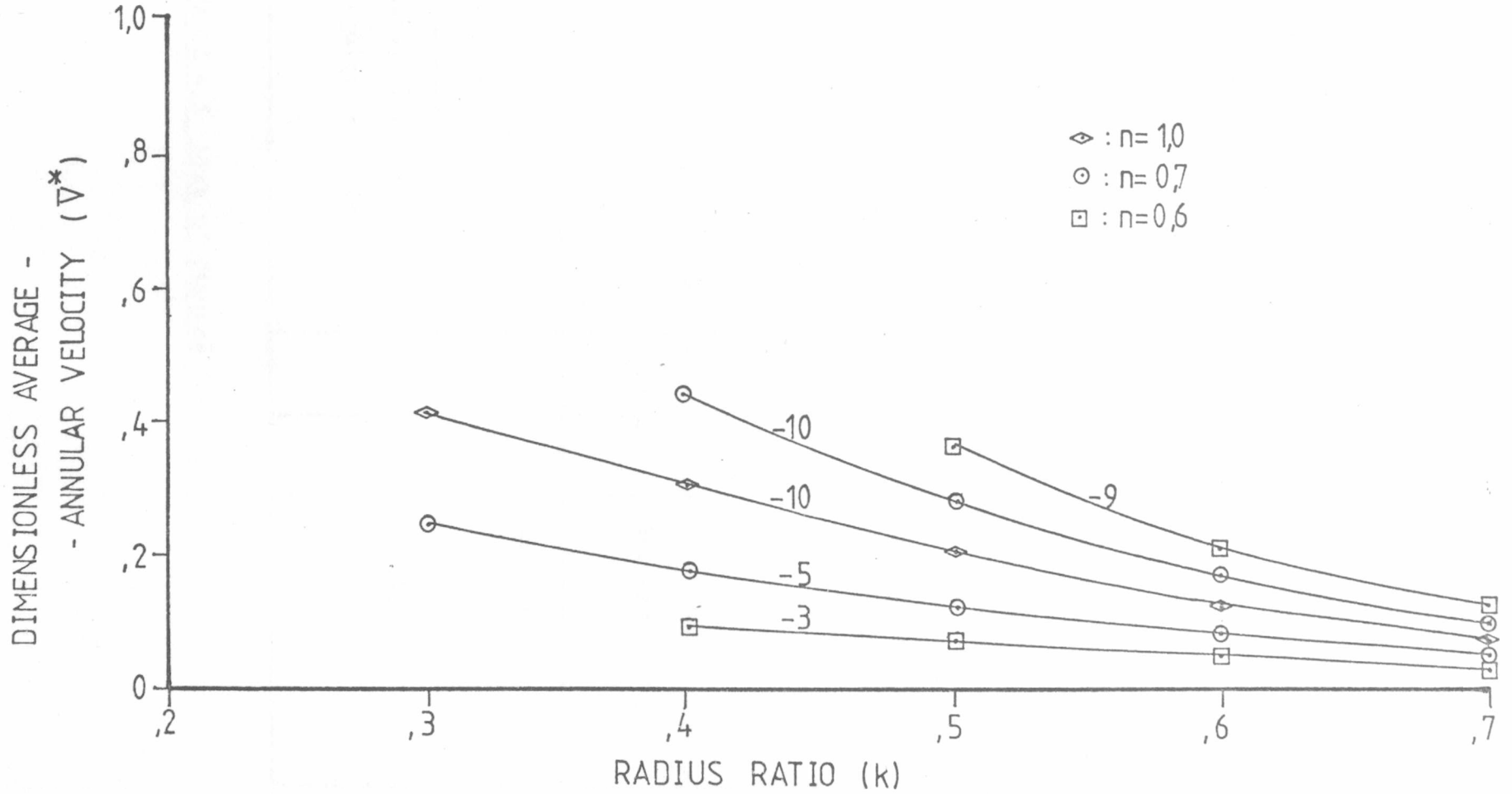
P = 3



# HELICAL FLOW OF A POWER LAW FLUID

Fig. 4.16

INDICATED PARAMETER IS P



### 4.2.3 Variable fluid index with other radius ratios.

In this section results are presented for the remaining values of power law fluid index and radius ratio. The characteristics of these results are similar to those of 4.2.1 and 4.2.2, and further discussion is therefore considered unnecessary. Table 4.5 lists the graphs presented in this section.

FIGURE	VERTICAL AXIS QUANTITY	n	k	$\beta$
4.17 A 4.17 R	axial velocity angular velocity	.9	.7	-200, -150, -100, -50, -25 .
4.18 A 4.18 R	axial velocity	.7	.7	-60, -45, -30, -15 .
4.19 A 4.19 R	axial velocity angular velocity	.5	.7	-30, -20, -10 .
4.20 A 4.20 R	axial velocity angular velocity	.9	.3	-20, -15, -10, -5 .
4.21 A 4.21 R	axial velocity angular velocity	.7	.3	-6, -4, -2 .

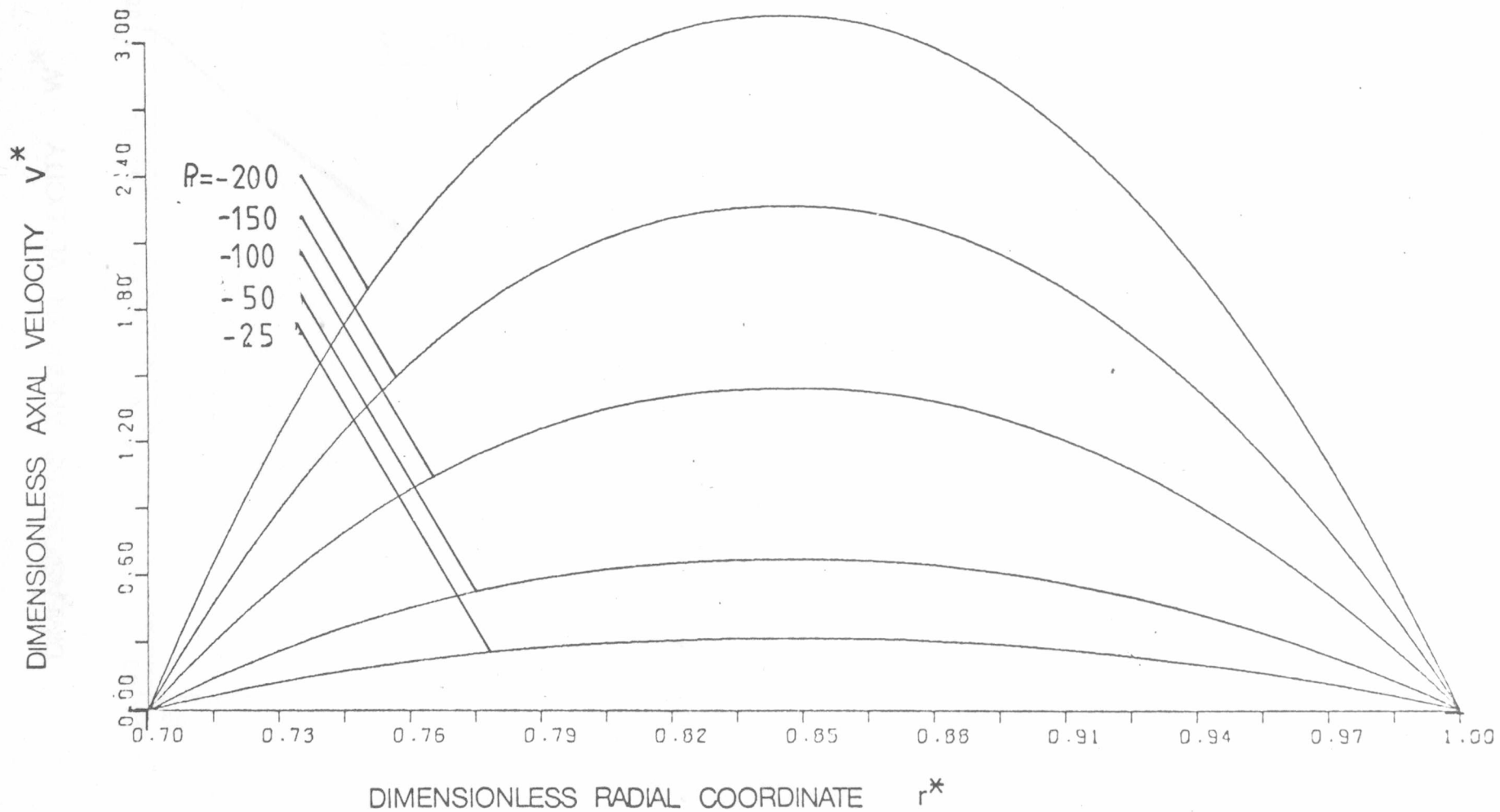
TABLE 4.5 List of figures for 4.2.3 .

HELICAL FLOW OF A POWER LAW FLUID

Fig. 4.17 A

$n = 0.9$

$k = 0.7$



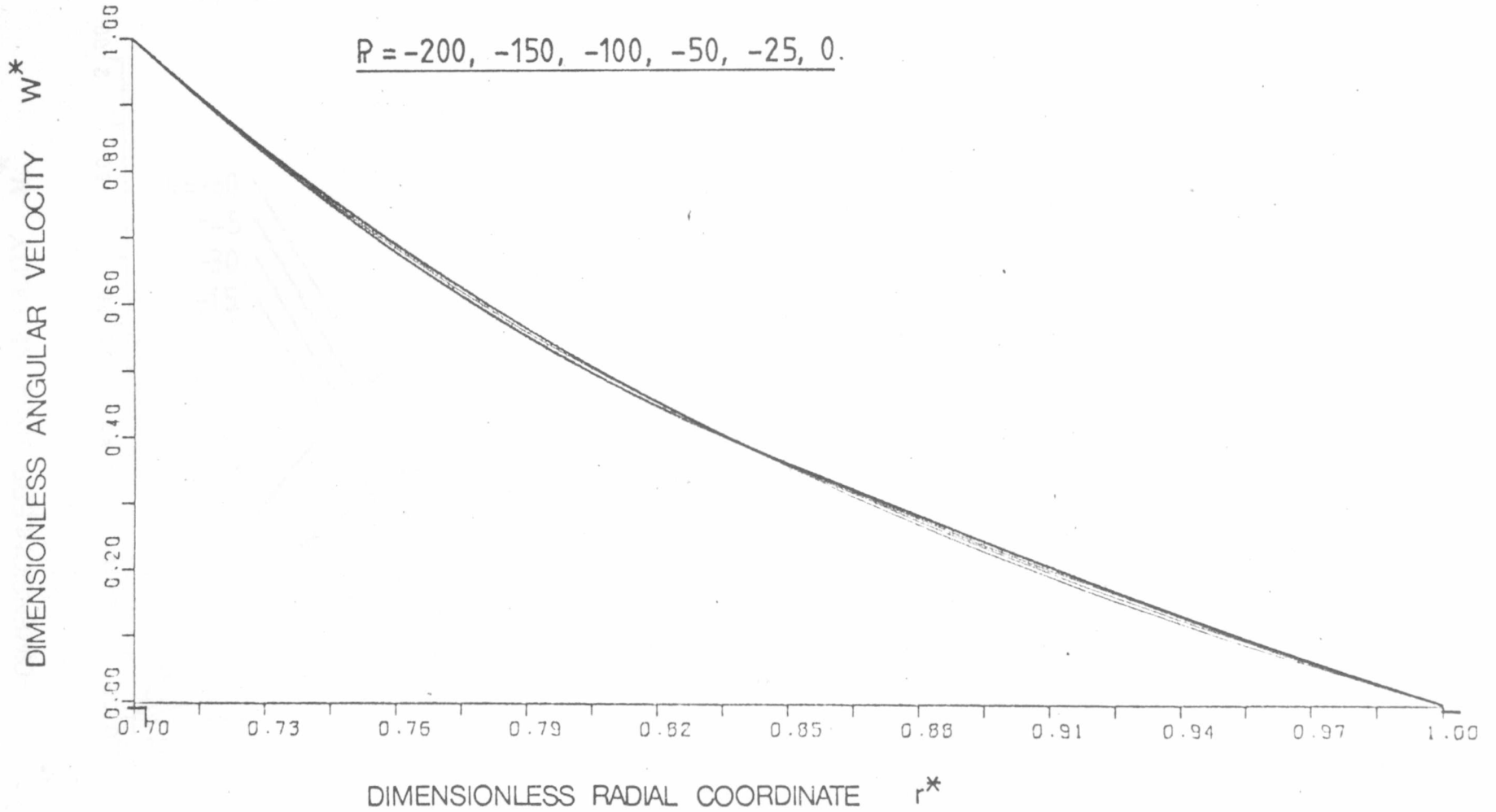
HELICAL FLOW OF A POWER LAW FLUID

Fig. 4.17 R

$n = 0.9$

$k = 0.7$

$R = -200, -150, -100, -50, -25, 0.$

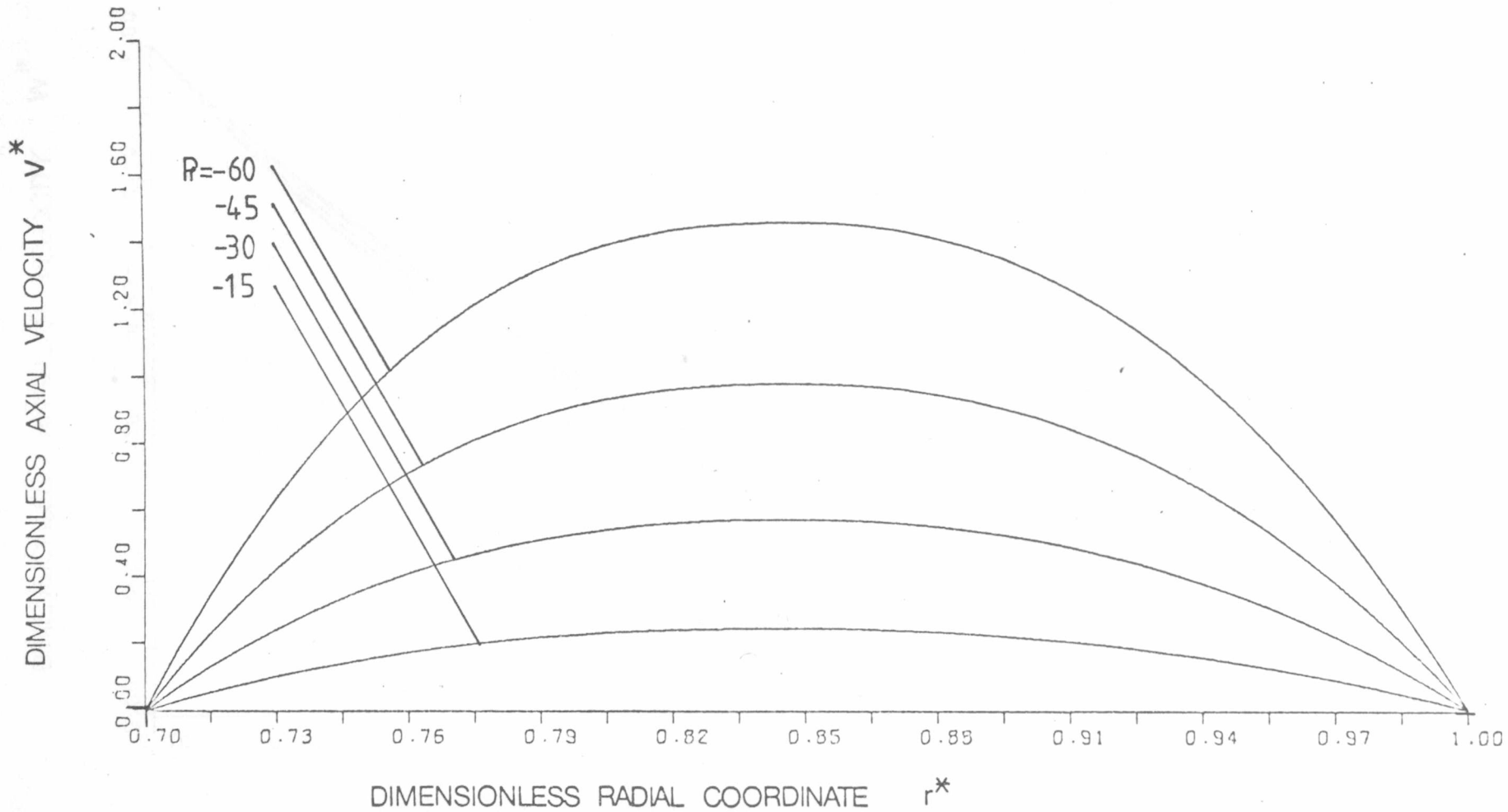


HELICAL FLOW OF A POWER LAW FLUID

Fig. 4.18 A

$n = 0.7$

$k = 0.7$



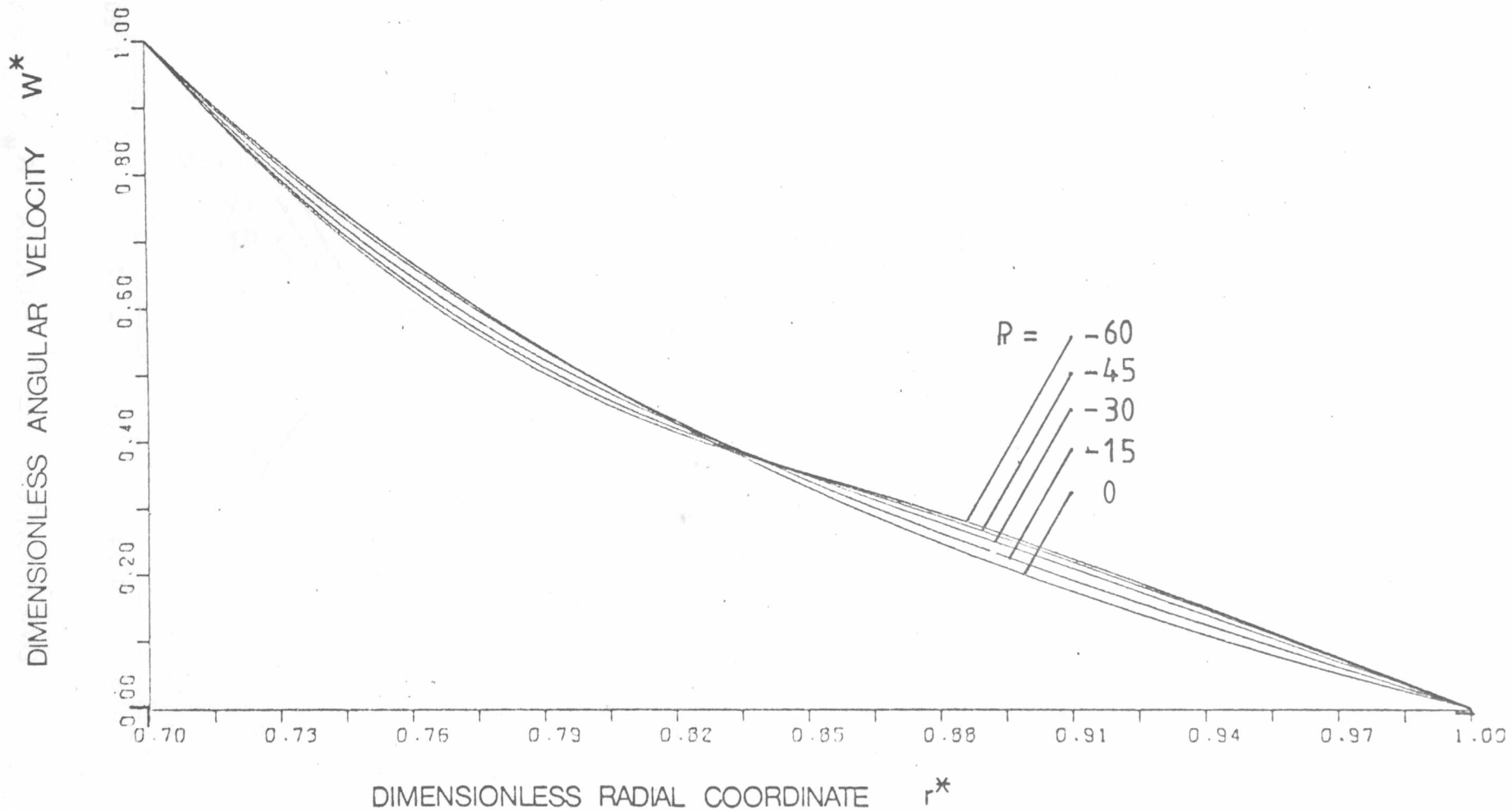
HELICAL FLOW OF A POWER LAW FLUID

Fig. 4.18 R

$n = 0.7$

$k = 0.7$

93

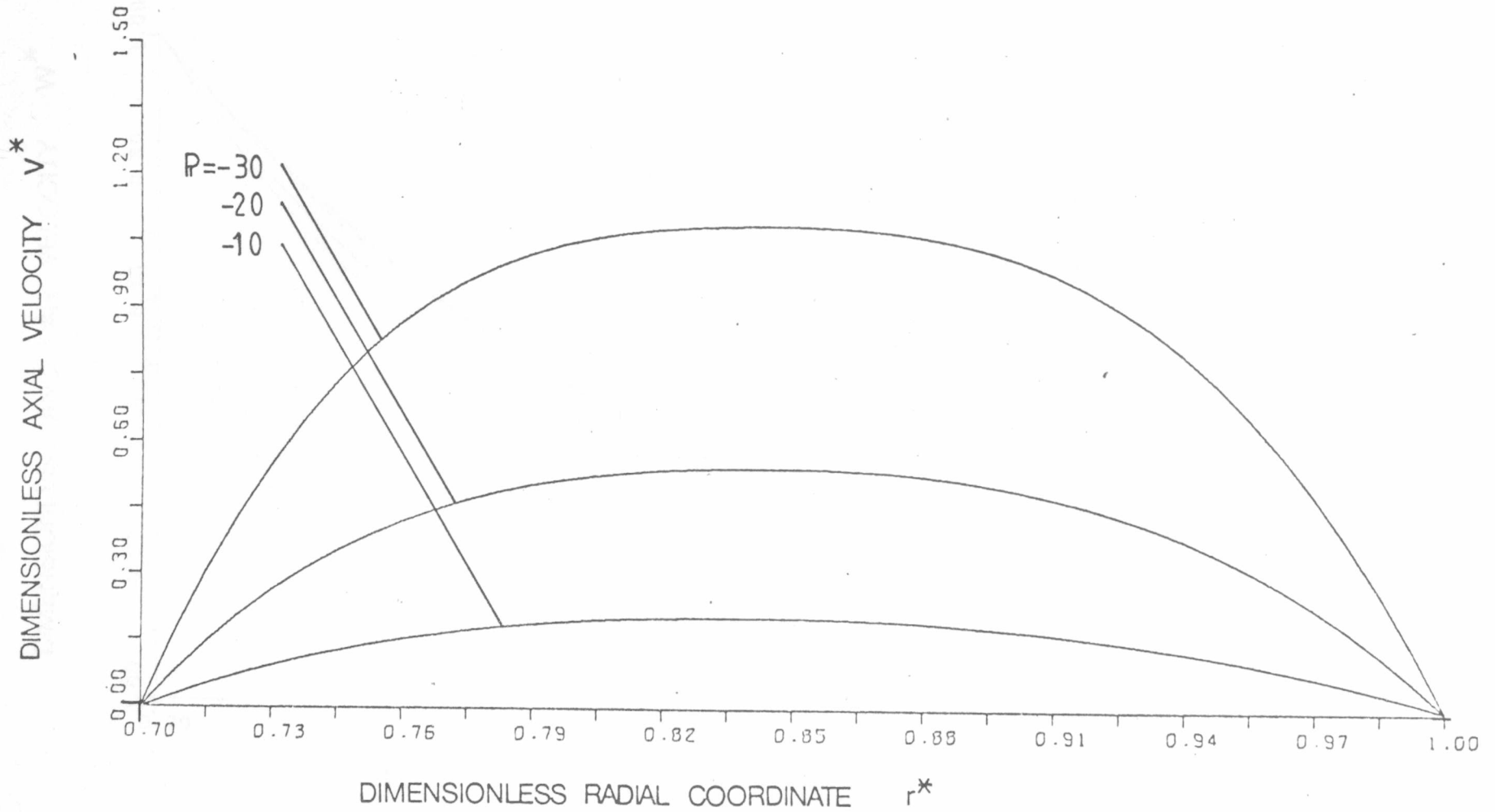


HELICAL FLOW OF A POWER LAW FLUID

Fig. 4.19 A

$n = 0.5$

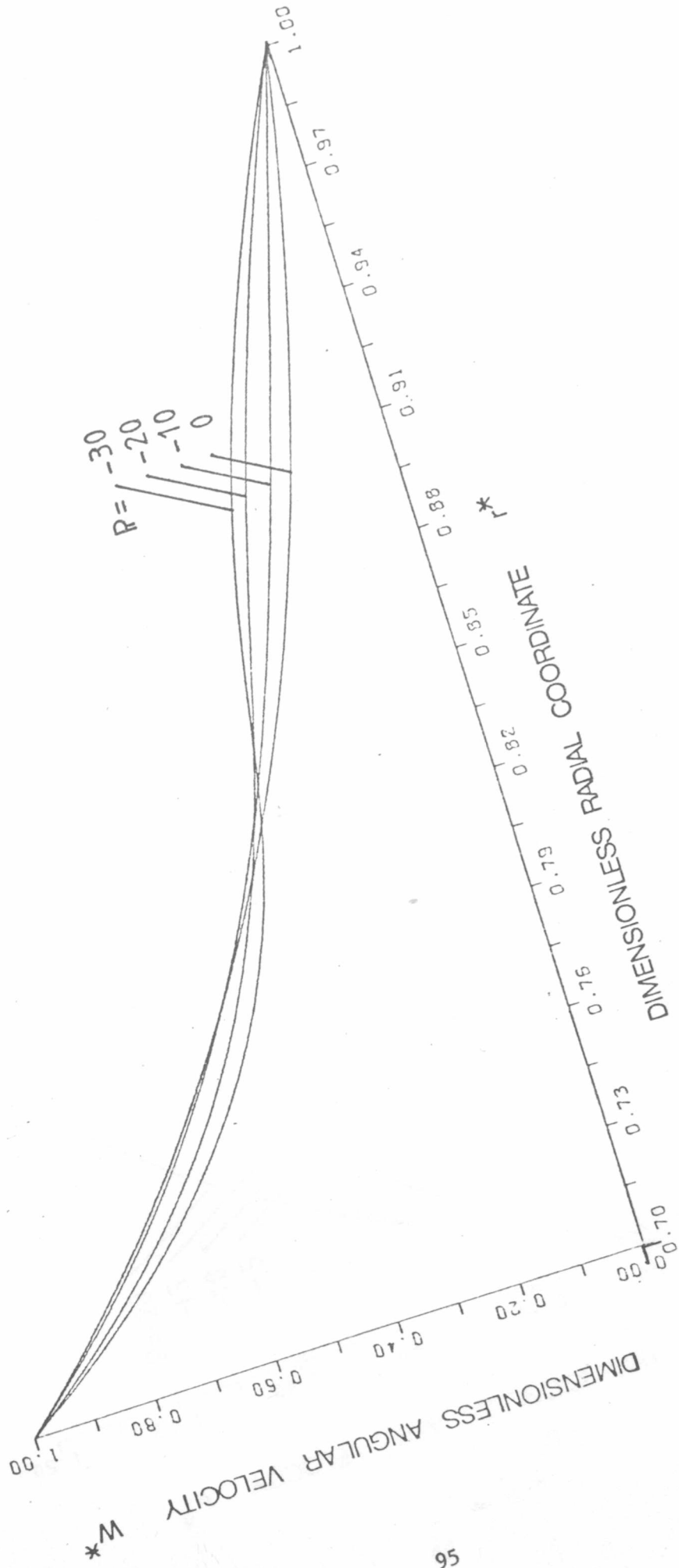
$k = 0.7$



$\kappa = 0.7$

HELIICAL FLOW OF A POWER LAW FLUID  
 $n = 0.5$

FIG. 4.19 R

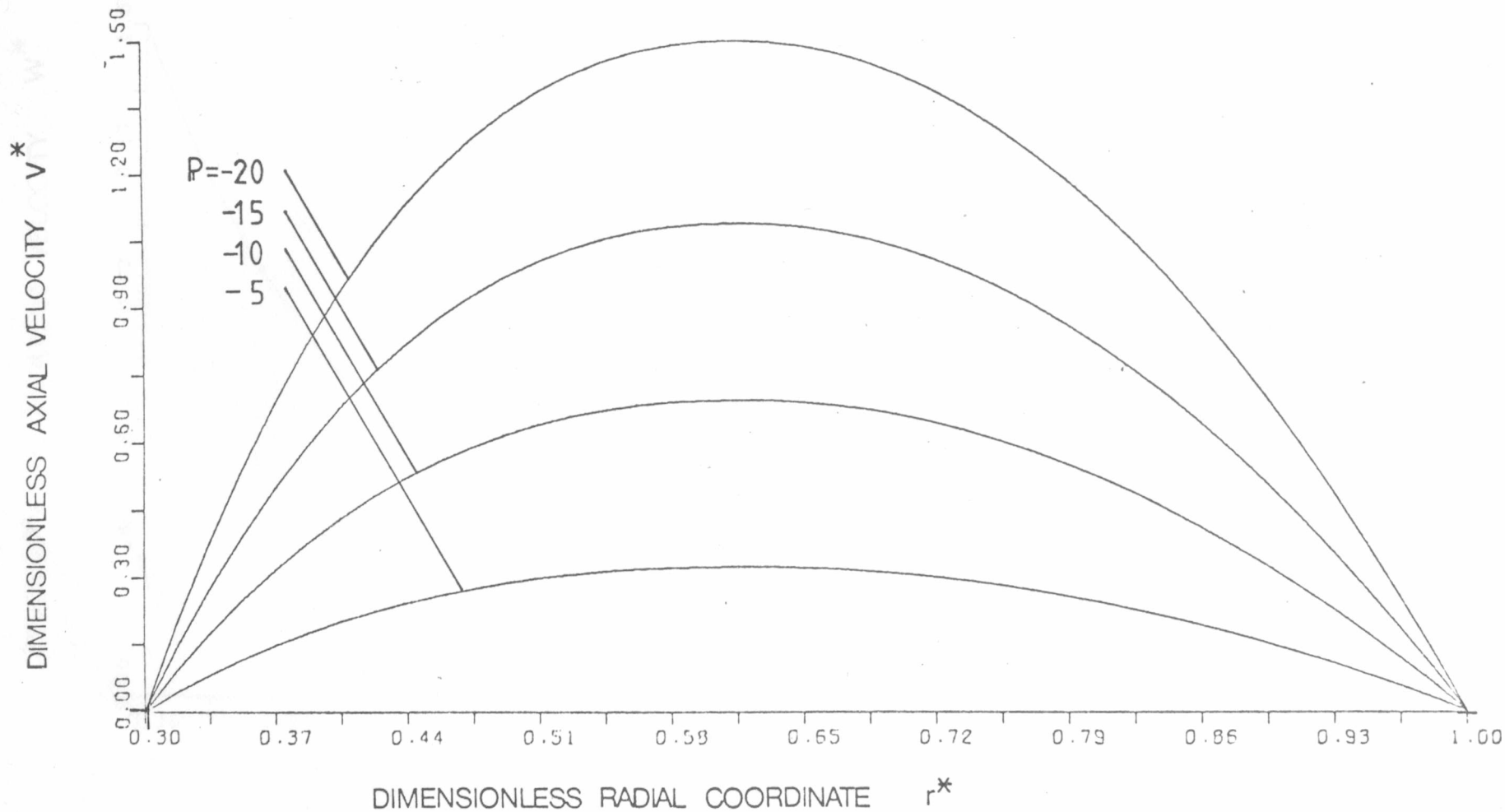


# HELICAL FLOW OF A POWER LAW FLUID

Fig. 4.20 A

$n = 0.9$

$k = 0.3$

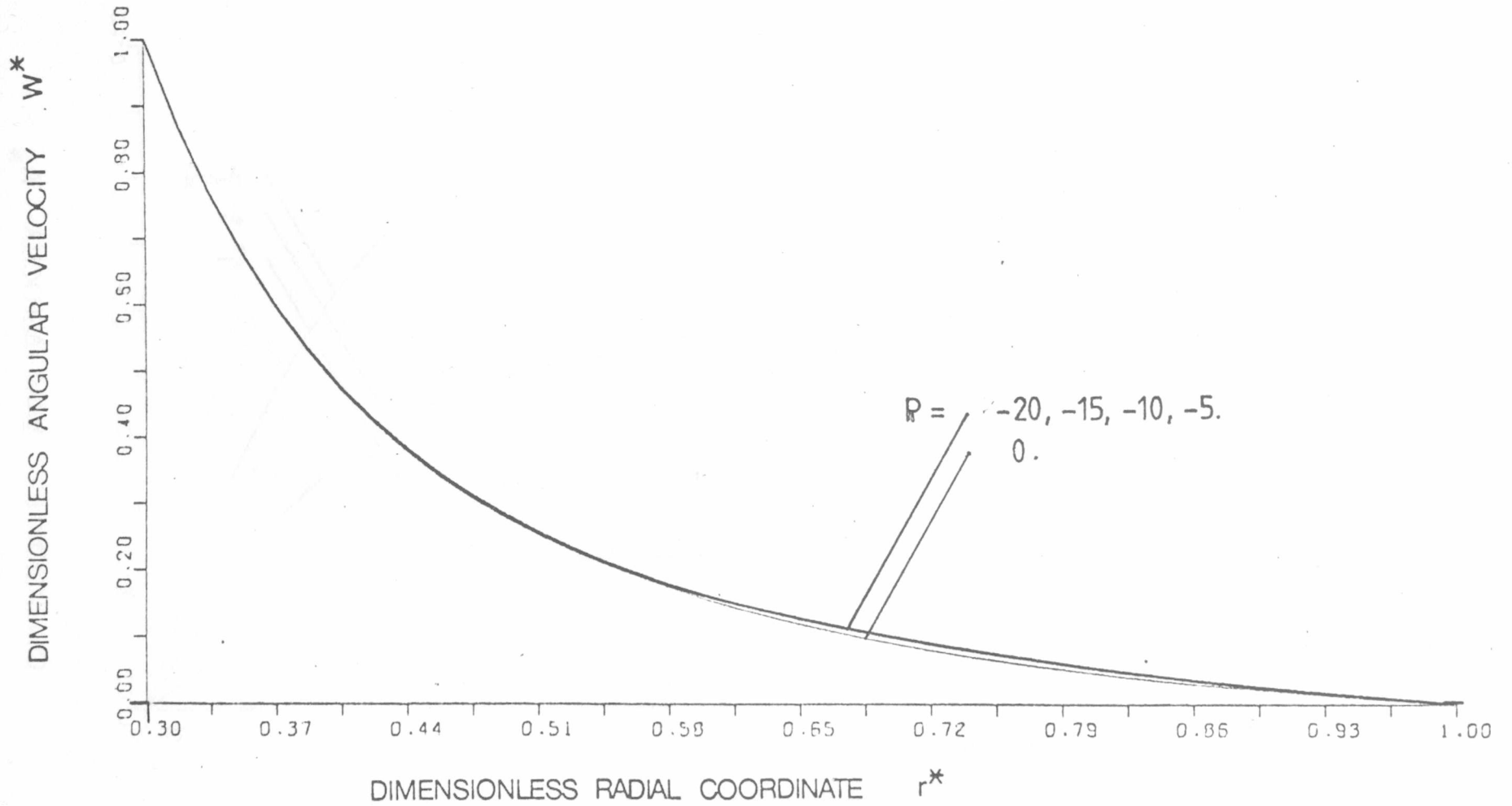


HELICAL FLOW OF A POWER LAW FLUID

Fig. 4.20 R

$n = 0.9$

$k = 0.3$

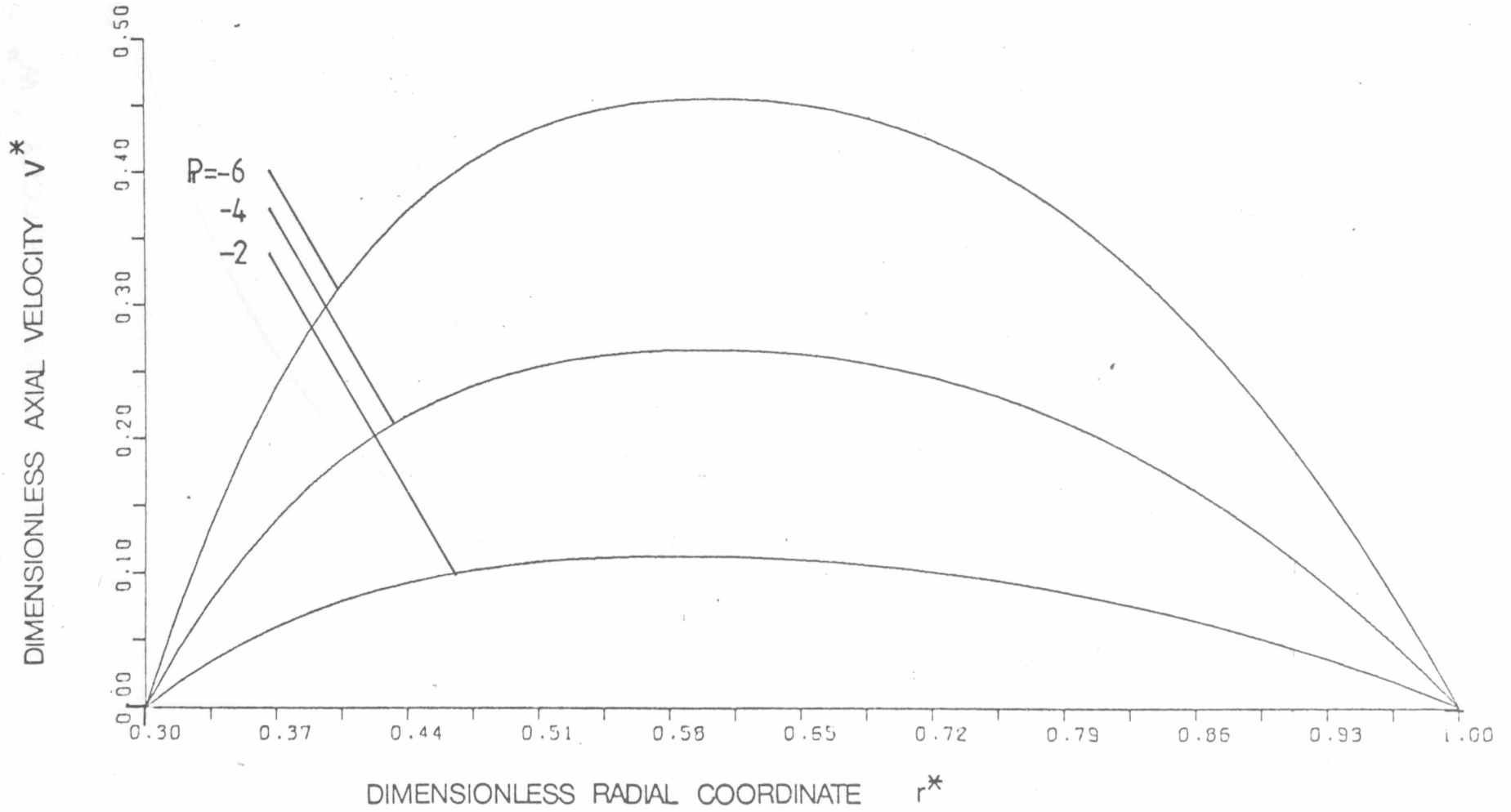


# HELICAL FLOW OF A POWER LAW FLUID

Fig. 4.21 A

$n = 0.7$

$k = 0.3$



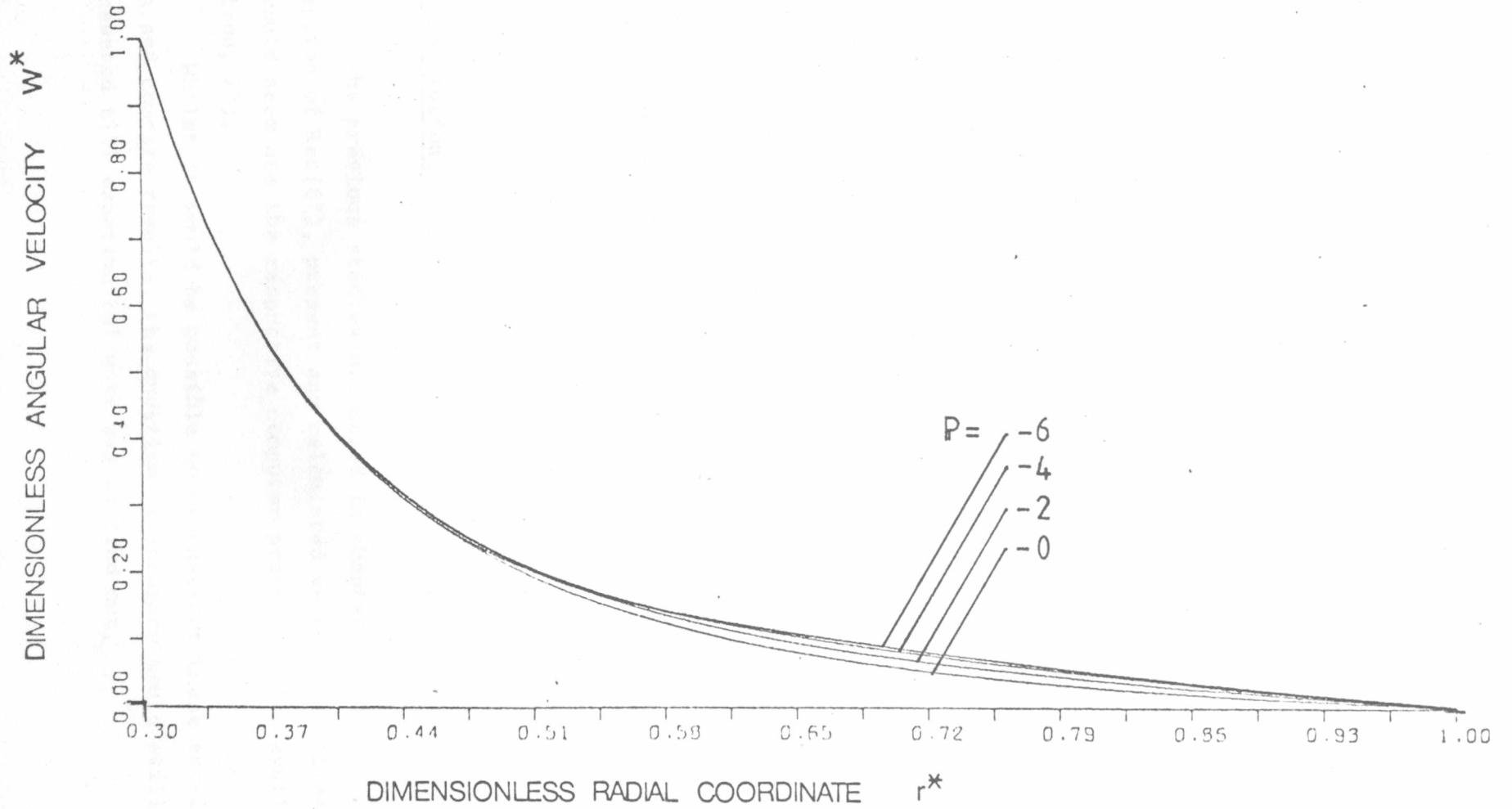
HELICAL FLOW OF A POWER LAW FLUID

Fig. 4.21 R

$n = 0.7$

$k = 0.3$

66



### 4.3 Physical representation of results.

In order to facilitate visualisation and discussion of results a physical model of the three dimensional flow field was constructed. The model represented a section of the annulus formed by the drill string and the outer casing. Radially positioned pins were used to represent the magnitude and direction of the flow field across the annulus. Realistic dimensions and parameters were used for the model and these are listed in table 4.6 . The model is illustrated in Fig. 4.7 .

INPUT PARAMATERS
Inner radius = 2.5 inches.
Outer radius = 9.5 inches.
Drill string rotation speed = 100 RPM.
Fluid : Power law with $n = .7$ and $m = .2$ .
Axial pressure gradient = $-10.8 \text{ Kg(m s)}^{-2}$ .
OUTPUT PARAMETERS
Average annular velocity = 55 feet/minute.
Volumetric flow rate = 625 gallons/minute.

TABLE 4.6 Parameters used for physical model.

### 4.4 Conclusion.

The previous studies discussed in chapter 3 did not, with the exception of Rea(67), present any calculated velocity profiles. Nor, it would seem are the respective computer programs still available (Watson, 77).

Whilst it would be possible to reconstruct these earlier programs and compare results, the question of accuracy would still remain unanswered till experimental work was carried out.

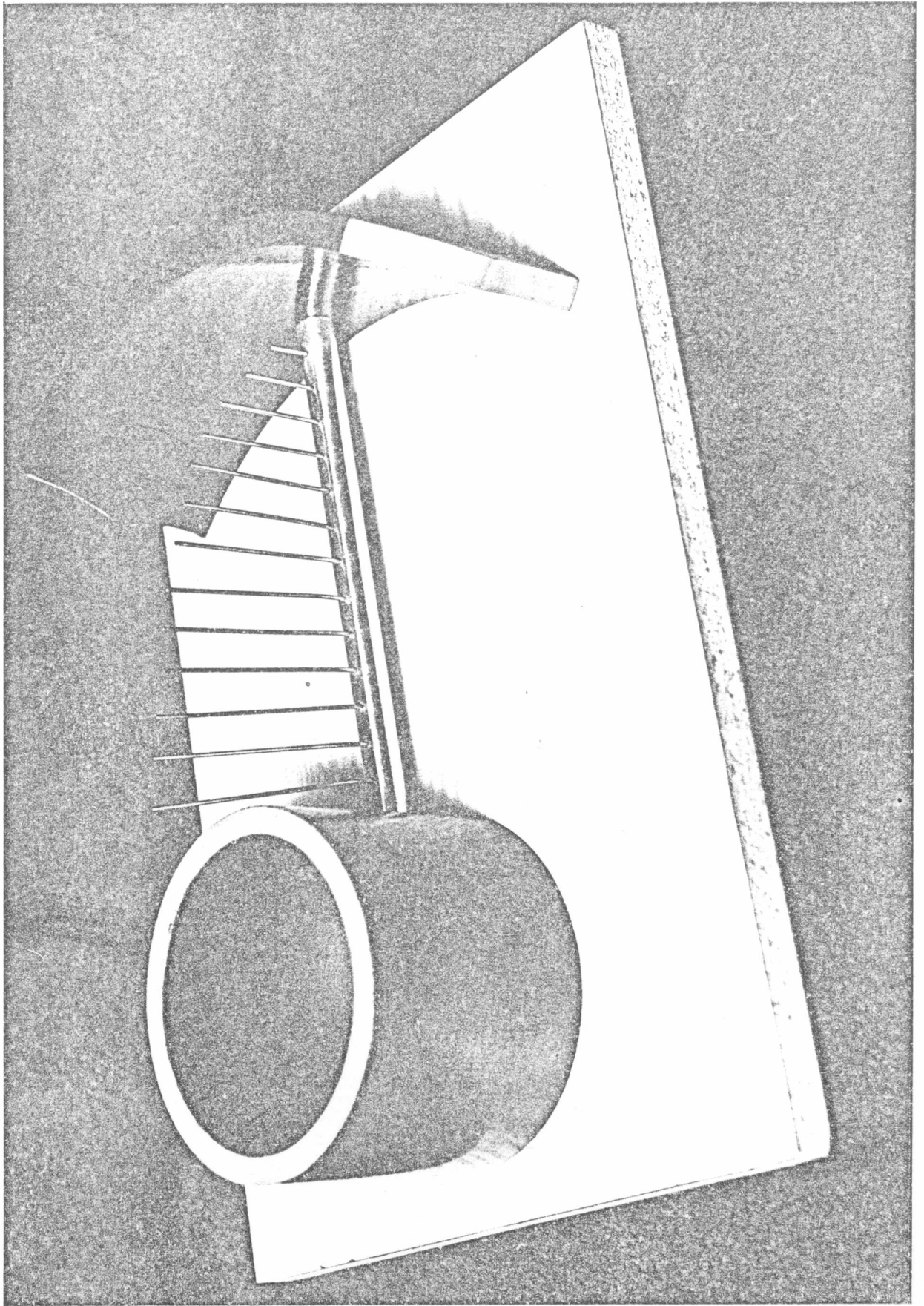


Fig. 4.7 PHYSICAL REPRESENTATION OF RESULTS

In view of the excellent agreement with Rea's experimental results reported in 4.1, it is hoped that future experimental results will support the predicted velocity profiles presented above.

In 4.2, the results obtained using MUDFLO were discussed using simple arguments to explain their characteristics. Since the results were found to be both explicable and sensible, it would seem reasonable to expect that this hope will be realised.

CHAPTER 5  
REVIEW, CONCLUSIONS AND RECOMMENDATIONS.

In the final chapter of this thesis, we review the previous chapters (5.1); restate the conclusions drawn (5.2) ; and make recommendations for further research into drilling fluid flow.

5.1 REVIEW.

5.1.1 Chapter 1 : Introduction

To provide suitable background for the present thesis, we gave an introductory discussion of drilling fluids and their purpose in chapter 1. We indicated that it is desirable to understand the nature of the flow of drilling fluids, but explained that geometric and rheological complexities preclude an exact analysis of the flow. The central aim of the thesis was introduced as ' the solution of the problem of predicting velocity profiles for non-Newtonian fluids flowing in an annulus with a rotating inner cylinder '. It was hoped that greater understanding of drilling fluid flow would be achieved through the solution of this problem.

To elucidate the scale of the problem, and to provide data for later calculations, typical values for the parameters involved were listed in 1.3 . It was noted however that, as with any such list, the values quoted could only be considered as ' representative ', with some omissions being inevitable.

5.1.2 Chapter 2 : Theoretical description.

In chapter 2, the governing equations for the flow of drilling fluid were discussed. It was shown that without several simplifying approximations, the equations are so complex as to be, for practical purposes at least, insoluble. The introduction of these simplifications led to the final mathematical model of ' Helical Flow ' given in 2.1 . This model describes a flow far removed from the flow of drilling fluids in oil wells, but it was argued that greater understanding of the original flow should be possible through understanding of this helical flow model.

In 2.2, the term ' fluid model ' was introduced as being some relation between shear rate and stress for the fluid in question. It was shown that for the helical flow model, fluid models of the form :

$$\underline{\tau} = f(\underline{a}:\underline{a}) \underline{a}$$

are of general applicability, and several examples were discussed. It was shown that, in helical flow at least, the fluid properties of viscoelasticity and thixotropy are unimportant.

A general system of non-dimensional variables was introduced in 2.3 and was extended for two particular fluid models.

### 5.1.3 Chapter 3 : Work on drilling fluid flow.

In 3.1, previous literature relevant to the problems of drilling fluid flow was reviewed and it was established that all previous work had used the mathematical model of helical flow, or a particular simplified case of it. Previous studies were found to have used one of two analysis methods, referred to as the ' integral formulation ' and the ' differential formulation ' . It was established that the more complex analyses involving partial differential equations had used the latter approach and the suggestion was made that it would be difficult to extend the former method to these cases. On this basis it was decided that, with a view to its later extension, the present thesis should adopt the differential formulation. It was noted that an additional advantage of this approach was its applicability to any fluid model of the type

$$\underline{\tau} = f(\underline{a}:\underline{a}) \underline{a} .$$

The computer algorithm developed for this thesis was described in 3.2 and reference made to the program listing in the appendices.

As experimental verification of results was outwith the scope of this research, a ' result assessment criterion ' based on the integral formulation was established.

It was noted that computational difficulties were encountered in calculations where very low velocity gradients occurred over large sections of the annular gap.

The difficulties appeared similar to those reported by Guickes (75) and were manifested in two ways :

- i) Calculations for Bingham plastics failed to converge in most cases.
- ii) The result assessment criterion was not satisfied in calculations for power law fluids with very low index  $n$ , especially when the radius ratio  $k$  was small.

These were taken to be limitations of the present algorithm, and their circumvention left as a matter for further research to be carried out after experimental verification of the results presented in chapter four.

#### 5.1.4 Chapter 4 : Results.

In 4.1, the velocity profiles predicted by MUDFLO were shown to be in excellent agreement with those measured experimentally by Rea(67) . This was taken as being indicative of the applicability of the finite difference approach to the helical flow problem.

In 4.2, the results of many calculations were presented using dimensionless variables. The results presented form a ' data base ' from which the velocity profiles for most practically occurring flows may be interpolated. The results were shown to be both 'explicable' and 'sensible' by discussion of their characteristics with reference to the shear rate profiles associated with each flow component.

#### 5.2 RESULTS AND CONCLUSIONS.

This research was motivated by a desire to understand better the flow of drilling fluids. To this end an analysis of the approximate model of helical flow has been performed with the result that a considerable amount of data for any particular flow condition is available through interpolation of the graphs presented in chapter 4, or by running the computer programme MUDFLO.

Many direct applications of these results to the practical problems of drilling fluid flow are possible. For example, estimates of the torque required to rotate the drill string in the fluid may be made, and thus the torque required at surface level to apply a certain torque to the drill bit may be deduced.

Similarly, the lift exerted on the drill string by the fluid may be estimated and the required load on the drill string to produce a certain load on the drill bit may be determined.

The interaction among the axial flow rate, the fluid parameters, and the axial pressure gradient can also be determined for any particular case, and the best combination of parameters for a given flow rate may be determined.

The initial motivation has thus been fulfilled to some extent. Immediate extensions of the work of this thesis are possible, affording even greater understanding of drilling fluid flow. These extensions are described in the section entitled ' further work ' .

The central aim of this thesis was to predict the velocity profiles for non-Newtonian fluids flowing in an annulus with a rotating inner cylinder. This too has been achieved, though to a lesser extent than the motivation discussed above. Solution of this problem has not however been achieved for cases in which low velocity gradients occur over large sections of the annular gap; in particular, no solution was obtained for Bingham plastics, and for power law fluids with low index  $n$  .

From the work of the thesis the following conclusions may be drawn ;

- 1) Whilst there are many variables to be specified for a particular helical flow of a power law fluid, the flow may be completely described by only three independent parameters:  $n$ ,  $k$ , and  $P$ .

A similar result holds for Bingham plastics.

- 2) The present work has resulted in the development of a computer programme which may be used with either dimensional or non-dimensional variables to give comprehensive information on many problems concerning the helical flow of non-Newtonian fluids.
- 3) Despite the occurrence of computational difficulties when very low velocity gradients were present over large sections of the annular gap, the iterative finite difference approach appears a useful technique for many of the problems of

drilling fluid flow. Its advantage over integral formulation based methods lies in its adaptability to more complex fluid flow situations. Problems arising from the computational difficulties described above are minimal since adequate indication of the quality of results is given by the computer program itself.

- 4) The results presented in chapter 4 have been supported both by the comparison with the experimental measurements of Rea (67) and by the integral formulation based data assessment criterion; with satisfaction of the latter criterion implying good agreement with integral formulation calculations.
- 5) It is apparent from the discussions in chapter 4 that much qualitative information on the nature and behaviour of velocity profiles in helical flow may be obtained by consideration of the shear rate profiles arising from each velocity component.
- 6) An incidental conclusion from the present work is that the technique of upwind differencing is not always suitable for use in an iterative calculation procedure.

### 5.3 RECOMMENDATIONS FOR FURTHER WORK.

Recommendations for further work may be divided into both short term investigations which can be carried out at the present time, and long term aims for future research. We consider each separately below.

#### A) SHORT TERM.

##### i) Experimental verification of results.

Of immediate importance is the experimental verification of the results presented in chapter 4. The techniques of Rea(67) may still be suited to this task, though use of a more sophisticated method such as laser Doppler or hot film anemometry (Frene,75) would possibly provide more accurate results and would facilitate later investigation of flow instabilities.

In conjunction with this, a preliminary investigation on stability could be carried out to see whether MUDFLO computational

difficulties reflect a physical flow instability. Full investigation of flow stability is however a long term project and is discussed below.

ii) Particle transport.

Another area of immediate interest is to assess particle transport capabilities of drilling muds under various flow conditions (Mayes & Walker, 75 ; Sifferman, 74).

B) LONG TERM.

Longer term aims of any research programme must be the full investigation of flow instabilities in the helical flow of non-Newtonian fluids, and their effect on particle transport properties; and the study of the flow of drilling fluids in conduits more complex than the idealistic concentric annulus used for the present work.

Starting points for the former study may be obtained from the following initial literature survey, whilst no literature is currently available on the latter topic.

5.3.1 Initial literature survey on instability in the helical flow of non-Newtonian fluids.

Denn and Roisman (69) discussed the onset of Taylor vortices in Couette flow of viscoelastic fluids and compared theoretical predictions with experimental work. A similar study was reported by Graebel (61).

McEachern (69) studied the transition from laminar to non-laminar flow with viscoelastic fluids flowing axially in an annulus. References are cited to indicate that a generalised Reynolds number does not provide a good criterion by which to judge the end of the laminar flow regime. The paper reports some success in the use of an alternative criterion. A similar criterion was also proposed by Walker and Korry (74).

Finally, a general reference on all aspects of instability in non-Newtonian fluid flow is given by Pearson(76).

The success of research programmes in the above areas should provide considerably deeper understanding of drilling fluid flow and its associated problems than is currently available.

APPENDIX A.      DERIVATION OF THE COMPONENTS OF THE SHEAR RATE TENSOR  
IN HELICAL FLOW.

In this appendix, we derive the components of the shear rate tensor  $\underline{\underline{\Delta}}$  for helical flow from the general expression for three dimensional flow in polar coordinates.

We recall from 2.2 that the components of  $\underline{\underline{\Delta}}$  for a general flow are

$$\begin{aligned} \Delta_{rr} &= 2 \left\{ \frac{\partial v_r}{\partial r} \right\} - \frac{2}{3} (\nabla \cdot \underline{v}) \\ \Delta_{\theta\theta} &= 2 \left\{ \frac{1}{r} \frac{\partial v_\theta}{\partial \theta} + \frac{v_r}{r} \right\} - \frac{2}{3} (\nabla \cdot \underline{v}) \\ \Delta_{zz} &= 2 \left\{ \frac{\partial v_z}{\partial z} \right\} - \frac{2}{3} (\nabla \cdot \underline{v}) \\ \Delta_{r\theta} &= r \frac{\partial}{\partial r} \left\{ \frac{v_\theta}{r} \right\} + \frac{1}{r} \frac{\partial v_r}{\partial \theta} = \Delta_{\theta r} \\ \Delta_{\theta z} &= \frac{\partial v_\theta}{\partial z} + \frac{\partial v_z}{\partial \theta} = \Delta_{z\theta} \\ \Delta_{rz} &= \frac{\partial v_z}{\partial r} + \frac{\partial v_r}{\partial z} = \Delta_{zr} \end{aligned}$$

where

$$(\nabla \cdot \underline{v}) = \frac{1}{r} \frac{\partial}{\partial r} \{ r \cdot v_r \} + \frac{1}{r} \frac{\partial v_\theta}{\partial \theta} + \frac{\partial v_z}{\partial z}$$

We first note that since  $v_r$  is zero and since all derivatives with respect to  $\theta$  and  $z$  are zero in helical flow,

$$(\nabla \cdot \underline{v}) = 0.$$

Using this result, we consider each component of  $\underline{\underline{\Delta}}$  in turn.

$$\underline{\underline{\Delta}}_{rr}$$

$$\Delta_{rr} = 2 \left\{ \frac{1}{r} \frac{\partial v_r}{\partial r} + \frac{v_r}{r} \right\}$$

= 0, since  $v_r = 0$  and all derivatives with respect to  $\theta$  and  $z$  are zero.

$$\underline{\Delta_{\theta\theta}}$$

$$\Delta_{\theta\theta} = 2 \left\{ \frac{1}{r} \frac{\partial v_\theta}{\partial \theta} + \frac{v_r}{r} \right\}$$

= 0, since  $v_r = 0$  and all derivatives with respect to  $\theta$  and  $z$  are zero.

$$\underline{\Delta_{zz}}$$

$$\Delta_{zz} = 2 \frac{\partial v_z}{\partial z} = 0, \text{ since all derivatives with respect to } z \text{ are zero.}$$

$$\underline{\Delta_{r\theta}}$$

$$\Delta_{r\theta} = r \frac{\partial}{\partial r} \left\{ \frac{v_\theta}{r} \right\} + \frac{1}{r} \frac{\partial v_r}{\partial \theta}$$

=  $r \frac{d}{dr} \left\{ \frac{v_\theta}{r} \right\}$  since all derivatives with respect to  $\theta$  and  $z$  are zero.

$$\underline{\Delta_{\theta z}}$$

$$\Delta_{\theta z} = \frac{\partial v_\theta}{\partial z} + \frac{\partial v_z}{\partial \theta}$$

= 0, since all derivatives with respect to  $\theta$  and  $z$  are zero.

$$\underline{\Delta_{rz}}$$

$$\Delta_{rz} = \frac{\partial v_z}{\partial r} + \frac{\partial v_r}{\partial z}$$

=  $\frac{dv_z}{dr}$  since all derivatives with respect to  $\theta$  and  $z$  are zero.

Thus in helical flow,

$$\underline{\underline{\Delta}} = \begin{bmatrix} 0 & r \frac{d}{dr} \left( \frac{v_\theta}{r} \right) & \frac{dv_z}{dr} \\ r \frac{d}{dr} \left( \frac{v_\theta}{r} \right) & 0 & 0 \\ \frac{dv_z}{dr} & 0 & 0 \end{bmatrix}$$

APPENDIX B. COMPUTER PROGRAM.

B.1 Description.

The computer program consists of one main routine ' MUDFLO ' and seven subroutines. Each subroutine is self contained and performs only one function. Another program ' DATIN ' is used to create an input data file on disc store.

The main program is divided into four main subsections, each performing only one function, and several small sections to control the operation of the subroutines. The functional sections of the main program and the subroutines are listed in table B.1, and the operation procedure is shown in figure B.2. Note that figure B.2 makes no distinction between main program subsections and subroutines.

The program is self documenting and is listed in B.2 . A list of variable names has been included in B.3 to aid interpretation of the listing.

Copies of the programs have been archived on magnetic tape by the Computing Services Unit, RGIT, Aberdeen ; and may be accessed using the archive numbers listed in B.4 .

TABLE B.1

SECTION NAME	FUNCTION	LOCATION
DATIN	Create input data file.	Separate program
PPRO	Read input data file; initialise and preprocess data.	MAIN
CNVRG	Control iteration cycle and test for convergence.	MAIN
DATOUT	Generate program output.	MAIN
CRASH	Print diagnostic information if the program run is aborted.	MAIN
MOVSET	Set up finite difference matrix.	Subroutine
SOLVSR	Solve finite difference matrix by successive over-relaxation methods.	Subroutine
SOLDR	Solve finite difference matrix using direct method.	Subroutine
VISCO	Update viscosity profile vector.	Subroutine
DIFF	Numerical differentiation.	Subroutine
VARIAN COORD	Post processing of results.	Subroutine

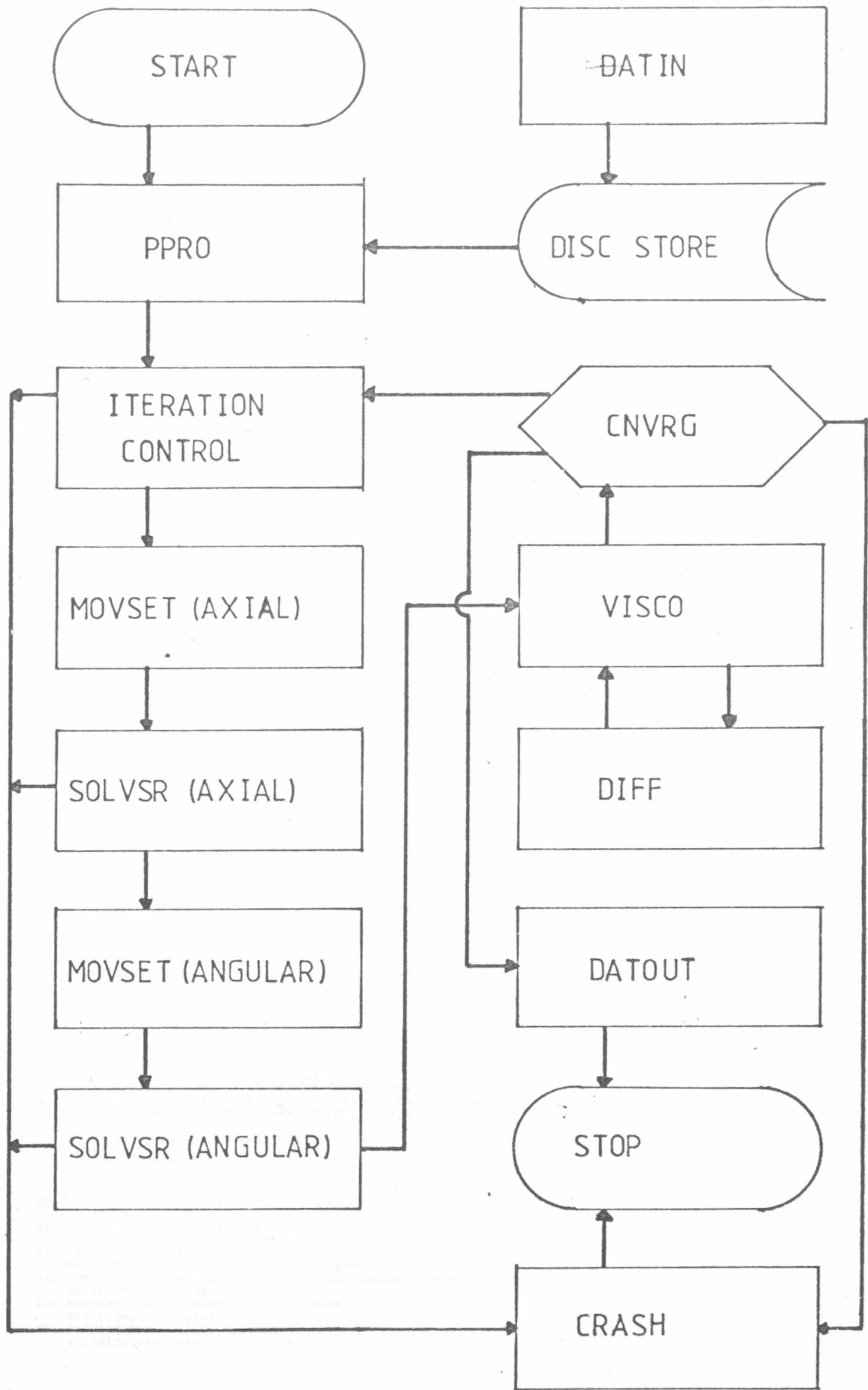


Fig. B.2

```

DIMENSION FLUID(6),RADIUS(60),VISCY(60),DVISCY(60),VZ(60),RVZ(60),
1DDVZ(60),VA(60),DVA(60),DDVA(60),VSOL(4,5R),ANGLE(60),ALPHA(60),
2CONST(60)
REAL LASTVZ(60),LASTVA(60),MODY(60)
INTEGER CRASH,DUMP,BATCH,BCHKNT,SET,CNTRL
EXTERNAL DIFF
C *****
C THE MUDFLO PROGRAM AND SUBROUTINES WERE WRITTEN BETWEEN OCT
C 76 AND MAY 78 BY JOHN MORTON AS PART OF A RESEARCH PROJECT FOR
C THE DEGREE OF M.PHIL. IN THE SCH. OF MECH. ENG., PGIT, ABERDEEN.
C
C THE PROGRAM IS DESIGNED TO PREDICT VELOCITY PROFILES THAT
C OCCUR WHEN NON-NEWTONIAN FLUIDS FLOW THROUGH AN ANNULUS WITH
C A ROTATING INNER CYLINDER. (E.G. DRILLING FLUID FLOW).
C
C A FINITE DIFFERENCE PROCEDURE IS USED WITH AN ITERATIVE LOOP :
C 1) GUESS INITIAL VISCOSITY PROFILE.
C 1-->2) CALCULATE VELOCITY PROFILES USING (1) OR (4).
C 1 3) TEST FOR CONVERGENCE. (STOP IF SO)
C 1-->4) CALCULATE NEW VISCOSITY ESTIMATE USING (2).
C
C THE SEPARATE PROGRAM 'DATIN.FOR' SHOULD BE RUN FIRST TO
C CREATE THE DATA FILE FOR36.DAT WHICH MUDFLO USES.
C
C OUTPUTS FROM MUDFLO ARE:
C CHANNEL 5 TTY: (KEY INFORMATION)
C " 25 LPT: (FULL PRINTOUT)
C " 40 DSK: (COPY OF ROTATIONAL VELOCITY PROFILE
C " COORDS FOR GRAPH PLOTS)
C " 41 DSK: ( " AXIAL " )
C *****
WRITE(5,10)
10 FORMAT(1H ,20X,' * * * * * ',/,
1 20X,' * M-U-D-F-L-O * ',/,
2 19X,' * * * * * ',/)
C ***
C ***
C P=P-R=0
C *** TO READ, PREPROCESS AND INITIALISE DATA. (22 MAY 77)
C *** TRANSFER OF DATA FROM FILE FOR36.DAT ***
OPEN(UNIT=36,DEVICE='DSK',FILE='FOR36.DAT')
READ(36,200)N,DUMP
200 FORMAT(I4)
MEMORY=DUMP
READ(36,205)RADIUS(1),RADIUS(N),VA(1),P ;! VA(1) FOR OIL BUT VA(N) FOR REA
205 FORMAT(2F10.4)
READ(36,210)(FLUID(I),I=1,6)
210 FORMAT(3F12.6)

READ(36,215)TOL,TOLMAT,LIM,LIMAT,SORFCT
215 FORMAT(2F11.5,2I4,F10.4)
CLOSE(UNIT=36,DEVICE='DSK',FILE='FOR36.DAT')
C *** END OF DATA TRANSFER ***
C DATA INITIALISATION
C BOUNDARY VALUES
I
VZ=AXIAL VELOCITY ,VA=ANGULAR VELOCITY
C VA(1) HAS BEEN READ,VA(1),VA(N),VZ(1),VZ(N) MAY ALSO BE SUPPLIED AS
C ...DATA BUT ARE 0 IN OIL WELL DRILLING (EXCEPT VA(1) )
C RADIUS(N) *MATRIX CONSTRUCTION
C CALCULATE F.D. INCREMENT H.
H=(RADIUS(N)-RADIUS(1))/(N-1)
DO 220 I=1,N
C IS REVALUING 1ST AND NTH ENTRIES REDUNDANT?
RADIUS(I)=RADIUS(1)+H*(I-1)
220 CONTINUE
C ITERATION CONVERGENCE? COUNTERS
KOUNT=0 ;KOUNT=0
TOL=TOL/1000000 ; TOLMAT=TOLMAT/1000000 ;TOL'S IN P.P.M. !!
C VISCOSITY MATRIX (NEWTONIAN APPROXIMATION)
DO 225 I=1,N
VISCY(I)=FLUID(6)
DVISCY(I)=0
225 CONTINUE
I
END OF DATA INITIALISATION
IF (FLUID(1).LE.10.0) WRITE(5,305)
IF (FLUID(1).LE.10.0) WRITE(25,305)
305 FORMAT(///,' DVISCY TO BE SET UP BY DIFFERENTIATING VISCY',/
1,' THIS IS UNRELIABLE IF LOW SHEAR-RATE OCCURS IN THE ANNULUS',/
2,' CHECK APPLICABILITY ! (SEE VISCO LISTING) ')
IF (DUMP.LT.1) GOTO 230
C *** OPTIONAL DUMPING OF VALUES ***
WRITE(25,300)
300 FORMAT(' P=P-R=0 ')
IF (DUMP.LT.2) GOTO 230
WRITE(25,310)
310 FORMAT(' DUMP VALUES : ')
WRITE(25,235)N,H
235 FORMAT(' N = ',I4,10X,' H = ',F10.4)
WRITE(25,240)VA(1),VA(N),VZ(1),VZ(N),P
240 FORMAT(' EDY,VALS.: ',4F10.4/' P = ',F10.4)
WRITE(25,245)TOL,TOLMAT,LIM,LIMAT,SORFCT
245 FORMAT(' CONVERGENCE PARAMETERS ',2F11.5,2I6,F10.4)
WRITE(25,250)(FLUID(I),I=1,6)
250 FORMAT(' FLUID PARAMETERS ',3F12.6)
WRITE(25,255)(I,I=1,N)
255 FORMAT(' NODE ',5(4X,I4,3X))
WRITE(25,260)(RADIUS(I),I=1,N)

```

MAIN(2)

```

260 FORMAT(' PAD: ',5(X,F10.4))
WRITE(25,265)(VISCY(I),I=1,N)
265 FORMAT(' VISCY',5(X,F10.4))
C *** END OF VALUE DUMP ***
230 CONTINUE !! END OF PPRO
C 0-P-P-P
C ***
C ***
      BATCH=5
1000 CONTINUE !! 1-T-E-R-A-T-I-O-N C-Y-C-L-E-F S-T-A-R-T-S H-E-R-E
C *** FIRST CALCULATE VELOCITY DISTRIBUTIONS
      IF ((VA(1),EQ,0).AND.(VAC(N),EQ,0)) GO TO 2000 !! AXIAL FLOW ONLY
C *** COMPUTE THE ANGULAR VELOCITY DISTRIBUTION (VA(I))I=1,N)
      IF (CNTRL,EQ,3) CNTRL=7 !!RESET CNTRL
      IF (CNTRL,EQ,1) CNTRL=0 !!RESET CNTRL
400 DUMP=0
      CALL MOVSET(3,0,0,0,N,H,CNTRL,DUMP,RADIUS,VISCY,DVISCY,VA,
      VSOL)
C *** N,B. RECALL THAT THE FIRST TWO ARGUMENTS IN MOVSET DETERMINE
C *** WHICH VELOCITY COMPONENT IS CONSIDERED.
      DUMP=0
      CALL SOLVSR(VSOL,VA,LIMAT,TOLMAT,SORPECT,CNTRL,KOUNTN,DUMP,N)
C *** IF (CNTRL=2) THEN NO SOLN FOUND TO CENTRAL MATRIX.
C *** COULD 'GOTO 400' FOR F/R SCHEME MATRIX BUT AS A RESULT OF RUNS #22.1 & #22.2,
C *** THIS WAS DISSALLOWED ON 11DEC.
      IF (CNTRL,EQ,1) GO TO 405 !! SOLUTION O.K. (ORIGINALLY (.NE.4))
      CRASH=10 !! NO SOLN. TO MATRIX (ANGULAR COMPONENT)
      GO TO 5000 !! C-R-A-S-H
405 CONTINUE !! VA(60) NOW HOLDS ANGULAR VELOCITY DISTRIBUTION
      IF ((VZ(1),EQ,0).AND.(VZ(N),EQ,0)).AND.(P,EQ,0) GO TO 430
C *** IF SO, THEN ROTATIONAL FLOW ONLY.
      CONTINUE !! COMPUTE AXIAL VELOCITY DISTRIBUTION (VZ(I))I=1,N)
2000 IF (CNTRL,EQ,3) CNTRL=2 !! RESET CNTRL
410 IF (CNTRL,EQ,1) CNTRL=0 !!RESET CNTRL
420 DUMP=0
      CALL MOVSET(1,0,P,N,H,CNTRL,DUMP,RADIUS,VISCY,DVISCY,VZ,VSOL)
      DUMP=0
      CALL SOLVSR(VSOL,VZ,LIMAT,TOLMAT,SORPECT,CNTRL,KOUNTN,DUMP,N)
C *** IF (CNTRL=2) THEN NO SOLN TO CENTRAL MATRIX.
C *** COULD 'GOTO 420' FOR F/R MATRIX,BUT AS A RESULT OF RUNS #22.1 & #22.2 .
C *** THIS WAS DISSALLOWED ON 11DEC.
      IF (CNTRL,EQ,1) GO TO 425 !! SOLUTION O.K. (ORIGINALLY (.NE.4))
      CRASH=1 !! NO SOLN. TO F/R MATRIX (AXIAL COMPONENT)
      GO TO 5000 !! C-R-A-S-H
425 CONTINUE !! VZ(60) NOW HOLDS AXIAL VELOCITY DISTRIBUTION
430 CONTINUE
C *** NOW HAVE CURRENT VELOCITY DISTRIBUTIONS FOR THIS ITERATION
C *** SET UP VISCOSITY DISTRIBUTION HERE FOR CONVENIENCE

C V-I-S-C-O-S-I-T-Y
      IF (FLUID(1),EQ,0) GO TO 4000 !! D-A-T-O-U-T FOR NEWTONIAN FLUID
C *** SECTION TO UPDATE VISCOSITY PROFILE ESTIMATE
      DUMP=0
      CALL VISCO(FLUID,VZ,VA,RADIUS,N,H,DUMP,VISCY,DVISCY,CRASH,DVA,DDVA
      I,DVZ,DDVZ,P,ALPHA)
C *** VISCY NOW HOLDS VISCOSITY ESTIMATE
C *** NOTE THAT A WARNING SHOULD BE PRINTED IF FLUID(1) IS L.T. 10 !
      IF (CRASH,EQ,2) GO TO 5000 !! C-R-A-S-H (NO SUCH MODFL)
C Y-T-I-S-O-C-S-I-Y
C *** TEST FOR CONVERGENCE USING SECTION C-N-Y-R-G
C C-N-Y-R-G
      RCHKNT=RCHKNT+1 !! RESET BATCH-CONTROLLER
      KOUNT=KOUNT+1 !! RESET ITERATION COUNTER
      IF (FLUID(1),EQ,0) GO TO 4000 !! D-A-T-O-U-T FOR NEWTONIAN FLUID
C *** IF ((KOUNT,GT,5).OR.(RCHKNT,EQ,BATCH)) GO TO 505
C *** PRINT FROM FIRST FEW ITERATIONS
C *** WRITE(25,530)KOUNT
C *** WRITE(25,550)(VZ(I),I=1,N)
C *** WRITE(25,560)(VA(I),I=1,N)
505 IF (RCHKNT,LT,(BATCH-1)) GO TO 1000 !! BATCH NOT COMPLETE !NEXT ITERATION
C *** INTEGER BATCH INITIALISED AT BEGINNING OF MUDFLO !
C *** COULD BE READ BY P-P-R-O THROUGH.
      IF (RCHKNT,EQ,BATCH) GO TO 500 !! BATCH COMPLETE ! TEST CONVERGENCE
C *** ON MULTIMATE ITERATION OF BATCH,STORE LASTVA + LASTVZ FOR TEST
      DO 510 I=1,N
          LASTVA(I)=VA(I)
          LASTVZ(I)=VZ(I)
510 CONTINUE
      GO TO 1000 !! NEXT ITERATION TO COMPLETE THE BATCH
C *** END OF BATCH-CONTROLLER
500 CONTINUE !! BATCH COMPLETE SO SET UP CONVERGENCE TEST
C *** IF BATCH=1,THERE MAY BE PROBLEMS !
      DO 520 I=1,N
          DIVDR = ABS(VA(I))
          DIZDR = ABS(VZ(I))
          IF ((DIVDR,LT,(10**10)).AND.(DIZDR,LT,(10**10))) GO TO 525
          CRASH=4 !!SOLUTION TENDING TO INFINITY
          GO TO 5000 !! C-R-A-S-H
525 CONTINUE
          IF (DIVDR,LT,0.0001) DIVDR=0.0001 !! TO AVOID DIVISION BY 0
          IF (DIZDR,LT,0.0001) DIZDR=0.0001 !! TO AVOID DIVISION BY 0
          ACHECK = ABS(VA(I)-LASTVA(I))/DIVDR
          ZCHECK = ABS(VZ(I)-LASTVZ(I))/DIZDR
999 IF (ACHECK,GT,TOL) GO TO 527 !!FAIL TEST BY ANGULAR COMPONENT
      IF (ZCHECK,GT,TOL) GO TO 527 !!FAIL TEST BY AXIAL COMPONENT
520 CONTINUE
      GO TO 4000 !! TEST PASSED SO PRINT RESULTS (D-A-T-O-U-T)

```

```

R24 FORMAT(1H1,///,' ROTATIONAL COMPONENT (I.E. ANGULAR VELOCITY)')
WRITE(25,828)(I,I=1,N)
WRITE(25,830)(VA(I),I=1,N)
WRITE(25,832)(LASTVA(I),I=1,N)
WRITE(25,834)(DVA(I),I=1,N)
DO 833 I=1,N
  CONST(I)=RADIUS(I)*DVA(I)
833 CONTINUE
WRITE(25,835)(CONST(I),I=1,N)
WRITE(25,836)(DVA(I),I=1,N)
WRITE(25,838)
838 FORMAT(1H1,///,' AXIAL COMPONENT ')
WRITE(25,840)(I,I=1,N)
WRITE(25,842)(VZ(I),I=1,N)
WRITE(25,844)(LASTVZ(I),I=1,N)
WRITE(25,846)(DVZ(I),I=1,N)
WRITE(25,848)(DDVZ(I),I=1,N)
WRITE(25,848)
848 FORMAT(1H1,///,' VISCOSITY')
WRITE(25,850)(I,I=1,N)
WRITE(25,852)(VISCY(I),I=1,N)
WRITE(25,854)(DVISCY(I),I=1,N)
WRITE(25,854)(ALPHA(I),I=1,N)
DO 856 I=1,N
  IF (ALPHA(I).NE.0.00001) GOTO 856
  WRITE(25,857)
  GOTO 858
856 CONTINUE
857 CONTINUE
858 FORMAT(/,' MODF ',R(X,F12.6))
859 FORMAT(/,' VA ',R(X,F12.6))
860 FORMAT(/,' LASTVA ',R(X,F12.6))
861 FORMAT(/,' DVA ',R(X,F12.6))
862 FORMAT(/,' DDVA ',R(X,F12.6))
863 FORMAT(/,' VZ ',R(X,F12.6))
864 FORMAT(/,' LASTVZ ',R(X,F12.6))
865 FORMAT(/,' DVZ ',R(X,F12.6))
866 FORMAT(/,' DDVZ ',R(X,F12.6))
867 FORMAT(/,' VISCY ',R(X,F12.6))
868 FORMAT(/,' DVISCY ',R(X,F12.6))
869 FORMAT(/,' ALPHA ',R(X,F12.6))
870 FORMAT(/,' MINIMUM SHEAR RATE LIMIT HAS BEEN APPLIED')
1 ' ...SEE ALPHA VECTOR')
C
C=N-O-R-D
CALL COORD(RADIUS,VZ,VZ,MODV,ANGLE,N)
WRITE(25,860)
WRITE(25,870)(MODV(I),I=1,N)

WRITE(25,880)(ANGLE(I),I=1,N)
860 FORMAT(1H1,///,' VECTORIAL SUM OF AXIAL AND ROTATIONAL VELOCITY')
870 FORMAT(/,' V ',R(X,F12.6))
880 FORMAT(/,' ANGLE ',R(X,F12.6))
C
D=P-O-T-C
I=N-T-F-G-P-A-T-O-P
C *** WE USE THE TRAPEZOIDAL RULE TO CALCULATE VOLUMETRIC FLOW RATE (Q)
C *** ...AND AVERAGE ANNUAL VELOCITY (AVANVZ)
Q=RADIUS(1)*VZ(1) + RADIUS(N)*VZ(N)
DO 890 I=2,N-1
  Q=Q + 2*RADIUS(I)*VZ(I)
890 CONTINUE
AVANVZ = Q*H / ((RADIUS(N)**2) - (RADIUS(1)**2))
Q=Q*H * 3.141592654
WRITE(25,892)
892 FORMAT(1H1,///,' AXIAL FLOW RATES THROUGH THE ANNULUS '///)
QIMP=Q*60.0 * 1000.0 / 4.546
QUSA=QIMP / .8327
WRITE(25,894),QIMP,QUSA
894 FORMAT(' VOLUMETRIC FLOW RATE =',F12.6,/,
1 ' ( =',F12.6,' IMPERIAL GALS/MIN IF MKS INPUT DATA USED )'
2 ' ( =',F12.6,' U.S.A. GALS/MIN IF MKS INPUT DATA USED )')
WRITE(5,896)AVANVZ
WRITE(25,896)AVANVZ
896 FORMAT(/,' AVERAGE ANNUAL VELOCITY IS ',F12.6,/,
1 ' NOTE: AVERAGE ANNUAL VELOCITY DEFINED AS...',/
2 ' [(VOLUMETRIC FLOW RATE) / (DISCHARGE AREA)] ')
C
P=O-T-I-P-G-F-T=N-I
A=N-A-L-Y-S-I-S
C *** TO ANALYSE RESULTS,CALCULATE FORCES ON CYLINDERS,
C *** ...AND ENABLE COMPARISON WITH OTHER AUTHOR'S RESULTS
C *** [SEE "INTEGRAL EQUATION DESCRIPTIONS..." 1DEC77 NOTES]
WRITE(25,900)
900 FORMAT(1H1,///,' RESULT ANALYSIS')
DO 902 I=1,N
  CONST(I)=2.0*3.141592654*VISCY(I)*DVA(I)*(RADIUS(I)**3)
902 CONTINUE
WRITE(25,904)
WRITE(5,904)
904 FORMAT(/,' CONSTANT = (ROTATIONAL TORQUE APPLIED)')
WRITE(25,920)(CONST(I),I=1,N)
WRITE(5,920)(CONST(I),I=1,N)
CALL VARIAL(P,CONST,AV,STDDEV,PERCNT)
WRITE(25,906)AV
906 FORMAT(/,' THROU PER UNIT LENGTH REQUIRED ON CYLINDERS =',F12.6)
WRITE(5,922)STDDEV,PERCNT
WRITE(25,922)STDDEV,PERCNT
DO 908 I=1,N

```

```

527 IF (KOUNT.LT.LIM) GO TO 529
    CRASH=5 ;!TOO MANY ITERATIONS
    GOTO 5000 ;! C-R-A-S-H
529 CONTINUE ;! RESET PARAMETERS FOR NEXT BATCH OF ITERATIONS
    ACHECK=0
    ZCHECK=0
    BCHKNT=0 ;DUMPEMEMORY
C *** RECALL THAT LASTVZ + LASTVA ARE RESET ON THE PENULTIMATE ITERATION
C *** .. OF A BATCH.
    IF (DUMP.LT.2) GOTO 1000;! START NEW BATCH
C *** OPTIONAL PRINT
    WRITE(25,530)KOUNT
530 FORMAT(//,' MUDFLO AT ITERATION',I6)
    IF (DUMP.LT.3) GO TO 1000;! NEXT BATCH
    WRITE(25,540)
540 FORMAT(' PRESENT VALUES')
    WRITE(25,550)(VZ(I),I=1,N)
550 FOPMAT(/(' VZ ',R(X,E12.6)))
    WRITE(25,560)(VA(I),I=1,N)
560 FOPMAT(/(' VA ',R(X,E12.6)))
    GO TO 1000;! START NEXT BATCH OF ITERATIONS
C *** END OF CONVERGENCE TEST SECTION
C C-R-V-A-C
C ***
C D-A-T-O-U-T
4000 CONTINUE ;! DATOUT TO PRINT RESULTS
    WRITE(5,800)KOUNT
    WRITE(25,800)KOUNT
800 FORMAT(1H1,///,' MUDFLO CONVERGENCE ATTAINED AFTER'
    I ,I6,' ITERATIONS')
    GO TO 4100
C
C-R-A-S-H
5000 CONTINUE ;! CRASH (SUBSECTION OF DATIN)
    WRITE(5,600)
    WRITE(25,600)
600 FORMAT(1H1,///,10X,' C-R-A-S-H'//)
    WRITE(5,605)CRASH,KOUNT
    WRITE(25,605)CRASH,KOUNT
605 FORMAT(' CRASH TYPE',I3,' AFTER ',I5 ' ITERATIONS'//)
C *** SOLYSR CRASH ANALYSIS
    IF ((CRASH.NE.1).AND.(CRASH.NE.10)) GOTO 610 ;! NOT A SOLYSR CRASH
C *** WE CALL MOVSET AND SOLYSR WITH HIGH DUMP AND THEN STUDY THE DIAGONAL
C *** DOMINANCE OF THE VSOL MATRICES.FINALLY WE RESET THE COMPONENT
C *** CAUSING THE CRASH (V% ) TO ZERO,AS V% WILL NOT HAVE BEEN UPDATED AND
C *** SO WILL BE EQUAL TO LASTV%
    WRITE(25,615)
615 FORMAT(' CRASH DUE TO SOLYSR FAILURE'//,4X,
    I ' CRASH ANALYSIS DATA AS FOLLOWS'//)

C *** ANGULAR FIRST
    CALL MOVSET(3,0,0,0,N,H,0,3,RADIUS,VISCY,DVISCY,VA,VSOL)
    CALL SOLYSR(VSOL,VA,LIMAT,TOLMAT,SORFCT,CNTRL,KOUNTM,3,N)
C *** NOW AXIAL
    CALL MOVSET(1,0,P,N,H,0,3,RADIUS,VISCY,DVISCY,VZ,VSOL)
    CALL SOLYSR(VSOL,VZ,LIMAT,TOLMAT,SORFCT,CNTRL,KOUNTM,3,N)
C *** DIAGONAL DOMINANCE
    WRITE(25,620)
620 FORMAT(//,' ROW',RX,' 1/R',11X,' 3/P',6X,' DVISCY/VISCY',
    I ' H*PEA POTL',3X,' H*PEA AXIAL')
    DO 625 I=1,N
        R1=1/RADIUS(I)
        R3=3*R1
        DVIVI=DVISCY(I)/VISCY(I)
        PEAROT=(R1+DVIVI)*H
        PEAAXI=(R3+DVIVI)*H
        WRITE(25,630)I,R1,R3,DVIVI,PEAROT,PEAAXI
630 FORMAT(1H ,I4,X,5(3X,E12.6))
625 CONTINUE
    IF (CRASH.EQ.1) GOTO 635
    DO 640 I=1,N
        VA(I)=0 ;! NOT YET UPDATED !
640 CONTINUE
    GOT 645
635 DO 650 I=1,H
        VZ(I)=0 ;! NOT YET UPDATED !
650 CONTINUE
645 CONTINUE
C *** SISTLANA HSAPC RSVLOS
610 CONTINUE
C
H-S-A-R-C
4100 WRITE(25,810)
810 FORMAT(' INPUT DATA AS FOLLOWS: '//)
C *** WE USE THE P-P-R-O FORMAT STATEMENTS
    WRITE(25,235)N,H
    WRITE(25,240)VA(1),VA(N),VZ(1),VZ(N),P
    WRITE(25,245)TOL,TOLMAT,LIM,LIMAT,SORFCT
    WRITE(25,250)(FLUID(I),I=1,6)
    WRITE(25,812)
    WRITE(25,814)(RADIUS(I),I=1,N)
812 FORMAT(//,' RADIAL COORDINATE OF NODES AS FOLLOWS :')
814 FORMAT(/(' RADIUS',R(X,E12.6)))
    IF (CRASH.FQ.2) GO TO 6000 ;! STOP
    IF (CRASH.FQ.0) WRITE(25,820)
    IF (CRASH.NE.0) WRITE(25,822)
    WRITE(25,824)
820 FORMAT(/////,' RESULTS AS FOLLOWS'//)
822 FORMAT(/////,' VALUES AT TIME OF CRASH AS FOLLOWS'//)

```

MAIN(5)

```

CONST(I)=RADIUS(I) * (VISCY(I)*DVZ(I) - 0.5*P*RADIUS(I))
908 CONTINUE
WRITE(25,910)
WRITE(5,910)
910 FORMAT(// ' CONSTANT A : [AXIAL] ')
WRITE(25,920)(CONST(I),I=1,N)
WRITE(5,920)(CONST(I),I=1,N)
CALL VARIAN(N,CONST,AV,STODEV,PERCNT)
WRITE(25,912)AV
912 FORMAT(// ' CONSTANT A =',E12.6)
WRITE(5,922)STODEV,PERCNT
WRITE(25,922)STODEV,PERCNT
C *** CALCULATE DRAG LIFT ON CYLINDERS
DRAGI=3.141592654*(2.0*AV + P*(RADIUS(I)**2))
DRAGO=3.141592654*(2.0*AV + P*(RADIUS(N)**2))*(-1)
WRITE(25,914)DRAGI,DRAGO
914 FORMAT(// ' DRAG LIFT ON INNER CYLINDER =',E12.6/
' DRAG LIFT ON OUTER CYLINDER =',E12.6)
C *** FIND PLANE OF ZERO (Z,R)-SHEAR-STRESS
ALAMD2=-2.0*AV/P
IF (ALAMD2.LT.0.0) WRITE(25,916)
IF (ALAMD2.LT.0.0) GO TO 924
916 FORMAT(// ' NO PLANE OF ZERO (Z,R)-SHEAR-STRESS EXISTS')
ALAMDA=-2.0*(AV+STODEV)/P**0.5
ALAMDII=(-2.0*(AV+STODEV)/P)**0.5
ALAMDLI=(-2.0*(AV-STODEV)/P)**0.5
WRITE(25,918)ALAMDA,ALAMDII,ALAMDLI
918 FORMAT(// ' PLANE OF ZERO (Z,R)-SHEAR-STRESS OCCURS AT RADIUS =',
'E12.6/' WITH UPPER BOUND =',E12.6/
' AND LOWER BOUND =',E12.6)
920 FORMAT(//(' ',R(X,E12.6)))
922 FORMAT(' WITH STANDARD DEVIATION',E12.6/
' AND MAX PERCENT DIFFERENCE',E12.6,/'W=A-R=N-I=N=G I'/
' IF MAX PERCENT DIFFERENCE IS GREATER THAN 1/2,THEN'/
' RESULTS OF THIS RUN MAY BE UNRELIABLE')
924 CONTINUE
C S-I-S-Y-L-A-N-A
C G-R-A-P-H
C *** CREATE GRAPH DATA FILES
OPEN(UNIT=40,DEVICE='DSK',FILE='FOR40.DAT')
OPEN(UNIT=41,DEVICE='DSK',FILE='FOR41.DAT')
WRITE(40,930)((RADIUS(I),VA(I)),I=1,N)
WRITE(41,930)((RADIUS(I),VZ(I)),I=1,N)
930 FORMAT(1H ,E12.6,3H , ,E12.6)
CLOSE(UNIT=40,DEVICE='DSK',FILE='FOR40.DAT')
CLOSE(UNIT=41,DEVICE='DSK',FILE='FOR41.DAT')
C *** H-P-A-R-G
GO TO 6000 !I FINNISH AND STOP

C *** END OF DATOUT
C T-U-O-T-A-D
6000 CONTINUE
STOP
END

```

## MOVSET

```

SUBROUTINE MOVSET(SCALER,PRESSR,N,H,CNTRL,DUMP,RADIUS,VISCY,DVISCY
1,V,VSOL)
DIMENSION RADIUS(60),VISCY(60),DVISCY(60),V(60),VSOL(4,58)
INTEGER CNTRL,DUMP,ONE,THREE
C
C
C ***      ***      ***      ***      ***      ***      ***
C ***      M=0-V-S-E-T      *      *      *      *      *
C *** SURPROGRAM 1 OF M-U-D-F-L-D      * (4 JULY 77)      *      *
C ***      *      *      *      *      *      *      *
C *** TO SET UP FIN,DIFF,MATRIX VSOL      *      *      *
C *** VSOL(4,58) IS THE AUGMENTED,COMPRESSED MATRIX OF...
C *** ...FIN,DIFF,COEFFTS.( 'ALTERNATIVE STOPAGE' USED )
C *** COL1=LOWER DIAG. ,COL2=MAIN ,COL3=UPPER ,COL4=R.H.S.
C ***      *      *      *      *      *      *      *
C *** IF (DUMP,GE,1) WRITE(25,10)
10 FORMAT(' M=0-V-S-E-T RUNNING ')
IF (CNTRL,EQ,2) GOTO 20 ;! FORWARD/BACKWARD SCHEME REQUIRED
C *** SET UP VSOL(4,58) USING CENTRAL FINITE DIFFERENCE SCHEME
C *** WE GO THROUGH A LOOP FOR ROWS 1 TILL N-2 ,
C *** AND THEN 'ADJUST' THE FIRST AND LAST ROWS
DO 30 I=1,N-2
C *** PROGRAM SETS UP VSOL FOR THE GENERAL BDY.VALUE PROBLEM :
C *** Y'' + PFA(X)Y' + QUU(X)Y = RPP(X) ON (A,B)
C *** WITH Y(A) AND Y(B) KNOWN , AND QUU(X) <= 0
C *** IN OUR CASE , QUU(X) = 0 ,BUT WE LEAVE IT IN FOR GENERALITY
C
C *** FIRST,EVALUATE PFA,QUU AND RPP AT NODE J=I+1*****N.B.THAT:
C *** ...VSOL IS (4,58),WHILST VECTORS ARE (60)
C *** .....HENCE VSOL ROW(I) CORRESPONDS TO VECTOR(J)
J=I+1
PFA=SCALER/RADIUS(J) + DVISCY(J)/VISCY(J) ;!VISCY SHOULDN'T BE 0 !
QUU=0
RPP=PRESSR/VISCY(J)
C *** PLACE ENTRIES IN MATRIX (REFC,MOVSET DOCUMENTATION P6 (1JULY77))
VSOL(1,I) = 2.0*(PFA*H) ;! LOWER DIAGONAL ENTRY
VSOL(2,I) = -4.0*(QUU*H*H*2.0) ;! MAIN DIAGONAL ENTRY
VSOL(3,I) = 2.0*(PFA*H) ;! UPPER DIAGONAL ENTRY
VSOL(4,I) = 2.0*(RPP*H*H) ;! R.H.S.CONSTANT ENTRY
30 CONTINUE
GOTO 40 ;!ADJUST FIRST AND LAST ROWS,OPTIONAL PRINT,THEN RETURN
20 CONTINUE ;!SET UP VSOL USING FORWARD/BACKWARD FIN,DIFF,SCHEME
DO 50 I=1,N-2
C *** FIRST EVALUATE PFA,QUU,RPP (AS ABOVE)
J=I+1 ;! SEE NOTE ABOVE
PFA=SCALER/RADIUS(J) + DVISCY(J)/VISCY(J)
QUU=0
RPP=PRESSR/VISCY(J)
C
C *** ONE=1 ; THREE=3
C *** THESE VALUES PRODUCE VSOL ENTRIES FOR FORWARD FIN,DIFF,SCHEME.
C *** USING FORWARD SCHEME WHEN ARS(PFA) >= 0 ,AND BACKWARD WHEN < 0..
C *** ...ENSURES NON-SINGULARITY OF VSOL (SEE DOCUMENTATION)
IF (PFA,GE,0) GOTO 70 ;! FORWARD SCHEME
ONE = 3 ; THREE = 1 ;!INTERCHANGE VSOL ENTRIES TO GIVE BACKWARD SCHEME
IF (DUMP,GE,2) WRITE(25,80)
80 FORMAT(' BACKWARD SCHEME IN ROW ',I4)
70 CONTINUE
C *** SET UP VSOL MATRIX (F/B SCHEME )
VSOL(ONE,I) = 1.0
VSOL(2,I) = -2.0 -(ARS(PFA)*H)+(QUU*H*H)
VSOL(THREE,I) = 1.0 + H*ARS(PFA)
VSOL(4,I) = RPP*H*H
50 CONTINUE
40 CONTINUE ;!ADJUST FIRST AND LAST ROWS
VSOL(4,1)=VSOL(4,1)-VSOL(1,1)*V(1)
C *** ;! ;! ;! N.B. * NOT 'ONE' !!!
VSOL(4,N-2)=VSOL(4,N-2)-VSOL(3,N-2)*V(N)
VSOL(1,1)=0 ; VSOL(3,N-2)=0 ;! NOT REALLY NECESSARY (NEVER USED)
C *** OPTIONAL PRINT
IF (DUMP,LT,2) GOTO 90 ;! RETURN
IF (CNTRL,EQ,0) WRITE(25,100)
100 FORMAT(' CENTRAL DIFFERENCE SCHEME USED')
IF (CNTRL,EQ,2) WRITE(25,110)
110 FORMAT(' FORWARD/BACKWARD DIFFERENCE SCHEME USED')
IF (SCALER,EQ,1.0) WRITE(25,120)
120 FORMAT(' AXIAL VELOCITY COMPONENT')
IF (SCALER,EQ,3.0) WRITE(25,130)
130 FORMAT(' ANGULAR VELOCITY COMPONENT')
IF (DUMP,LT,3) GOTO 90
WRITE(25,140)((VSOL(K,I),K=1,4),I=1,N-2)
140 FORMAT('12X,' VSOL:',4(X,E11.5))
90 RETURN
END

```

SOLVSR(1)

```

SUBROUTINE SOLVSR (VSOL,V,LIMAT,TOLMAT,SORFCT,CNTRL,KOUNTM,DUMP,N)
DIMENSION VSOL(4,58),V(60),EX(60),RFSIDL(60)
REAL LASTEX(60)
INTEGER CNTRL,LIMAT,DUMP ,DUMMY,SET,CNTR
C
C ***      ***      ***      ***      ***      ***      ***      ***
C ***      S-O-L-V-S-R
C *** SUBPROGRAM 2 OF M-U-D-F-L-O      * (RJUNE 77)
C ***
C *** TO DETERMINE THE SOLUTION VECTOR OF THE COMPRESSED
C *** TRIDIAGONAL LIN-SYSTEM VSOL(4,58) BY
C *** SUCCESSIVE OVER-RELAXATION METHODS
C ***      ***      ***      ***      ***      ***      ***
C
IF (DUMP,LT,1) GOTO 20
WRITE(25,10)
10 FORMAT(' S-O-L-V-S-R RUNNING')
20 CONTINUE
C *** DATA INITIALISATION
KOUNTM=0;CHECK=0;SET=5
EX(1)=0;EX(N)=0
DO 30 I=2,N-1
EX(I)=V(I) ! COPY V(2,N-1) INTO EX FOR INITIAL GUESS SOLN.1
C *** WE NOW DIVIDE THROUGH EACH VSOL ROW BY ITS DIAGONAL ENTRY,AS
C *** THIS SAVES DOING IT IN EACH ITERATION
K=1-1
DIAGEL=VSOL(2,K)
IF (DIAGEL,EQ,0) GOTO 90 ! ZERO IN MAIN DIAGONAL !
DO 40 J=1,4
VSOL(J,K)=VSOL(J,K)/DIAGEL
40 CONTINUE
30 CONTINUE
50 CONTINUE ! *** S-O-R C-Y-C-L-E STARTS HERE *** !
C *** WE NOW GO THROUGH EX(60) VECTOR APPLYING SOR EQUATION , AND
C *** COMPARING EX(60) WITH LASTEX(60)
C *** EX(60) HOLDS THE CURRENT SOLUTION ESTIMATE , AND LASTEX(60) THE
C *** PREVIOUS ONE .
C *** N.B. THAT DIVISION BY PARTIAL DERIVATIVES (=VSOL(2,K)) HAS BEEN
C *** CARRIED OUT ABOVE.
DO 65 DUMMY=1,SET
C *** ITERATIONS DONE A SET AT A TIME ***
DO 60 I=2,N-1
K=I-1
EX(I)=EX(I)-SORFCT*(VSOL(1,K)*EX(I-1)+VSOL(2,K)*EX(I)+
VSOL(3,K)*EX(I+1)-VSOL(4,K))
60 CONTINUE
C *** RESET COUNTER BEFORE NEXT ITERATION

KOUNTM=KOUNTM+1
65 CONTINUE
C *** SET UP CONVERGENCE CHECK (EVERY 'SET' OF ITERATIONS)***
IF (KOUNTM,LE,SET) GOTO 70 ! 1ST SET,SO CANT TEST CONVERGANCE !
DO 75 J=2,N-1
IF (CHECK,GT,TOLMAT) GOTO 70 ! IF SO,FAIL CONVERGANCE TEST !
DIVIDR=ABS(EX(J))
IF (DIVIDR,GT,10**10) GOTO 92 ! SOLN. TENDING TO INFINITY !
IF (DIVIDR,LT,0.0001) DIVIDR=0.0001 !: TO AVOID DIVISION BY ZERO !:
CHECK=ABS(EX(1)-LASTEX(1))/DIVIDR
75 CONTINUE
70 CONTINUE
IF ((CHECK,LE,TOLMAT),AND,(KOUNTM,GT,SET)) GOTO 80
C *** IF CHECK < TOLMAT,CONVERGANCE O.K. BUT...
C *** ...BUT IF KOUNTM <= SET ,1ST SET SO CAN'T TEST CONVERGANCE
IF (KOUNTM,GE,LIMAT) GOTO 94 ! IF SO,TOO MANY ITERATIONS
C
C *** RESET PAPAETERS BEFOPE NEXT SET OF ITERATIONS ***
DO 150 I=1,N
LASTEX(I)=EX(I)
150 CONTINUE
CHECK=0
C
IF (DUMP,LT,4) GOTO 50 !: START NEXT SET OF ITERATIONS !
C *** OPTIONAL PPRINT
WRITE(25,110)KOUNTM
110 FORMAT(' S-O-L-V-S-R RUNNING AT',I5,' TH ITERATION'//
' CONVERGANCE NOT YET ATTAINED'// ' PRESENT VALUES ARE1')
WRITE(25,120)(I,I=1,N)
120 FORMAT(' NODE:',5(X,I4,3X))
WRITE(25,130)(EX(I),I=1,N)
130 FORMAT(' EX ',5(X,E10.4))
GOTO 50 !: START NEXT SET OF ITERATIONS !
C
80 CONTINUE !: CONVERGANCE ATTAINED , SOLUTION FOUND !
CNTRL=CNTRL+1
IF (DUMP,LT,1) GOTO 160
WRITE(25,170)KOUNTM,SORFCT
170 FORMAT(' SOLUTION OBTAINED AFTER',I5,' ITERATIONS'//
' SOR FACTOR =',F8.3)
IF(DUMP,LT,2) GOTO 160
WRITE(25,180)
180 FORMAT(' SOLUTION VECTOR AS FOLLOWS')
WRITE(25,120)(I,I=1,N)
WRITE(25,130)(EX(I),I=1,N)
WRITE(25,140)(LASTEX(I),I=1,N)
140 FORMAT(' LASTX',5(X,E10.4))
160 CONTINUE

```

## SOLVSR(2)

```

C
C *** INSERT SOLUTION EX(2,59) INTO VELOCITY VECTOR V(2,59)
DO 190 I=2,N-1
  V(I)=EX(I)
190 CONTINUE
GOTO 210 ;! OPTIONAL PRINT, THEN RETURN I
C
90 CONTINUE ;! OUTPUT FOR 3 CASES WHEN NO SOLN. FOUND I
WRITE(25,91)
91 FORMAT(' ZERO ELEMENT IN MAIN DIAGONAL OF VSOL(4,58) !')
GOTO 96
92 WRITE(25,93)
93 FORMAT(' SOLUTION IS TENDING TO INFINITY I ( > 10**10 )')
GOTO 96
94 WRITE(25,95)
95 FORMAT(' TOO MANY ITERATIONS !')
96 CONTINUE ;! MANDATORY OUTPUT IF NO SOLUTION
IF (DUMP.LT.1) WRITE(25,97)
97 FORMAT(' <<... IN SUBROUTINE S=O=L-V=S=R >>')
CNTPL=CNTPL+2; CNTR=CNTPL-2
WRITE(25,200) KOUNTM, CNTR, CNTPL
200 FORMAT(' NO SOLUTION AFTER', 15, ' ITERATIONS !/' CNTPL=14,
1' =', 14)
WRITE(25,120)(I, I=1, N)
WRITE(25,130)(EX(I), I=1, N)
WRITE(25,140)(LASTEX(I), I=1, N)
C *** DO NOT ALTER V(60) !!!
IF ((CNTPL.NE.4).AND.(DUMP.LT.3)) GOTO 210
C *** PRINT MANDATORY IF CNTPL=4
WRITE(25,215)
215 FORMAT(' NR. VSOL ROWS DIVIDED BY DIAGONAL ENTRY !')
WRITE(25,220)((VSOL(K,I), K=1,4), I=1, N-2)
220 FOPMAT('11X, VSOL:', 4(X, F11.5))
210 IF ((CNTPL.NE.4).AND.(DUMP.LT.3)) GOTO 240 ;! RETURN I
C *** CALCULATE RESIDUALS
DO 230 I= 2, N-2
  RESIDL(I)=VSOL(1,I)*EX(I-1)+VSOL(2,I)*EX(I)+VSOL(3,I)*EX(I+1)-
  VSOL(4,I)
1
230 CONTINUE
WRITE(25,120)(I, I=2, N-1)
WRITE(25,250)(RESIDL(I), I=2, N-1)
250 FOPMAT(' RESDL', 5(X, E10.4))
C
240 CONTINUE
IF (CNTPL.EQ.2) WRITE(25,260)
260 FORMAT(' S=O=L-V=S=R COULD BE RECALLED WITH DIAGONALLY DOMINANT *
1, MATRIX I/' .., BUT F/R F.D. SCHEME FOUND TO BE'
2, ' INACCURATE FOR M/N FLUIDS &SO IS DISALLOWED. '/')

IF (CNTPL.EQ.4) WRITE(25,270)
270 FORMAT('=MUDFLO SYSTEM C-R=A-S-H FROM SUBROUTINE SOLVSR !!'////)
RETURN
END

```

SOLDR

```

SUBROUTINE SOLVSP(VSOL,V,LMAT,TOLMAT,SORFCT,CNTRL,KOUNTM,DIMP,N)
DIMENSION VSOL(4,58),V(60)
DOUBLE PRECISION BETA(58),GAMMA(57),ZFD(58),EX(58)
INTEGER CNTRL,DIMP
C ***      ***      ***      ***      ***      ***      ***
C ***      SUBPROGRAM 2-R OF MUDFIO : S=O=L=D=R (10JAN78) ***
C ***      COMPATIBLE WITH SOLVSP (PARAMS 3,4,5,7 ARE DIMMIES) ***
C ***      TO DETERMINE THE SOLN. OF A TRIDIAGONAL SYSTEM DIRECTLY ***
C ***      REF: D.GHEFNSPA: INTRODUCTION TO NUMERICAL ANALYSIS AND ***
C ***      ...APPLICATIONS 1971 MARKHAM SECTION 3.4 ***
C ***      ***      ***      ***      ***      ***
C ***      GENERATE UPPER AND LOWER TRIANGULARISATION VECTORS
      BETA(1)=VSOL(2,1) !! MAIN DIAGONAL
      IF (PBETA(1),EQ,0) GOTO 35 !! SINGULAR MATRIX
      DO 40 I=2,N-2
        J=I-1 !! SO J=1,2,3,...,N-3
        GAMMA(I)=VSOL(3,J) / BETA(J)
        BETA(I)=VSOL(2,I) -VSOL(1,I) * GAMMA(J)
        IF (BETA(I),EQ,0) GOTO 35 !! SINGULAR MATRIX
40    CONTINUE
C ***      SET UP ZFD VECTOR
      ZFD(1)=VSOL(4,1)/BETA(1)
      DO 60 I=2,N-2
        ZFD(I) = ( VSOL(4,I)-VSOL(1,I)*ZFD(I-1) ) / BETA(I)
60    CONTINUE
C ***      SET UP EX VECTOR [SOLUTION]
C ***      [SETTING UP ERROR EQUATIONS WOULD ALTER COL4 OF VSOL TO CURRENT
C ***      VECTOR OF RESIDUALS. ERROR FOR SOLN INVOLVES ADDING PARTS ONTO
C ***      VECTOR V(60) , SO V WOULD HAVE TO BE ZERO'D AT THE START]
      EX(N-2)=ZFD(N-2)
      DO 70 I=1,N-3
        J=(N-2)-I !! SO J= N-3,N-4,N-5,...,1
        EX(J)=ZFD(J) - EX(J+1)*GAMMA(J)
70    CONTINUE
100   CONTINUE !! EX NOW CONTAINS THE SOLUTION
C ***      COPY SOLUTION TO V(60)
      DO 105 I=1,N-2
        V(I+1)=EX(I)
105   CONTINUE
      CNTRL=CNTRL+1
      IF (DIMP,LT,2) GOTO 180
      WRITE(25,190)
190   FORMAT(/' SOLUTION OBTAINED BY S=O=L=D=R')
      WRITE(25,200)(V(I),I=1,N)
200   FORMAT(/(' V : ',4(X,E12.6)))
180   GOTO 210 !! RETURN
35    CONTINUE !! MATRIX SINGULAR,SO INSOLVABLE
      CNTRL=CNTRL+2 ; DIMP=4 ; NTRL=CNTRL-2

      WRITE(25,240)NTRL,CNTRL
240   FORMAT(/' SINGULAR MATRIX : INSOLVABLE'/' CNTRL=',I4,' =>',I4//)
      WRITE(25,260)((VSOL(I,J),I=1,4),J=1,N)
260   FORMAT(/(' VSOL : ',4(X,E12.6)))
210   CONTINUE
C ***      CALCULATE AND PRINT DETERMINANT WHEN NEEDED
      IF (DIMP,LT,2) GOTO 300
      DTRMNT=1.0
      DO 270 I=1,N-2
        DTRMNT=DTRMNT*BETA(I)
270   CONTINUE
      WRITE(25,280)DTRMNT
280   FORMAT(/' DETERMINANT OF VSOL IS',E12.6,/' BETA VECTOR IS:')
      WRITE(25,290)(BETA(I),I=1,N-2)
290   FORMAT(/(' BETA : ',4(X,E12.6)))
300   RETURN
      END

```

NOTE : SOLDR is an alternative routine to SOLVSR.



VISCO(2)

```

C ***
70 CONTINUE ;! CRASH : NO MODEL FOUND
  WRITE(25,80) FLUID(1)
80  FORMAT(' C-R-A-S-H FROM SUBROUTINE V-J-S-C-O' /
1     ' NO MODEL AVAILABLE FOR FLUID(1)=',FR.3, /
2     ' CHECK DOCUMENTATION OR LINE PRINT FOR MODELS AVAILABLE' /
3     ,/)
  CRASH=2 ;! INTEGER CRASH RECORDS REASON FOR FAILURE
  DUMP=4
  GO TO 210 ;! OPTIONAL PRINT THEN RETURN
C ***
200 CONTINUE ;! DVISCY TO BE SET UP BY DIFF
C ***  DDVISC  IS A DUMMY VARIABLE, AND IS NOT USED IN THE COMPUTATION
      CALL DIFF(VISCY,DVISCY,DDVISC,N,H,DUMP)
C ***
210 CONTINUE ;! OPTIONAL PRINT THEN RETURN
  IF (DUMP.LT.3) GO TO 220
  WRITE(25,230)(ALPHA(I),I=1,N)
230  FORMAT(/(' ALPHA',4(X,E12.6)))
  WRITE(25,240)(DALPHA(I),I=1,N)
240  FORMAT(/(' DALPHA',4(X,E12.6)))
  WRITE(25,250)(VISCY(I),I=1,N)
250  FORMAT(/(' VISCY',4(X,E12.6)))
  WRITE(25,260)(DVISCY(I),I=1,N)
260  FORMAT(/(' DVISCY',4(X,E12.6)))
270  RETURN
      END

```

## DIFF

```

SUBROUTINE DIFF(VCTR,DVCTR,DDVCTR,N,H,DUMP)
DIMENSION VCTR(60),DVCTR(60),DDVCTR(60)
INTEGER DUMP
C ***      ***      ***      ***      ***      ***      ***
C ***      D-I-F-F      *      *      *      *      *      ***
C ***      SUBPROGRAM 4 OF M-II-D-F-L-O SYSTEM (25 JULY 77)      *      ***
C ***      FULLY DEVELOPED VERSION 1.4 (8 AUGUST 77)      *      ***
C ***      EXTERNAL TO SUBPROGRAM Y-I-S-C-O      *      ***
C ***      *      *      *      *      *      *      ***
C ***      TO NUMERICALLY DIFFERENTIATE VECTOR:VCTR(60)      *      ***
C ***      DVCTR(60) STORES 1ST DERIVATIVE :DDVCTR(60) THE 2ND. ***
C ***      ***      ***      ***      ***      ***      ***
      IF (DUMP.GE.1) WRITE(25,10)
10  FORMAT(' D-I-F-F RUNNING')
      IF (N.LT.15) WRITE(25,20)
20  FORMAT(' *** INSUFFICIENT NODES FOR SUBROUTINE D-I-F-F')
C ***      SET UP DVCTR + DDVCTR (REF. GREENSPAN + M., J. JAMES + DOCUMENTATION )
C ***      7 POINT FORWARD F.D. FORMULAE AT NODES 1,2,3
      DO 25 I=1,3
      DVCTR(I)=(-147*VCTR(I)+360*VCTR(I+1)-450*VCTR(I+2)+400*VCTR(I+3)
1 -225*VCTR(I+4)+72*VCTR(I+5)-10*VCTR(I+6))/(60*H)
      DDVCTR(I)=(1624*VCTR(I)-6264*VCTR(I+1)+10530*VCTR(I+2)-10160*
1 VCTR(I+3)+5940*VCTR(I+4)-1944*VCTR(I+5)+274*VCTR(I+6))/(360*H*H)
25  CONTINUE
C ***      7 POINT BACKWARD F.D. FORMULAE AT NODES N-2,N-1,N
      DO 30 I=N-2,N
      DVCTR(I)=(147*VCTR(I)-360*VCTR(I-1)+450*VCTR(I-2)-400*VCTR(I-3)
1 +225*VCTR(I-4)-72*VCTR(I-5)+10*VCTR(I-6))/(60*H)
      DDVCTR(I)=(1624*VCTR(I)-6264*VCTR(I-1)+10530*VCTR(I-2)-10160*
1 VCTR(I-3)+5940*VCTR(I-4)-1944*VCTR(I-5)+274*VCTR(I-6))/(360*H*H)
30  CONTINUE
C ***      5 POINT CENTRAL F.D. FORMULAE AT NODES 4,.....,N-3
      DO 35 I=4,N-3
      DVCTR(I)=(-VCTR(I+2)+8*VCTR(I+1)-8*VCTR(I-1)+VCTR(I-2))/(12*H)
      DDVCTR(I)=(-VCTR(I+2)+16*VCTR(I+1)-30*VCTR(I)+16*VCTR(I-1)
1 -VCTR(I-2))/(12*H*H)
35  CONTINUE
C ***      OPTIONAL PRINT
      IF (DUMP.LT.3) GOTO 40
      WRITE(25,50)(I,I=1,N)
50  FORMAT('   NODE',4(5X,I4,4X))
      WRITE(25,60)(VCTR(I),I=1,N)
60  FORMAT('   VCTR',4(X,E12.6))
      WRITE(25,70)(DVCTR(I),I=1,N)
70  FORMAT('   DVCTR',4(X,E12.6))
      WRITE(25,80)(DDVCTR(I),I=1,N)
80  FORMAT('   DDVCTR',4(X,E12.6))
40  RETURN

```

END

```

SUBROUTINE COORD(RADIUS,VA,VZ,MODV,ANGLE,N)
DIMENSION RADIUS(60),VA(60),VZ(60),ANGLE(60)
REAL MODV(60)
C ***      ***      ***      ***      ***      ***      ***
C ***      C-O-O-P-D      *      *      *      ***
C ***      SUBPROGRAM 5 OF N-H-D-F-I-D (14 NOV 77)      ***
C ***      TO VECTORIALLY ADD THE AXIAL AND ROTATIONAL      ***
C ***      *      *      *      VELOCITY PROFILES      ***
C ***      ***      ***      ***      ***      ***      ***
DO 10 I=1,N
  RADVA = RADIUS(I)*VA(I)
C ***      RADVA = TANGENTIAL VELOCITY IN METRES/SECOND
  MODV(I) = ((RADVA**2) + (VZ(I)**2))**.5
  ANGLE(I) = (ATAN2(VZ(I),RADVA))*(180.0/3.1417) ;1 IN DEGREES
10 CONTINUE
RETURN
END

SUBROUTINE VARIAN(N,VCTR,AV,STDDEV,PERCENT)
DIMENSION VCTR(60)
C ***      ***      ***      ***      ***      ***      ***
C ***      V-A-R-I-A-N      *      *      *      ***
C ***      SUBPROGRAM 6 OF N-H-D-F-I-D      ***
C ***      CALCULATES AVERAGE,STANDARD DEVIATION AND      ***
C ***      MAX PERCENT DIFFERENCE OF VCTR(60)      ***
C ***      ***      ***      ***      ***      ***      ***
SUM=0
C ***      CALCULATE AVERAGE (AV)
DO 10 I=1,N
  SUM=SUM + VCTR(I)
10 CONTINUE
AV=SUM/N
SUM=0 ; PERCENT = 0
C ***      CALCULATE STALDARD DEVIATION (STDDEV) AND MAX.PERCENT DIFFERENCE
C ***      ... FROM AV (PERCENT)
DO 20 I=1,N
  SUM=SUM + (VCTR(I)-AV)**2.0
  DIFF=ABS(VCTR(I)-AV)
  PERCENT=AMAX1(PERCENT,DIFF)
20 CONTINUE
PERCENT = PERCENT * 100.0 / AV
STDDEV = (SUM/(N-1))**.5
RETURN
END

```

B.3 Variable names used in the program.

NAME	TYPE	USAGE AND COMMENTS
N	INTEGER	Number of nodes. Warning is printed if it is less than 15 .
P	REAL	Axial pressure gradient.
FLUID	REAL(60)	Fluid parameter matrix. First entry defines model ; sixth entry gives initial viscosity approximation ; entries 2 to 6 hold the fluid parameter values.
TOL	REAL	Tolerance limit for convergence of velocity distribution calculations.
TOLMAT	REAL	Tolerance limit for matrix solution calculations.
LIM	INTEGER	Max. N <sup>o</sup> . of iterations in velocity calculations.
LIMAT	INTEGER	Max. N <sup>o</sup> . of iterations in matrix solutions.
SORFCT	REAL	Successive over-relaxation factor for SOLVSR.
H	REAL	Distance between nodes.
RADIUS	REAL(60)	Nodal values of the radial coordinate.
VISCY	REAL(60)	Viscosity vector.
DVISCY	REAL(60)	Derivative of VISCY.
KOUNT	INTEGER	N <sup>o</sup> . of main program iterations so far.
KOUNTM	INTEGER	N <sup>o</sup> . of SOLVSR iterations so far.
VZ	REAL(60)	Axial velocity vector.
DVZ	REAL(60)	Derivative of VZ.
DDVZ	REAL(60)	Second derivative of VZ.
VA	REAL(60)	Angular velocity vector.
DVA	REAL(60)	Derivative of VA.
DDVA	REAL(60)	Second derivative of VA.
LASTVZ	REAL(60)	Copy of VZ from previous iteration block.
LASTVA	REAL(60)	Copy of VA from previous iteration block.
V	REAL(60)	Copy of VA or VZ in SOLVSR.

B.3 Contd.

NAME	TYPE	USAGE AND COMMENTS
VSOL	REAL(60)	Matrix of finite difference coefficients.
EX	REAL(60)	Current solution estimate in SOLVSR.
RESIDL	REAL(60)	Residuals in SOLVSR.
VCTR	REAL(60)	Vector to be differentiated in DIFF.
I,J,K	INTEGERS	Indices.
CRASH	INTEGER	Used to control subsection ' CRASH' of main prog. Its value depends on reason for programme failure.
DUMP	INTEGER	Controls amount of output generated by program. Normal value is 0; except when diagnosing faults.
BATCH	INTEGER	Number of iterations between convergence tests.
BCHKNT	INTEGER	No. of iterations since last convergence test.
SET	INTEGER	No. of iterations between convergence tests in SOLVSR.
CNTRL	INTEGER	Controls the interaction of MOVSET and SOLVSR.
SCALER	REAL	Used to control whether MOVSET sets up matrix for axial or angular velocity profile.
PRESSR	REAL	( As for SCALER )
ONE	INTEGER	Used in MOVSET U.D.S. to effect interchange of VSOL columns 1 and 3 when backward scheme is chosen.
THREE	INTEGER	( As for ONE )

B.4 Archive numbers.

Archive numbers may be used to retrieve magnetic tape copies of the program from the Computing Services library, RGIT.

FILE NAME	ARCHIVE NUMBER	DATE ARCHIVED
DATIN	ARC 017.018	28/04/78
MUDFLO	ARC 009.015	21/01/78
MOVSET	ARC 021.018	28/04/78
SOLVSR	ARC 023.018	28/04/78
SOLDR	ARC 019.018	28/04/78
VISCO	ARC 025.018	28/04/78
DIFF	ARC 018.18	28/04/78
COORD	ARC 024.018	28/04/78
VARIAN	( As COORD )	-

NOTATION

SYMBOLS

$f(\underline{\underline{\Delta}}:\underline{\underline{\Delta}})$	Apparent viscosity $(M L^{-1} T^{-1})$
$g$	Acceleration due to gravity $(L T^{-2})$
$k$	Radius ratio of an annulus
$m$	Power law fluid model parameter $(M L^{-1} T^{-n})$
$n$	Power law fluid model parameter
$P$	Pressure $(M L^{-1} T^{-2})$
$\rho$	Axial body force defined as $\rho g - \frac{dP}{dz}$ $(M L^{-2} T^{-2})$
$\bar{P}$	Dimensionless axial body force, defined in 4.2
$v$	Velocity (In axial direction unless otherwise indicated) $(L T^{-1})$
$w$	Angular velocity $(T^{-1})$
$W$	Angular velocity boundary value $(T^{-1})$
$r$	Radius $(L)$
$R$	Boundary value of radius $(L)$
$t$	Time $(T)$
$z(r)$	Stability parameter of Ryan and Johnstone, defined in 3.1.4
$\alpha$	Shear rate (equal to $(\underline{\underline{\Delta}}:\underline{\underline{\Delta}})$ ) $(T^{-2})$
$\underline{\underline{\Delta}}$	Shear rate tensor $(T^{-1})$
$\mu_0$	Bingham plastic model parameter $(M L^{-1} T^{-1})$
$\rho$	Density $(M L^{-3})$
$\underline{\underline{\tau}}$	Shear stress tensor $(M L^{-1} T^{-2})$
$\tau_w$	Shear stress at wall $(M L^{-1} T^{-2})$
$\tau_0, \tau_\infty$	Fluid model parameters $(M L^{-1} T^{-2})$
$\sigma_1, \sigma_2$	Fluid model parameters $(T)$
$\lambda_0, \lambda_\infty$	Fluid model parameters $(M L^{-1} T^{-1})$

SUBSCRIPTS

1,2	Used to indicate value at inner and outer wall respectively
$r, \theta, z$	Coordinate subscripts defined in the usual way
$\sim$	Indicates that the quantity is a vector
$\underline{\underline{\approx}}$	Indicates that the quantity is a tensor

## SUPERSCRIPTS

- Indicates an averaged quantity
- \* Dimensionless value as defined in 2.3

## OPERATIONS

( $\underline{I}:\underline{I}$ ) The second invariant of the tensor  $\underline{I}$  defined as

$$\sum_{i=1}^3 \sum_{j=1}^3 T_{ij} T_{ji}$$

where the subscripts  $i$  and  $j$  have the conventional meaning.

( $\underline{V}:\underline{v}$ )  $\frac{1}{r} \frac{\partial}{\partial r} \{r v_r\} + \frac{1}{r} \frac{\partial v_\theta}{\partial \theta} + \frac{\partial v_z}{\partial z}$

## BIBLIOGRAPHY

- Baroid,76. Manual of Drilling Fluids Technology, Baroid petroleum Services, Houston, Texas.
- Bird,R.B., Stewart,W.E. and Lightfoot,E.N. 65. Transport Phenomena; Wiley.
- Coleman,B.D. and Noll,W. 58. J. Applied Physics V30(10), p1508.
- Coulson,J.M. and Richardson,F. 71. Chemical Engineering V3; Pergamon.
- Denn,M.M. and Roisman,J.J. 69. A.I.Che.J. V15(3), p450.
- Dierckes,A.C. 65. Ph.D. thesis, Princeton University.
- Fredrickson,A.G. 64. Principles and Applications of Rheology; Prentice-Hall.
- Fredrickson,A.G. and Bird,R.B. 58. Industrial and Engineering Chemistry V50(3), p347.
- Frene,J. 75. Disa Information V17(Feb), p19.
- Graebel,W.D. 61. Physics of fluids V4,p362.
- Greenspan,D. 71. Introduction to Numerical analysis and Applications; Markham.
- Guickes,T.L. 75. Trans. A.S.M.E. : J.Engineering for Industry 75(May), p498.
- Laird,W.M. 57. Industrial and Engineering Chemistry 49(1), p347.
- Langlois,W.E. 64. Slow Viscous Flow; Macmillan.

- M<sup>C</sup>Eachern,D.W. 66. A.I.Che.J. V12(2), p328.
- M<sup>C</sup>Eachern,D.W. 69. A.I.Che.J. V15(6), p885.
- Martin,M 68. Les Fluides de Forage; Publications de l'Institute Fraincais du Petrol, p24.
- Mishra,P. and Mishra,I. 76. A.I.Che.J. V22(3), p617.
- Murphy,P.J. 75. D.Off.Tech. Thesis, RGIT.
- Noll,W. 58. Arch. Rational Mech. Anal. V2,p197.
- Parslay,P.R. 57. Petroleum Trans. A.I.M.E. V210; p310.
- Pearson,J.R.A. 76. Annual Review of Fluid Mechanics; p163.
- Rea,D.R. and Schowalter,W.R. 67. Trans. Soc. Rheology V11(1), p125.
- Rivlin,R.S. 56. J.Rational Mech. Anal. V5(1), p179.
- Robertson,R.E. 76. Soc. Petroleum Engineers J. 76(Feb),p31.
- Ryan,N.W. and Johnstone,M.M. 59. A.I.Che.J. V5(4), p433.
- Savins,J.G. and Wallick,G.C. 66. A.I.Che.J. V12(2), p357.
- Savins,J.G. and Wallick,G.c. 69. Soc. Petroleum Engineers J. 75(Sep), p311.
- Schowalter,W.R. and Dierckes,A.C. 66. Industrial and Engineering Chemistry Fundamentals V5(2), p263.
- Sifferman,T.R., Myers,G.M., Haden,E.L. and Wahl,H.A. 74. J. Petroleum Technology 74(Nov), p1295.

- Sivalingham, A. 77. British Petroleum Co. Ltd. Dyce. (Private communication)
- Skelland, A.H.P. 67. Non-Newtonian Flow and Heat Transfer; Wiley.
- Slawomirski, M.R. 74. Archiwum Gornictwa xix(2), p83.
- Slawomirski, M.R. 75. Int. J. Rock Mech. Min. Science and Gemoech. Abstr. v12, p115.
- Spalding, D.B. 70. Report No. BL/TN/A/39, Imperial College of <sup>Science and</sup> Technology.
- STEC, 76. Data Sheets for Oil Drilling Technology; Scottish Technical Education Council.
- Tiu, C. and Bhattach, S. 74. A.I.Che.J. V20(6), p1140(Oct).
- Walker, R.E. and Al-Rawi, O. 70. SPE of AIME paper No. 3108.
- Walker, R.E. and Holman, E. 71. Oil and Gas J. 71(Mar), p80.
- Walker, R.E. and Korry, D.E. 73. SPE of AIME paper No. 14321(Apr).
- Walker, R.E. and Korry, D.E. 74. J. Petroleum Technology 74(Feb), p167.
- Watson, R.J. 77. Mobil Oil Co., Dallas, Texas. (Private communication).
- Wilson, R.C. 76. D.Off.Tech. Thesis, RGIT.
- Zienkiewicz, O.C., Owen, D.R.J. and Lyness, J.F. Conference notes: Finite Element Methods in Fluid Flow Problems, Swansea. p489.